DOCKING OF THE p68 SUBUNIT OF DNA POLYMERASE α-PRIMASE ON THE SV40 HELICASE IS REQUIRED FOR THE VIRAL PRIMOSOME ACTIVITY

By

Hao Huang

Dissertation

Submitted to the Faculty of

Graduate School of Vanderbilt University

in partial fulfillment of the requirements

for the degree of

DOCTOR OF PHILOSOPHY

in

Biological Sciences

December, 2010

Nashville, Tennessee

Approved:

Ellen Fanning, Dr.rer.nat.

James G. Patton, Ph.D.

Katherine L. Friedman, Ph.D.

Brandt F. Eichman, Ph.D.

Walter J. Chazin, Ph.D.

ACKNOWLEDGMENTS

I am deeply indebted to my mentor, Dr. Ellen Fanning. Ellen dedicates her life to science and sets a great role model for me. She guided me through every step of my graduate career. She taught me how to design projects, how to write proposals, and how to do good presentations. She was always available and gave advice. She always encouraged me when I doubted myself. Her help and support over the past several years were invaluable to me.

I would like to thank Dr. Walter Chazin for his support as well. The work presented in this dissertation is a successful collaboration with his lab. Especially, I thank his former student, Dr. Brian Weiner, who conducted all the structural studies.

I would also like to thank the other members of my dissertation committee, Drs. James Patton, Katherine Friedman, and Brandt Eichman for their input into my dissertation project. In particular, I thank Jim and Kathy for their encouragement and help.

I want to thank all past and present members of the Fanning lab for providing such a great working environment. My special thanks give to Dr. Bob Ott who taught me to purify pol-prim and to set up the replication assays, to Dr. Haijiang Zhang who initiated this project, to Kun Zhao who maintains the lab and helped me purify Tag and RPA, to Diana Arnett who helped a lot with the two manuscripts and to Dr. Xiaorong Zhao, Dr. Xiaohua Jiang, and Wes Dulaney for their advice and friendship.

I also want to thank our collaborator Dr. James Pipas for providing the patch mutants of Tag.

I want to extend a special thanks to my family. They always appreciate who I am and

support all my decisions. I could not get to this point without their tremendous sacrifice and unconditional love.

Finally, I would like to thank the financial support of National Institute of Health and Vanderbilt University.

TABLE OF CONTENTS

Page

LIST OF TABLES

LIST OF FIGURES

LIST OF ABBREVIATIONS

aa	amino acids
AAA+	ATPases associated with a variety of cellular activities
ATP	Adenosine triphosphate
ATPγS	Adenosine 5'-O-(thiotriphosphate)
ATR	ATM and Rad3-related
BME	2-mercaptoethanol
bp	Base pair
BSA	Bovine serum albumin
C	Celsius
Cdc	Cell division cycle
CDK	Cyclin dependent kinase
Cdt1	Cdc10-dependent transcript 1
Ci	Curie
CMG	Cdc45/Mcm2-7/GINS
Co-IP	Co-immunoprecipitation
COSY	Correlation spectroscopy
cpm	Counts per minute
CTD	Carboxyl-terminal domain
CTP	Cytidine triphosphate

Da	Dalton
dATP	Deoxyadenosine triphosphate
DBD	DNA binding domain
Dbf4	Dumb bell forming 4
dCTP	Deoxycytidine triphosphate
dGTP	Deoxyguanosine triphosphate
DNA	Deoxyribonucleic acid
dNTP	Deoxyribonucleotide
dsDNA	double-stranded DNA
DTT	Dithiothreitol
dTTP	Deoxythymidine triphosphate
EDTA	Ethylenediaminotetraacetic acid
EM	Electron Microscopy
EP	Early panlindrome
EPR	Electron paramagnetic resonance
E.coli	Escherichia coli
g	Gram
GINS	*Go ichi ni san* (5, 1, 2, 3)
GST	Glutathione S-tranferase
h	hour
HCl	Hydrochloric acid

HD	Helicase domain
HEPES	N-[2-hydroxyethyl] piperazine-N'-[2ethansulfonic acid]
His	Histidine
HiPIP	High-potential iron protein
HR	host-range
HSQC	Heteronuclear single quantum coherence
Hsc70	Heat shock protein cognate 70
ID	Internal domain
IPTG	Isopropyl thio-beta-D-galactopyranoside
ITC	Isothermal titration calorimetry
kb	kilobase
Kd	Dissociation constant
kDa	kilo Dalton
KOH	Potassium Hydroxide
L	Liter
LB	Luria broth
M	Molar
MCM	Mini-chromosome maintenance
mg	Milligram
$MgCl_2$	Magnesium Chloride
min	Minute

ml	Milliliter
MRN	Mre11-Rad50-Nbs1
µg	Mirogram
µl	Microliter
µM	Miromolar
µCi	Microcurie
NaCl	Sodium Chloride
Ni-NTA	Nickel-nitrilotriacetic acid
ng	Nanogram
NLS	Nuclear localization signal
nm	Nanometer
nmol	Nanomol
NMR	Nuclear magnetic resonance
nt	Nucleotide
NTD	N-terminal domain
NOESY	Nuclear Overhauser effect spectroscopy
NP-40	Nonidet-P40
OB	Oligonucleotide/oligosaccharide-binding
OBD	Origin binding domain
OD	Optical density
ORC	Origin recognition complex

p58C	C-terminal domain of p58
p68N	the folded domain of the N-terminal region of p68
P4	Patch 4 mutant
Pab101	Polyomavirus monoclonal antibody 101
PBS	Phosphate buffered saline
PCNA	Proliferating cell nuclear antigen
PCR	Polymerase chain reaction
PDB	Protein databank
PMSF	Phenylmethylsulfonyl fluoride
pmol	Picomol
Pol	DNA Polymerase
Pol δ	DNA Polymerase δ
Pol ε	DNA Polymerase ε
Pol-prim	DNA Polymerase α-primase
Pre-RC	Pre-replication complex
Rb	Retinoblastoma
RFC	Replication factor C
RNA	Ribonucleic acid
RPA	Replication protein A
RPA70AB	the DNA binding domains A and B of RPA
RPA70N	the N-terminus of the RPA70 subunit

RPA32C	the C-terminus of the RPA32 subunit
rpm	revolutions pre minute
RT	room temperature
SDS	Sodium dodecyl sulfate
SDS-PAGE	Sodium dodecyl sulfate polyacrylamide gel electrophoresis
sec	Second
ssDNA	single-stranded DNA
Sc	Saccharomyces cerevisiae
SSB	Single stranded DNA binding protein
SV40	Simian Virus 40
Sso	*Sulfolobus solfataricus*
Tag	SV40 large tumor antigen
TBE	Tris borate EDTA buffer
TBS	Tris buffered saline
TBST	Tris buffered saline tween-20
TCA	Trichloroacetic acid
Tris	Tris-(hydroxymethyl-)aminomethane
TOCSY	Total correlation spectroscopy
TopBP1	Topoisomerase II binding protein 1
Topo I	Topoisomerase I
UV-vis	Ultraviolet-visible

VP	Viral protein
V	Volt
WT	Wild type

CHAPTER I

INTRODUCTION

DNA Replication Overview

In all organisms, cells accurately duplicate their genomic DNA during each cell division. This fundamental process, known as DNA replication, is essential to maintain genome integrity. DNA replication is precisely orchestrated and highly regulated to ensure faithful propagation of genetic information from one cell generation to another. Misregulation of DNA replication can lead to severe diseases such as cancer and developmental abnormalities.

DNA replication is carried out by a multi-protein machine termed the replisome [1]. The fundamental components of the replisome are highly conserved from prokaryotes to eukaryotes (Fig. 1.1) [2]. They include a helicase to unwind the parental double-stranded DNA (dsDNA) into two single stands served as template for replication, single-stranded DNA (ssDNA) binding proteins (SSBs) that coat ssDNA to prevent secondary structure formation, a primase to initiate *de novo* DNA synthesis by generating RNA primers that can be elongated by DNA polymerases, DNA polymerases (Pol) to synthesize new strands of DNA in a 5'-3' direction, a clamp that encircles DNA and tethers DNA polymerase to template to increase polymerase processivity, and a clamp loader that mediates the clamp loading. Replisome-mediated DNA replication is achieved through dynamic assembly of these fundamental components.

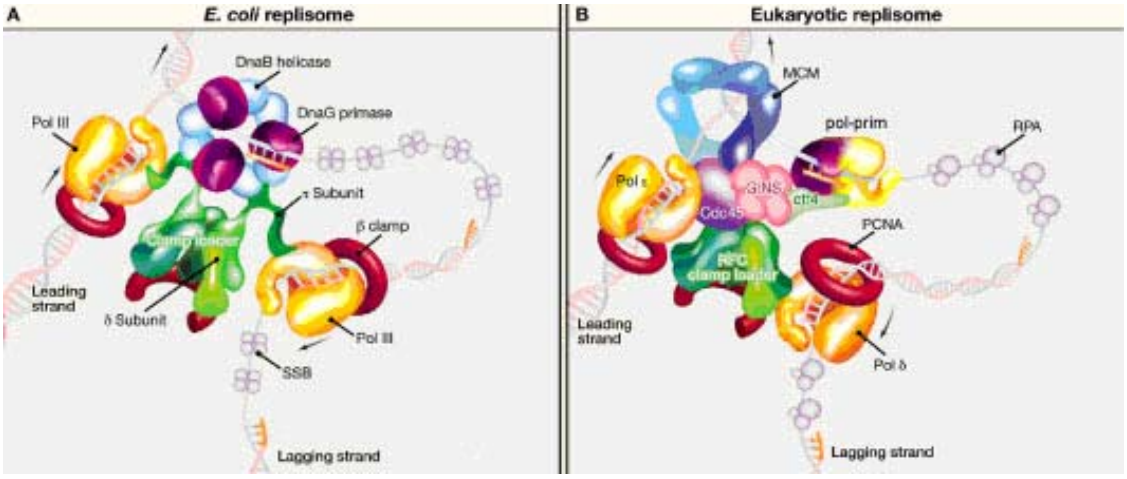

Figure 1.1. Replisomes of prokaryotic and eukaryotic systems [2]**.** (A) Model of the *E.coli* replisome. The DnaB helicase translocates along the lagging strand and unwinds the duplex DNA into two separate strands, which are coated by SSBs. Three monomers of the DnaG primase interact with DnaB and catalyze RNA primer synthesis. The two separated parental DNA strands are replicated by Pol III, continuously on the leading strand and discontinuously on the lagging strand in the form of Okazaki fragment. The β clamp tethers Pol III to the DNA and ensures that the polymerase stays attached to the DNA. Loading of the β clamp is mediated by the clamp loader. The τ subunits of the clamp loader organize the replisome by simultaneously binding Pol III and DnaB. (B) Model of the eukaryotic replisome. The MCM 2-7 helicase functions similarily to the DnaB helicase, it translocates along the leading strand and unwinds the duplex DNA. Eukaryotic SSB is the RPA protein. The primase in the eukaryotic replisome is Pol α-primase (pol-prim), which includes a primase and DNA polymerase. In addition, Pol α-primase creates an RNA-DNA hybrid primer. In eukaryotes, the polymerases on individual ssDNA are different, with Pol ε and Pol δ synthesizing the leading and lagging strands, respectively. The eukaryotic clamp, PCNA (proliferating cell nuclear antigen), performs a similar role as the *E. coli* β clamp. The RFC protein is the eukaryotic clamp loader. The eukaryotic replisome also contains factors not present in the *E. coli* replisome, like Cdc45, the GINS complex and Ctf4. They are essential components of the replisome, but their specific functions are currently not well-defined.

Priming is an important process that couples activities of the helicase and the primase. This process is performed by a sophisticated protein machinery called the primosome, which normally consists of a helicase, a primase, and SSBs. Primosomes have been well-characterized in prokaryotic systems such as *E.coli*. The *E.coli* primosome is composed of the DnaB heliase, the

DnaG primase and the SSBs (Fig. 1.1A) [3]. Dynamic physical association of the three proteins directs primosome assembly of *E.coli* [3]. Primosome activity is essential for priming on both leading and lagging strands at origins of replication, as well as for initiating synthesis of each Okazaki fragment on the lagging strand. The primosome activity has also been shown to be important for checkpoint activation at stalled replication forks and telomere maintenance. This dissertation will take advantage of the Simian Virus (SV40) *in vitro* replication system to explore the mechanism that regulates the viral primosome assembly.

SV40: A Model for Eukaryotic DNA Replication

SV40 has a well characterized origin with a specific DNA sequence, and a cognate initiator protein that also serves as the helicase for replication [4]. Importantly, except for this single viral protein, SV40 utilizes host replication proteins to replicate the viral genome. SV40 therefore has been a favored model for studying eukaryotic chromosomal replication for a long time. In particular, the development of a cell-free SV40 DNA replication system using purified proteins [5, 6] has been very useful for examining the protein-DNA and protein-protein interactions that ensure the progression of steps in the process of initiation of DNA replication.

The Virus

SV40 is a small DNA virus of the *Polyomaviridae* family [7]. It contains a double-stranded, closed circular DNA genome (~5.2 kb), which associates with histones to form a mini-chromosome with 24-25 nucleosomes [8, 9]. The SV40 mini-chromosome is surrounded by

a non-enveloped icosahedral capsid with 72 capsomeres. Each capsomere contains one VP1 pentamer and an interior VP2 or VP3 that contacts both the VP1 pentamer and the condensed mini-chromosome [10]. SV40 can infect a number of mammalian cell types. In permissive primate cells, such as kidney cells of its natural host Rhesus macaque, SV40 produces a persistent infection with little cytopathic effect. In contrast, in kidney cells of *Cercopithecus aethiops* (African green monkey), SV40 produces a lytic infection with release of thousands of progeny viruses [11]. In non-permissive cells, like rodent cells, SV40 infection does not produce progeny virions [7]. Integration of viral DNA into the cellular genome by non-homologous recombination can lead to stable transformation of non-permissive cells [12].

The SV40 genome can be divided into three distinct regions: the early transcription unit, the late transcription unit and the regulatory region (Fig. 1.2) [12]. The early unit encodes large T antigen (Tag), small t antigen, and 17K T antigen. The late transcription unit encodes four capsid proteins VP1, VP2, VP3 and VP4 [13], an agno protein that helps viral assembly, and a pre-micro RNA that is expressed (miRNA) late in infection and limits immune recognition by reducing early gene expression [14]. The regulatory region, located in between the early and late coding units, contains the viral origin of DNA replication, early and late promoters, enhancers of transcription and the viral packaging signal [12].

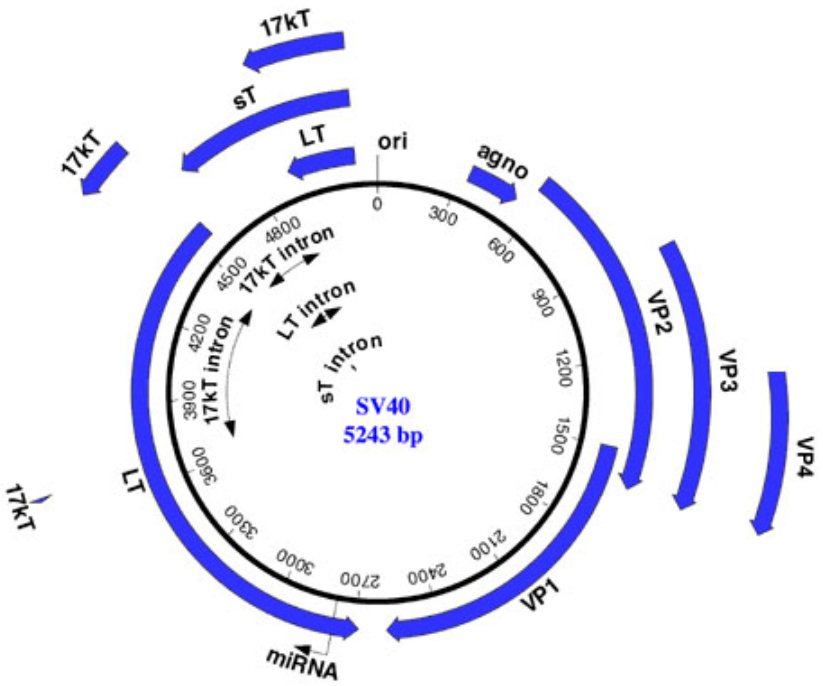

Figure 1.2. Map of the SV40 genome. SV40 genomic DNA is composed of three elements: the early and late coding units and the regulatory region. The early unit encodes large T antigen (LT), small t antigen (sT), 17K T antigen (17KT). The late unit encodes the three structural proteins (VP1, VP2, VP3 and VP4), the agnoprotein (agno) and a pre-microRNA (miRNA). The regulatory region (ori) contains sequences for the early and late promoter and the origin of replication. Adapted from [12].

The core of SV40 origin is 64 bp in length and contains three functional regions (Fig. 1.3) [4]: the early (imperfect) palindrome (EP), the pentanucleotide palindrome (PEN) which consists of four GAGGC pentanucleotides arranged as inverted repeats, and a 17 bp A/T rich domain (AT). All four pentanucleotides, as well as the spacing between these repeats, are critical for specific Tag binding. The AT region directs DNA bending and facilitates strand separation during DNA unwinding [15].

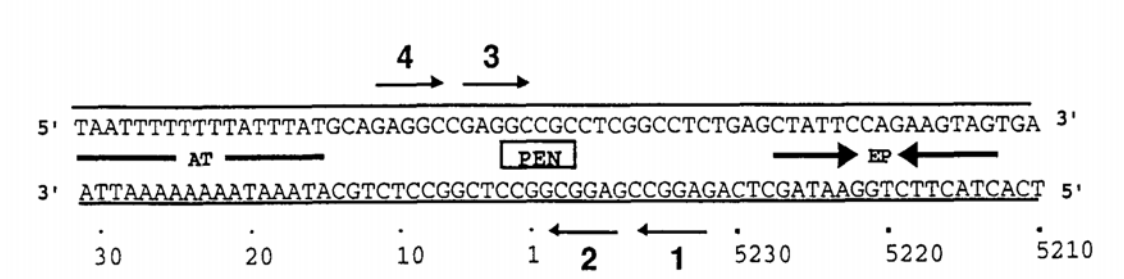

Figure 1.3. The SV40 core origin. The four GAGGC pentanucleotides are indicated by arrows numbered 1-4. Also shown are the locations of the early palindrome (EP) and the A/T-rich (AT) region [4].

Following attachment to the surface of a permissive cell, SV40 enters its host cell through caveolae-mediated endocytosis [16] and is sorted to the smooth endoplasmic reticulum (ER) directly through a microtubule-dependent pathway [17, 18]. The virus is uncoated in the ER [19, 20], the exposed viral mini-chromosome is then imported into the nucleus [21, 22]. Once in the nucleus, the viral chromatin undergoes remodeling and transcription initiates from the early promoter by the host transcription apparatus. Differential splicing of the early transcript results in expression of Tag and small t, which act cooperatively to drive the host cell into S phase and to reprogram the cellular environment for virus production [7]. Tag then initiates replication of the viral genome, activates late gene transcription, and promotes virion assembly [7] [4, 12, 23]. Tag plays an essential role during SV40 infection and is at the core of the SV40 DNA replication machinery.

Mechanism of SV40 DNA Replication in a Cell-free System

The SV40 *in vitro* replication system has served as an excellent model for studies of DNA replication in eukaryotes. The earliest *in vitro* replication system was established using human or monkey cell extract supplemented by the viral protein Tag [24]. The cell extract, together with a single viral protein Tag, is able to replicate plasmid DNA containing the SV40 origin of replication. Extensive fractionation studies were then conducted to identify the essential factors in host cell extract that are required for replication [5, 25-27]. Eventually, ten cellular protein complexes were isolated and shown to be sufficient to replicate SV40 DNA in the presence of Tag in a cell-free system [5]. The ten cellular complexes and their biochemical activities are listed in Table 1.1[6].

As the initiator for SV40 replication, Tag recognizes the origin of replication, melts and unwinds the duplex DNA, and recruits other replication factors required for initiation. The detailed mechanism of Tag-dependent origin recognition and DNA unwinding will be discussed in the Tag section of this chapter. Briefly, Tag specifically binds to the SV40 origin and assembles into a double hexamer with head-to-head orientation in the presence of ATP. Powered by ATP hydrolysis, Tag unwinds the parental dsDNA to generate ssDNA template for DNA synthesis. Topoisomerase I relieves the superhelical tension that accumulates during DNA unwinding ahead of the replication fork [28].

Table 1.1. Cellular proteins required for SV40 DNA replication and their functions.

Protein	*Subunit Composition*	*Functions*
Replication Protein A (RPA)	70, 32, 14 kDa	Single-stranded DNA binding
DNA polymerase α-primase (pol-prim)	180, 68,58,48 kDa	DNA polymerase, primase RNA-DNA primer synthesis
DNA polymerase δ	125, 66, 50,12 kDa	DNA polymerase, 3'-5' exonuclease
Proliferating Cell Nuclear Antigen (PCNA)	37 kDa	Clamp
Replication Factor C (RFC)	140, 40, 38, 37, 36 kDa	Clamp loader
Topoisomerase I	100 kDa	Relieves torsional stress in DNA
Topoisomerase II	140 kDa	Segregates daughter strands, Relieves torsional stress in DNA
RNase HI	68 kDa	Endonuclease for removal of RNA primers
FEN I	44 kDa	5'-3' flap exonuclease for removal of RNA primers
DNA ligase I	125 kDa	Ligation of DNA

While DNA unwinding is underway, Tag orchestrates the primosome assembly by recruiting the ssDNA-binding protein replication protein A (RPA) and DNA polymerase α-primase (pol-prim) [6]. RPA binds ssDNA and protects it from nuclease and hairpin formation [29]. The primase-containing pol-prim initiates *de novo* DNA synthesis by generating a chimeric DNA-RNA primer that can be elongated by DNA polymerases [30, 31]. Tag interactions with RPA and pol-prim are essential for primosome assembly and will be discussed further (Table 1.2; Fig 1.14) in this chapter.

Once the RNA-DNA primer is synthesized, a switch from pol-prim to DNA po δ occurs at the primer-template junction. The polymerase switch is mediated by two accessory proteins: Replication Factor C (RFC) and Proliferating Cell Nuclear Antigen (PCNA) [32-34]. RFC is the

clamp loader; it binds to the 3'-end of the primer-template junction, displaces pol-prim and loads the sliding clamp PCNA onto the primer-template junction. The clamp PCNA encircles DNA and binds pol δ. Association of pol δ with PCNA then enables its processive DNA extension without dissociating from the template [35, 36]. The observation that pol-prim, RFC, and pol δ compete with one another for RPA binding at the primer-template junction suggests that this process is highly coordinated [37]. The switching from pol-prim to pol δ occurs during initiation on the leading strand and during synthesis of each Okazaki fragment on the lagging strand. On the leading strand, DNA synthesis by the PCNA- pol δ complex is continuous after this switch. On the lagging strand, DNA synthesis proceeds until pol δ encounters the previously synthesized Okazaki fragment, resulting in gapped Okazaki fragments of ~200bp in size.

The short Okazaki fragments synthesized discontinuously on the lagging strand are further processed into complete, ungapped DNA product [38]. Two nucleases, RNaseHI and Fen I, catalyze the complete removal of the RNA primer. RNase HI has endonucleolytic activity that cleaves the RNA primer but leaves one single ribonucleotide at the 5' end of the RNA-DNA primer junction [39]. Fen I, which has 5' to 3' flap exonuclease activity, removes the remaining ribonucleotide [40]. The gap after primer removal can be filled by pol δ, and DNA ligase I then joins the adjacent Okazaki fragments together to form a continuous DNA strand [5].

When the two replication forks converge, replication terminates, resulting in two intertwined circular daughter molecules [41]. Topoisomerase II segregates the two daughter molecules by inducing transient double-strand breaks, resulting in two separated circular DNA strands [28].

In SV40 DNA replication, Tag serves as the initiator by binding to the SV40 origin and the

helicase at the replication fork, but its functional equivalent in eukaryotic cells has not been identified yet. Nonetheless, the ten cellular protein complexes identified through the SV40 replication system also function to duplicate chromosomal DNA. Thus, elucidating the functional role of individual proteins as well as the mechanism that directs the replisome assembly by using this simple model system will yield significant insight into the complex eukaryotic DNA replication. However, it is still noteworthy that there are major differences between the viral and host replication. The DNA pol ε, which is responsible for copying the leading strand during chromosomal replication [42, 43], is not required for SV40 DNA replication (Fig. 1.4). Also it has been recognized recently that host DNA damage pathways are activated during SV40 DNA replication [44] [45], which allows viral replication to escape from the strict control of chromosomal DNA replication. These differences raise a key question that whether SV40 replication mimics a host chromosomal replication or an alternative DNA repairing process.

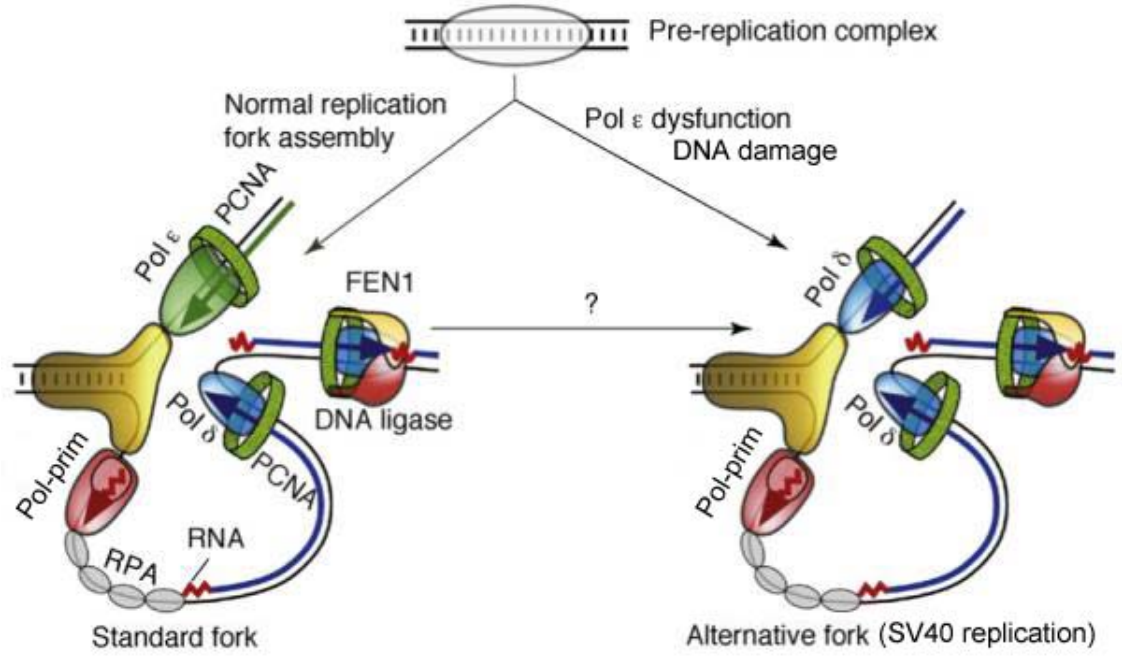

Figure 1.4. Models for eukaryotic DNA replication fork and SV40 replication fork. On the left is a model illustrating primary roles for Pol ε and Pol δ in leading and lagging strand replication, respectively. Other proteins shown include the Pol-prim (red), the MCM helicase (yellow), RPA (gray), the sliding clamp PCNA; green) and the FEN1-DNA ligase complex (yellow-red). On the right is a model wherein Pol ε dysfunction causes formation of an alternative fork. Conditions other than Pol ε dysfunction might also cause formation of alternative fork, like the DNA damage signaling conditions during the SV40 DNA replication. Adapted from [43].

The SV40 Primosome Trinity

As stated before, a primosome usually consists of three components: a helicase, a primase and SSBs. In the case of SV40 DNA replication, Tag, pol-prim and RPA compose the SV40 primosome, with Tag as the helicase, pol-prim as the primase, and RPA as the SSB. A detailed discussion of each component follows below.

Tag

Tag is the major early gene product encoded by the SV40 genome. It is a multifunctional

protein composed of 708 amino acids and has a predicted molecular weight of 82.5kDa [7]. Biochemical and genetic studies demonstrated that Tag is essential to drive infected cells into S phase, to initiate viral DNA replication, to activate late gene expression, to promote virion assembly and to induce cellular transformation [4, 7, 12, 23]. The diverse functions of Tag are mediated by its structural and functional domains (Fig. 1.5). Tag is composed of four functional domains: an N-terminal J domain (a.a. 1-102), an origin binding domain (OBD) (a.a. 131-259), a helicase domain (a.a. 260-627), and a C-terminal host range domain (a.a. 628-708). Structures of these individual domains [46, 47] [48] have been determined except for the HR domain which is thought to be, at least in part, unstructured. Although a crystal structure of the intact Tag protein is not available yet, cryo-EM structures of double hexamers of Tag bound to SV40 origin DNA with atomic structure fitted were reported recently [49].

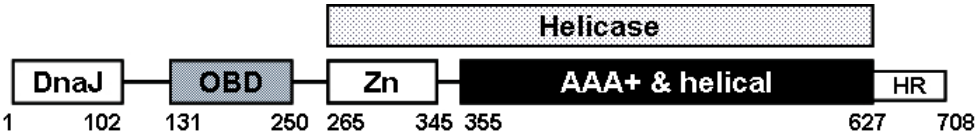

Figure 1.5. Structural and functional domains of Tag. The known functional domains are represented by colored boxes and flexible linkers by thin lines. Residue numbers are indicated below. OBD, SV40 origin-DNA-binding domain; ZnD, zinc domain; AAA+, ATPases associated with a variety of cellular activities; HR, host range. Adapted from [50].

The J domain of Tag is essential to drive infected cells into S phase and to induce cell transformation [12]. It composed of four α-helices (a.a. 7-102) with an extended loop (a.a. 103-117) containing the LxCxE motif, which binds to the retinoblastoma (Rb) tumor suppressor (Fig. 1.6, red) [46]. Rb bound to E2F inhibits E2F-dependent transcription activation required for

G1/S transition. The J domain acts in concert with the LxCxE motif to disrupt Rb-E2F complexes. The J domain recruits Hsc70 and the LxCxE motif associates with Rb. The energy derived from ATP hydrolysis of Hsc70 induces release of E2F from Rb, resulting in E2F-DP1 dependent transcription of genes that promote S phase entry [23]. The J domain is dispensable for SV40 DNA replication *in vitro* [51], but it is essential for viral replication in infected cells [4, 23]. The host range domain is not required for replication or for cellular transformation, but it is involved in host range determination as well as virion assembly [52].

The OBD is involved in sequence-specific binding to the origin of SV40 replication. Mutagenesis analysis identified two elements, termed A (~ a.a. 152-155) and B2 (a.a. 203-207), to be essential for origin specific recognition [53]. The structure of the OBD was initially determined by NMR [47]. It is composed of a central five-stranded antiparallel β-sheet flanked by two α-helices on one side and by one α-helx and one 3_{10}-helix on the other (Fig. 1.6, green) [47]. The origin DNA binding surface was mapped to two closely juxtaposed loops forming a continuous surface, which corresponds with the elements A and B2, respectively [47]. Crystal structures of OBD in complex with origin DNA showed that the A loop travels back and forth along the major groove of the DNA and accounts for most contacts with the GAGGC pentanucleotides of the origin core [54, 55]. Although a hexameric structure of OBD was determined [56], the OBDs do not contact one another when bound to origin DNA [54, 55]. The OBD is also involved in non-specific dsDNA and ssDNA binding, which are thought to be essential for helicase activity of Tag [57]. The DNA binding surface of OBD is also involved in its interactions with RPA70AB and RPA32C [58, 59]. In the context of intact Tag protein, the

OBD plays roles in oligomerization, origin melting, DNA unwinding, helicase activity, RPA loading and RPA ssDNA binding mode remodeling [4], [58, 59].

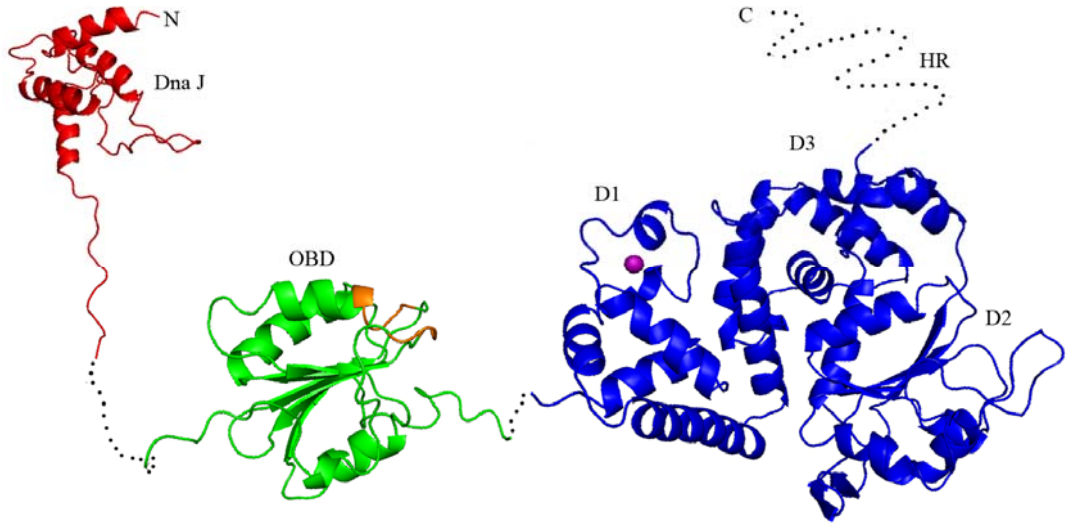

Figure 1.6. Overall structure of SV40 large Tag. Tag is composed of three structural domains connected by flexible peptides: the DnaJ domain (red); the OBD (green); and the helicase domain (blue) which contains three sub-domains D1, D2 and D3. The structure of HR has not been investigated. Elements A1 and B2 in the OBD are colored yellow. The zinc is colored magenta. Structures of each domain were determined independently and are linked by dot lines.

The helicase domain is composed of three subdomains: D1, a zinc domain; D2, an AAA+ domain; D3, an α-helical domain (Fig. 1.6, blue) [48]. The zinc domain is a globular fold stabilized by a non-canonical zinc motif that is not directly involved in DNA binding. The zinc domain is important for Tag hexamerization. The AAA+ domain is quite typical: it contains all the signature motifs of the AAA+ family proteins: a Walker A motif for ATP binding, a Walker B motif for ATP hydrolysis and the motif C, which detects ATP/ADP in the nucleotide binding pocket [60]. The AAA+ domain is also involved in hexamerization. The hexameric helicase

domains appear like a double donut consisted of a smaller ring containing the zinc domains and a large ring containing the AAA+ and the helical domains (Fig. 1.7A).

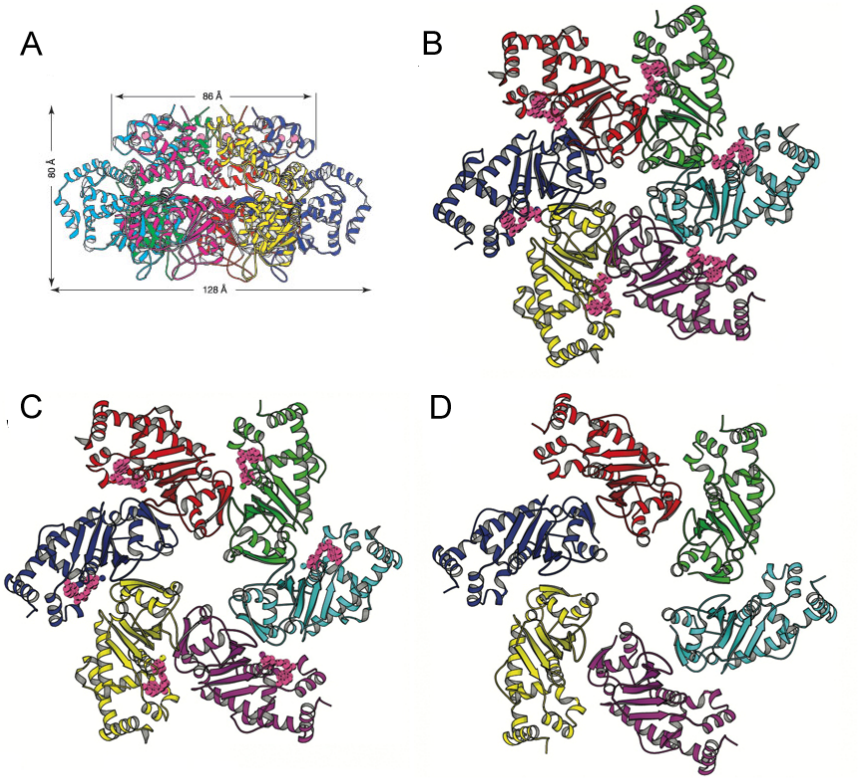

Figure 1.7. Tag hexameric structures in different nucleotide binding states. Viewing from the side (A) and from the C-terminal end (B, C, D). Each monomer is depicted with a distinct color. (A) The Nt-free hexamer structure. The pink balls represent Zn atoms. (B) The ATP bound hexamer structure. The six ATPs at the cleft between two monomers are in pink. (C) The ADP bound hexamer structure, showing ADP (pink) at the cleft. (D) The Nt-free hexamer structure. Adapted from [48, 61].

Structures of the hexameric helicase domain have been solved in various nucleotide binding states (Fig. 1.7), revealing a potential mechanism that may couple ATP hydrolysis with conformational changes to drive DNA unwinding (Fig. 1.8) [61, 62]. The six subunits of the Tag

helicase hexamer bind and hydrolyze ATP in an unusual all-or-none mode, unlike the sequential mechanism of other known hexameric helicases [63, 64]. The hexamer has a strongly positive-charged central channel [48]. Six β hairpins, one from each of the six subunits, protrude into the central channel for interacting with DNA (Fig. 1.8B). The size of the central channel changes according to the nucleotide binding state of the hexamer, with the smallest opening (14Å) in the ATP-bound form (Fig. 1.7B) and the widest opening in the nucleotide-free state (22 Å) (Fig. 1.7D) [61]. Upon ATP binding, the D2/D3 swings toward D1 by using a flexible helix that connects D1 and D2 as a hinge. This conformational change triggers movement of the β hairpins, a key observation that forms the foundation for a model for the unwinding mechanism. The β hairpins are proposed to pull dsDNA into the channel for unwinding (Fig. 1.8C). The unwound ssDNA is proposed to then extrude from side channels of the hexamer [48]. ATP hydrolysis and ADP release restore the original position of the β hairpins (Fig. 1.8D, E) and re-set the helicase hexamer for another round of DNA unwinding (Fig. 1.8A). Although this model is very appealing, the idea that the hexamer central channel could accommodate dsDNA remains controversial and the exit of the two separated strands is still unresolved. Structures of Tag in complex with DNA are expected to solve these puzzles.

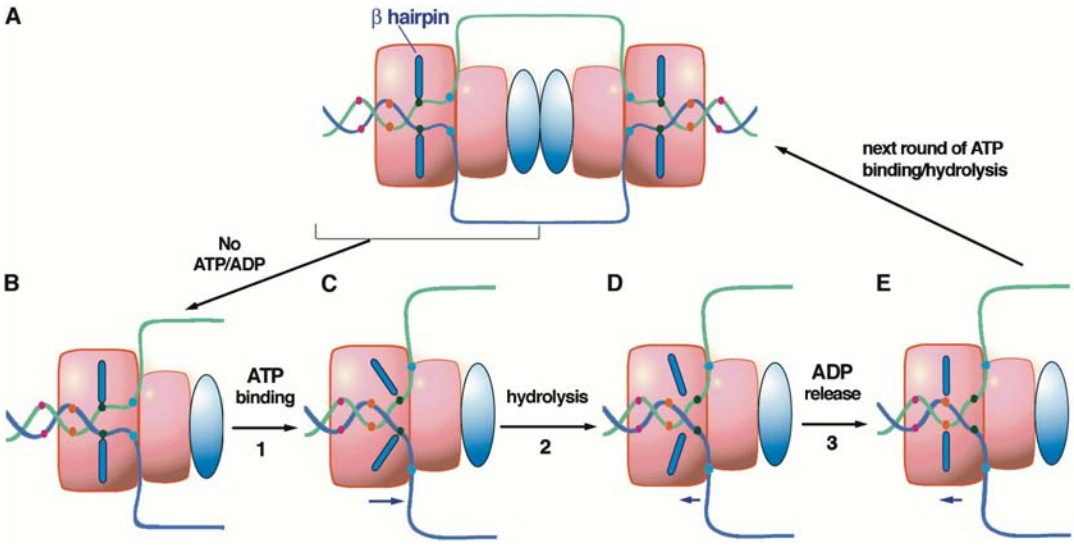

Figure 1.8. A Looping model showing the coupling of the β hairpin movement to the dsDNA translocation into Tag double hexamer for unwinding. The β hairpins move along the central channel in response to ATP binding (step 1), hydrolysis (step 2), and ADP release (step 3). (A) Tag double hexamer with two ssDNA loops coming out from the side channels. Each hexamer contains a helicase domain (represented by two squares in pink) and an OBD (oval in light blue). The β hairpin structure is represented by two bars (in blue) within the helicase domain. The colored dots on the DNA (red, orange, black, and blue) are position markers for translocation. (B) A Tag hexamer corresponding to the left half of the double hexamer in (A) in the Nt-free state. (C) The movement of β hairpins upon ATP binding, which serves to pull dsDNA into the helicase for unwinding. The unwound ssDNA extrudes from the side channels. For clarity, only one hexamer is shown. (D) The β hairpins move back about halfway toward the Nt-free position after ATP hydrolysis. (E) The ADP is released from the LTag hexamer, and the β hairpins return to the original Nt-free position. From [61].

The capability of Tag to serve as the initiator and the helicase for SV40 DNA replication is largely attributed to the cooperative activities of the OBD and the helicase domain. Structures of Tag assembled as double hexamer at the SV40 origin have been determined by electron microscopy [65-67] [49]. Detailed 3D analysis showed that the double hexamer is asymmetrical and adopts different degrees of bending along the DNA axis. Based on currently available structural and biochemical data, a favorable model for Tag-mediated origin melting and DNA

unwinding has been proposed (Fig. 1.9) [47-49, 54-56, 61, 62, 65-70]. At first, four Tag OBDs specifically bind to the four GAGGC sites in the origin (Fig. 1.9A). These binding events likely bring the associated helicase domains to the DNA (Fig. 1.9B). Hexamerization of the helicase domain recruits the additional eight Tags to the origin to form a double hexamer. Through nonspecific DNA binding, the additional eight OBDs bind to DNA side by side with the initial four OBDs forming a spiral double hexamer (Fig. 1.9C), which has been observed by cryo-EM (Fig. 1.9C')[49]. Conformational rearrangements of subunits of the two hexamer activate the double hexamer to unwind DNA. Powered by ATP, the helicase double hexamer melts and unwinds duplex DNA bidirectionally (Fig. 1.9D), resulting in the rabbit ear-like structure as seen by electron microscopy (Fig. 1.9D') [71]. Recent findings suggest the possibility that duplex melting is accomplished by crushing the duplex when ATP binds to Tag, constricting the central channel, which forces several bases in the AT-rich region to flip out of the double helix, thereby melting the duplex (X.S. Chen, 2010, in press). Several models have been proposed to explain the path of the DNA strands through the double hexamer [48, 61, 66, 67, 70], but they are all speculative at the moment.

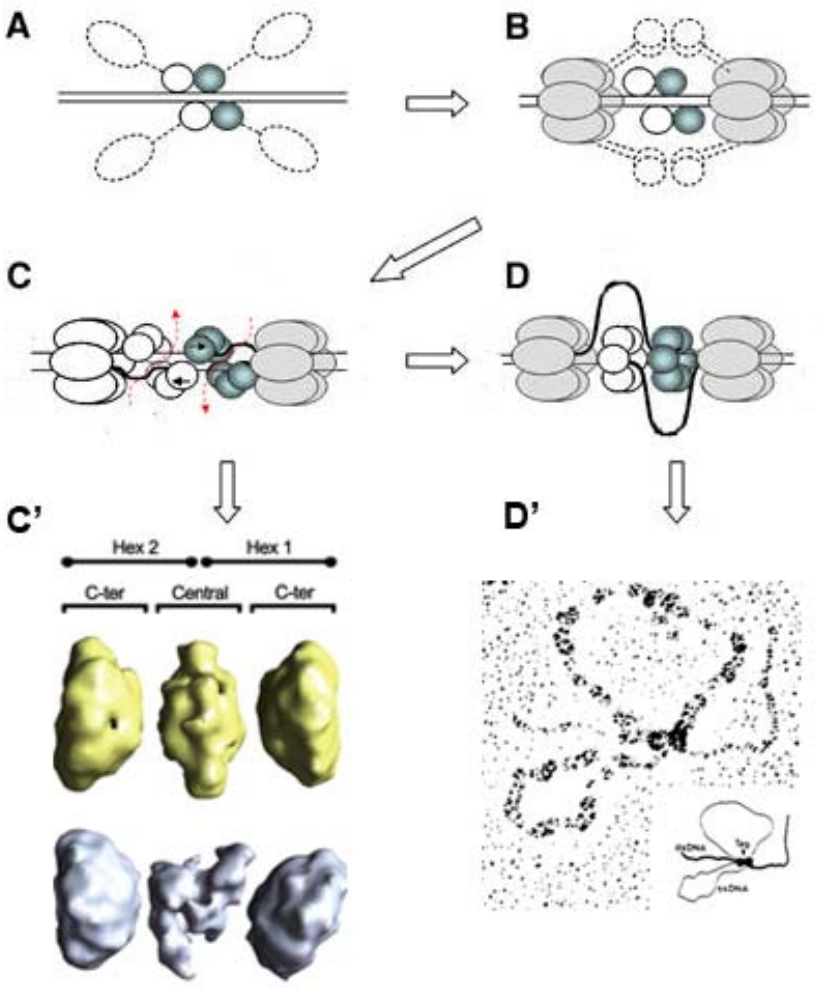

Figure 1.9. Model for origin melting and DNA unwinding by Tag. (A) Four OBDs bind the origin and bring monomeric domains of helicase in proximity to the DNA. (B) Helicase domains are assembled in two hexamers encircling DNA; this brings an additional eight OBDs in proximity to the origin. (C) Using a nonspecific DNA-binding mode, the eight additional OBDs bind side by side with the four initial OBDs forming a spiral double hexamer. The helicase distorts and melts the origin. (C') Cryo-EM maps of Tag hexamers in the parallel (upper) and displaced conformations (bottom) [49]. (D) The helicase pulls the most distant OBD and induces switching of an open (spiral) OBD hexamer to closed hexamer. OBDs are represented as circles. OBDs that mediate assembly of the right-hand hexamer are colored in blue and those for the left-hand hexamer are white. Monomers of the helicase domain are represented as ellipses and shadowed in gray [54]. (D') Electron micrograph of unwinding intermediate (rabbit ears-containing structure) started from the SV40 origin of DNA replication [71].

DNA pol -prim

DNA polymerases are specialized enzymes that catalyze DNA synthesis. These enzymes play essential roles in DNA replication, DNA recombination and DNA repair [72]. Currently, nineteen human DNA polymerases have been identified, and they have been grouped in five different families (A, B, C, X, Y) based on sequence homology and structural similarities. [73] DNA polymerases catalyze phosphoryl transfer reactions and require a primer with a 3'-OH terminus for nucleotide addition [72]. DNA pol-prim is unique among all the polymerases as it is the only one that contains an associated DNA primase activity to make an RNA primer with a free 3'-OH terminus [72]. Thus, pol-prim serves as the initiator polymerase during DNA replication. In addition, pol-prim plays important roles in DNA repair and telomere maintenance [74-76].

DNA pol-prim is composed of four subunits named according to their molecular weights in kDa: p180, p68, p58 and p48, each of which possesses distinct functions (Fig. 1.10) [72].

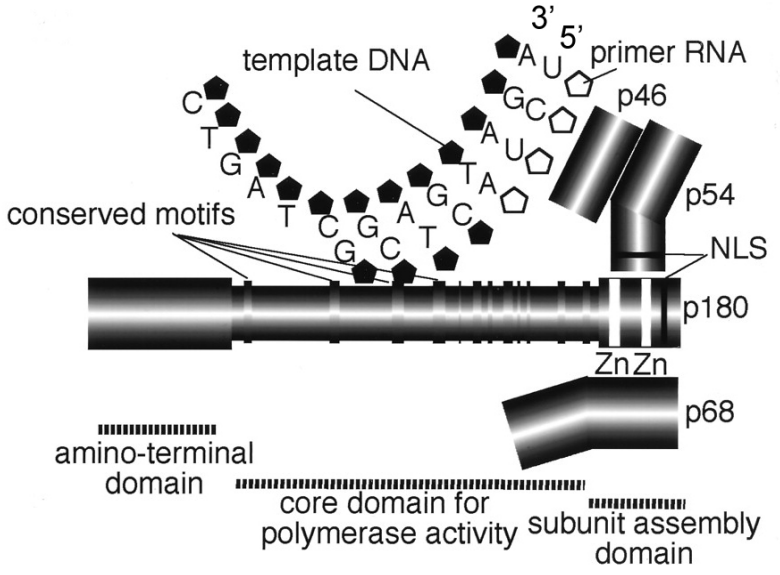

Figure 1.10. Molecular architecture of DNA pol-prim. Adapted from [77].

The p180 subunit contains the polymerase activity. p180 can be divided into three domains: an N-terminal protein interaction domain (a.a. 1-329); the minimal core polymerase domain (a.a. 330-1279); and a C-terminal, Zn-containing subunit assembly domain (a.a. 1280-1465) [77]. Pol-prim, together with pol δ and pol ε, belongs to the B family of polymerases. The core polymerase domain of p180 contains all conserved motifs among family B polymerases and it is predicted to fold into a human right hand-like structure with three distinct subdomains designated as palm, thumb, and fingers [72]. The palm contains the catalytically active sites, where two conserved aspartic acid residues function to coordinate two Mg^{2+} ions involved in a phosphoryl transfer reaction via a two-metal-ion mechanism. The fingers position the template and interact with the incoming dNTP. Concerted movement of the fingers toward the palm results in a conformational switch from an "open" to a "closed" mode, forming a binding pocket for nucleotides. The thumb interacts with duplex DNA. The C-terminal domain of p180 serves as an anchor for both p68 and p58. p180 contains a nuclear localization signal, but nuclear translocation of p180 depends on its association with p68 [78]. p180 is phosphorylated throughout the cell cycle, but becomes hyperphosphorylated in G2/M phase [79, 80]. Cyclin E and cyclin A-dependent protein kinases are able to phosphorylate p180, but the functional importance of p180 phosphorylation is still unknown.

The p68 subunit, also known as the B subunit, does not contain any enzymatic activity, but serves a regulatory role (Fig. 1.11). p68 is required for cell viability and executes an essential function in an early stage of S phase in yeast [81]. Association with p68 facilitates production and nuclear translocation of p180 [78] [82]. The region required for p180 association is localized at a

large C-terminal region of p68 [77], and this region is highly conserved among different species. Unlike the C-terminal domain, the N-terminal region of p68 shows very little sequence conservation, and is predicted to be largely disordered. p68 can also be phosphorylated by cyclin-dependent kinases in a cell cycle-dependent manner [80, 83]. The phosphorylation sites are located within residues 141-160 of the N-terminal domain. Phosphorylation of p68 by cyclin A/E-Cdk2 inhibits the primosome activity on RPA-coated template, but not primer extension activity of pol-prim activity in initiation of SV40 replication *in vitro* [84]. However, the underlying mechanism by which p68 phosphorylation regulates SV40 DNA replication remains unclear.

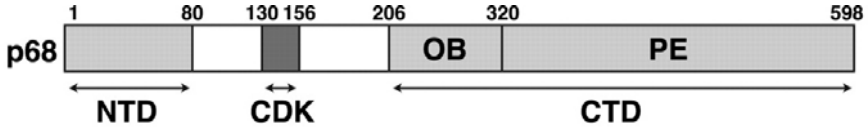

Figure 1.11. A schematic diagram of the p68 subunit of human pol-prim. NTD, N-terminal domain; CDK, cluster of sites phosphorylated by cyclin A-dependent kinase; CTD, C-terminal domain composed of an oligonucleotide-oligosaccharide binding (OB) subdomain and a phosphoesterase (PE) subdomain.

A crystal structure of the C-terminal domain (a.a. 1263-1468, CTD) of yeast p180 in complex with the C-terminal domain of yeast p68 (a.a. 246-705) has been determined (Fig. 1.12A) [85]. The CTD of p180 adopts an elongated, bilobed structure resembling a saddle. Each lobe contains a Zn motif, and the two lobes are connected by a three-helix bundle that represents the central portion of the saddle. The CTD of yeast p68 is composed of an N-terminal oligonucleotide/oligosaccharide (OB) domain with a C-terminal phosphoesterase (PE) domain

(Fig. 1.12A). Both the OB domain and the PE domain of make contacts with p180CTD: the OB domain contacts the N-teminal Zn motif, whereas the PE domain interacts with the N-terminal lobe. The electron microscopic (EM) image reconstructions of yeast p180 (a.a. 346-1468) -p68 (a.a. 246-705) heterodimer revealed that a bilobal shape with two dictinct regions. Docking of the p180CTD-p68CTD complex in the EM reconstruction showed that the p180CTD-p68CTD interaction module was tethered to the polymerase domain of p180 through a flexible linker (Fig. 1.12B) [85].

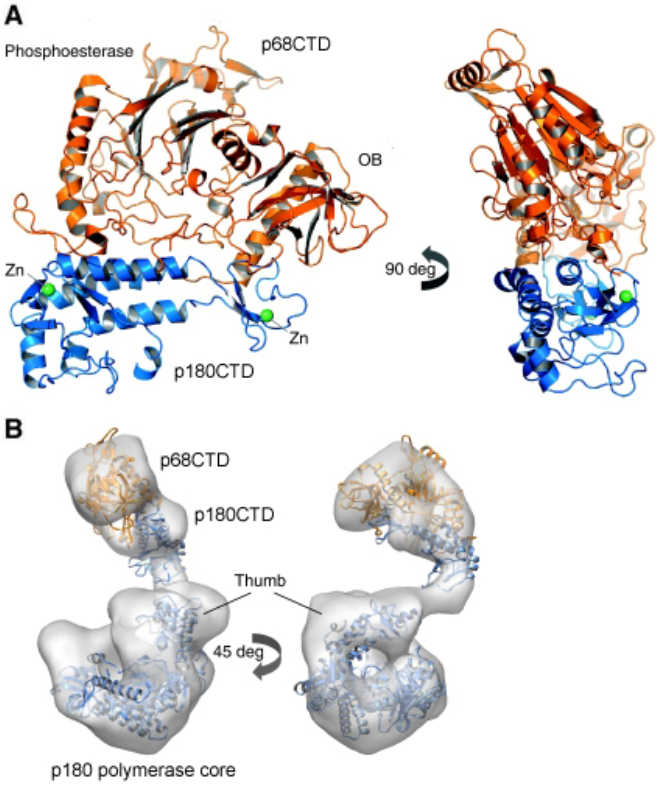

Figure 1.12. Crystal structure of the yeast p180CTD-p68CTD complex. (A) Ribbon diagram of the crystal structure of the yeast p180CTD-p68CTD complex, showing two orientations of the complex related by a 90 degree rotation. The p180CTD is drawn in blue and the p68CTD in orange. The positions of the phosphoesterase and OB domains in the p68CTD are indicated. The zinc atoms are shown as green spheres.

Figure 1.12, continued. (B) Ribbon models for the crystal structures of the p180CTD-p68CTD complex and the catalytic domain of the archaeal polymerase from *T. gorgonarius* are fitted to the EM reconstruction of yeast p180 (a.a. 349-1468)-p68 (a.a. 246-705) heterodimer. Two rotated views of the EM reconstruction are shown, represented as white transparent density. The p180CTD and the catalytic domain of the archaeal polymerase are shown in blue and the B subunit in orange. Adapted from [85].

The p48 and p58 subunits of pol-prim function together as the primase, with the catalytic activity residing in p48 [31]. p48 shares sequence homology with DNA polymerase β, a member of the polymerase X family, and is thought to catalyze nucleotide addition via a similar two-metal-ion mechanism [86]. Three aspartates in p48, Asp109, Asp111 and Asp306, have been proposed to appropriately position a pair of Mg^{2+} to assist in catalysis of the phosphoryl transfer reaction [87]. The p58 subunit has no known catalytic activity. It tethers p48 to p180, stabilizes p48 and enhances primase efficiency [88]. A nuclear localization signal in p58 can direct both p58 and the p58/48 complex to the nucleus [77]. p58 has been proposed to function in regulating primer initiation, elongation, length counting [89], as well as transfer of primers from the primase active site to the polymerase active site of p180 [90]. A unique 4Fe-4S cluster in the C-terminal domain of p58 was identified and shown to be essential for primer synthesis [91, 92]. The crystal structure of this unique C-terminal 4Fe-4S domain has recently been reported [93, 94]. Initiation of primer synthesis requires both p48 and p58 subunits.

Primer synthesis by pol-prim involves an ordered steps of template binding, NTP binding, initiation, extension and transfer of the primer to be extended by pol α [31]. The rate-limiting step of initiation is the dinucleotide formation from the first two individual ribonucleotides [95]. The primase first synthesizes a 7-10 nucleotide RNA primer; and then without dissociation of

pol-prim, the RNA primer is handed off to the p180 subunit, which extends the primer, yielding a chimeric RNA-DNA primer of ~30 nucleotides [96].

Eukaryotic pol-prim is structurally and functionally different from its counterpart in prokaryotes [31]. Prokaryotic primases are monomers with three distinct domains: an N-terminal domain with a zinc-binding motif that is critical for recognizing initiation sites on template ssDNA, a RNA polymerase domain, and a C-terminal region that either interacts with the helicase or is a helicase itself. Instead of making chimeric DNA-RNA primers, prokaryotic primases synthesize only small RNA primers.

RPA

RPA is the major eukaryotic ssDNA binding protein [97]. It was first identified as an essential cellular factor required for SV40 DNA replication [29]. RPA plays important roles in many pathways of DNA metabolism, including DNA replication, repair and homologous recombination [98]. The primary function of RPA in these pathways is to protect ssDNA from nucleases and to prevent hairpin formation and reannealing. RPA also interacts with many DNA processing proteins. These interactions are thought to remodel the ssDNA binding mode of RPA and to help DNA processing proteins trade places on ssDNA [98].

RPA has three subunits RPA70, RPA32 and RPA14 that are conserved in eukaryotes. It is a highly modular protein with multiple domains connected by flexible linkers (Fig. 1.13). RPA has six oligonucleotide/oligosaccharide binding (OB)-fold domains: RPA70N, RPA70A, RPA70B, RPA70C, RPA32D and RPA14. RPA32C is a winged-helix-turn-helix fold [99]. Four of the

OB-fold domains (RPA70A, RPA70B, RPA70C and RPA32D) constitute the DNA binding domains (DBDs). RPA binds to ssDNA with a 5'-3' polarity with RPA70A at the 5' end and RPA32D at the 3' end [100], in order of decreasing affinity for ssDNA. RPA has been shown to adopt three distinct binding modes distinguished by the number of DBDs involved and the length of ssDNA that it covers [101-103] [58] . In the compact binding mode, two DBDs (RPA70A and RPA70B) bind 8-10 nucleotides. An intermediate binding mode involves three DBDs (RPA70A, RPA70B and RPA70C) covering 12-23 nucleotides. In the fully extended binding mode, all four DBDs are engaged in binding to 28-30 nucleotides.

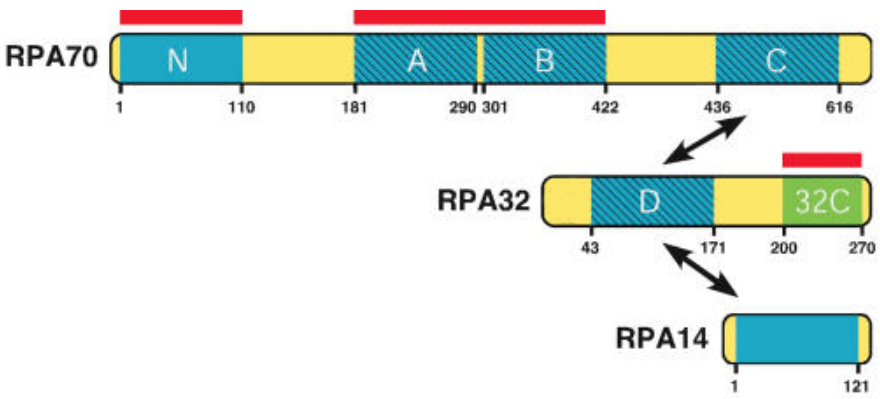

Figure 1.13. RPA is a modular protein. Schematic diagram: arrows indicate intersubunit associations; protein-binding domains are denoted by red bars; ssDNA binding domains A-D by hatching; OB-folds by blue boxes; linkers by yellow boxes; winged helix by a green box. From [98].

RPA interacts with a variety of DNA processing proteins. These interactions coordinate the recruitment and displacement of DNA processing proteins on ssDNA [98]. Particularly, the modular property of RPA guides proteins to trade places on ssDNA via a hand-off mechanism [104]. RPA70N, RPA70A, RPA70B and RPA32C have been shown to be involved in

protein-protein interactions. The basic cleft of RPA70N mediates interactions with multiple proteins including p53, ATRIP, RAD9 and MRE11 [105-107]. The larger module RPA70AB can interact with pol-prim [108]. RPA32C physically interacts with Tag, Rad52, XPA, Smarcal 1 and p58 [58, 94, 99, 109]. Studies of interaction between Tag and RPA32C suggest that proteins binding to RPA32C may facilitate the displacement of RPA from ssDNA [58].

Interactions within the SV40 Primosome

Tag, RPA and pol-prim compose the SV40 primosome. How these proteins come together and assemble into a functional primosome to initiate SV40 DNA replication is an intriguing, but poorly understood process. As we are beginning to appreciate, the dynamic assembly of DNA processing machinery often involves multiple protein-protein interactions that drive the hand-off of DNA from one protein to another [104]. Pair-wise protein interactions have been observed in the SV40 viral primosome [108, 110-115] [58, 59] (Table 1.2). Particularly, the interactions between Tag and RPA have been systematically investigated using a combination of structural and functional approaches in a collaboration between the Fanning and Chazin labs. Physical interaction of Tag-OBD with the RPA high-affinity ssDNA-binding domains RPA70AB actively loads RPA on emerging ssDNA during the activation of the SV40 pre-replication complex. Loading of RPA proceeds through a ternary complex of RPA70AB, Tag-OBD, and 8-10 nt ssDNA oligomer [59]. Physical interaction between the Tag-OBD and RPA32C remodels the binding mode of RPA on ssDNA to transiently create a short stretch of unbound ssDNA for pol-prim loading and primer synthesis (Fig 1.14A, B) [58]. The subsequent primer extension by

pol-prim does not require Tag, but may be facilitated by RPA through its interaction with pol-prim (Fig. 1.14 D).

Table 1.2. Protein-protein interactions involved in SV40 primosome assembly. ?, unknown; ND, not determined.

Interaction	*Interacting domains*	*Binding site mapped*	*Role of interaction*
Tag-RPA	OBD-70AB	Yes	RPA loading
	OBD-32C	Yes	RPA conformation remodeling, pol-prim loading
Tag-pol-prim	?-p68 a.a.1-240	No	pol-prim loading
	?-p180 a.a.195-313	No	pol-prim loading
	?-p58/p48	No	ND
RPA-pol-prim	RPA 32C-p58C	Yes	ND
	RPA 70NAB-p58/p48	No	ND

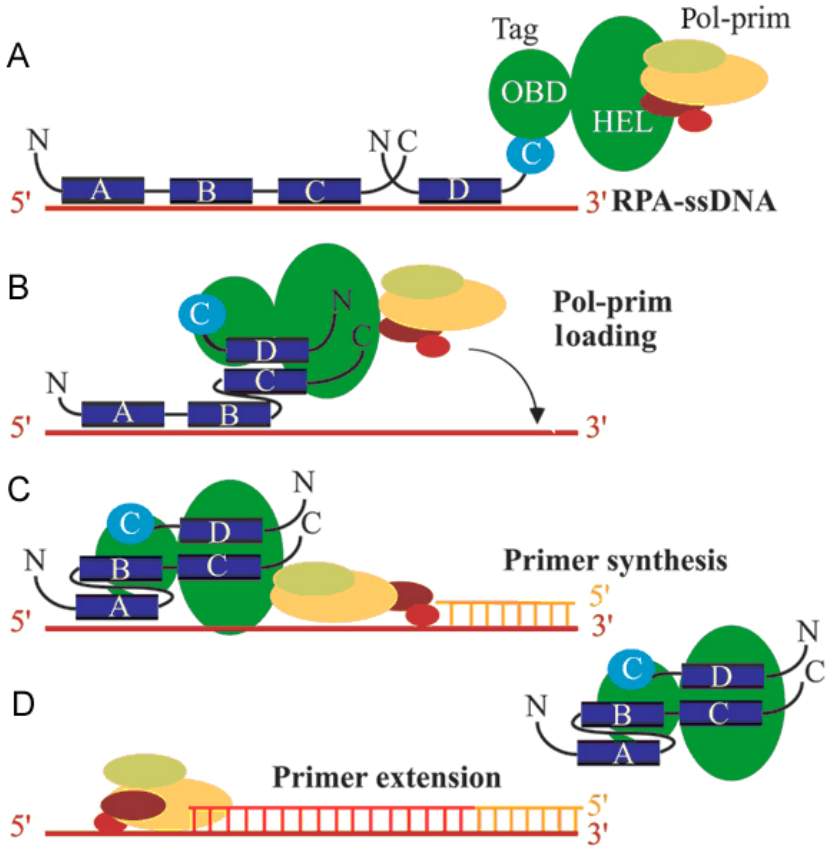

Figure 1.14. Model for SV40 primosome activity on RPA-coated ssDNA. (A) RPA (blue) is schematically depicted in the high-affinity 28−30 nt binding mode with all four ssDNA binding domains (A−D) bound to ssDNA. RPA14 is omitted for simplicity. The helicase domain (HEL) of a Tag hexamer [62] can associate with a pol-prim heterotetramer. Antibodies against Tag that specifically inhibit either hRPA binding to Tag-OBD or pol-prim binding to the helicase domain prevent primer synthesis. (B) We suggest that primosome assembly begins when Tag-OBD associates first with RPA32C and then with RPA70AB, transiently creating a short stretch of unbound ssDNA. (C) In concert with this RPA remodeling, pol-prim associated with the Tag hexamer would be poised to access the free ssDNA and begin primer synthesis. (D) Primer extension by pol-prim is likely coupled with RPA and Tag dissociation, and followed by the RFC- and PCNA-mediated switch to DNA polymerase δ (not shown) [58].

In the well characterized prokaryotic *E.coli* primosome, the interaction between the DnaB helicase and the DnaG primase coordinates DNA unwinding and primosome activity at a replication fork (Figure 1.1 A) [116]. The conservation of helicase-primase coordination among

prokaryotic replication systems suggests that the functional importance of Tag association with pol-prim should be investigated. The Tag hexamer interacts with the pol-prim heterotetramer with nanomolar affinity and in a 1:1 stoichiometry [117]. At least three subunits of pol-prim make physical contacts with Tag [110-112, 118], but the functional role of these physical contacts in SV40 primosome activity remains elusive [3]. Elucidating the functional roles of these physical contacts has been a longtime goal of our lab.

When I started my dissertation project, the p68 subunit of pol-prim had been shown to be required for SV40 viral primosome activity and to bind directly to Tag [84, 110]. Thus, I aimed to explore a functional link between p68-Tag interaction and SV40 primosome activity through a combination of structural and functional approaches in collaboration with the Chazin lab. Yeast two-hybrid and pull-down assays were used to identify the minimal interaction regions of Tag and p68. NMR spectroscopy was used by the Chazin lab to determine the solution structure of the p68 minimal interacting domain and to map the interaction surface on p68. Structure-guided mutagenesis was used to confirm and pinpoint mutual interaction sites of the two proteins. The identified mutant proteins that were deficient in binding with each other were then generated for use in functional assays. Two different functional assays, the SV40 monopolymerase assay and the primosome assay, were used to test primosome activity of mutant proteins at the origin of SV40 replication and on the lagging strand, respectively. Studies in this dissertation offer deeper understanding of the SV40 primosome operation and provide significant insight into the complexity of eukaryotic DNA replication initiation.

CHAPTER II*

STRUCTURE OF A DNA POLYMERASE α-PRIMASE DOMAIN THAT DOCKS ON THE SV40 HELICASE AND ACTIVATES THE VIRAL PRIMOSOME

Introduction

De novo DNA replication begins with RNA primer synthesis on a DNA template, followed by primer extension and processive DNA synthesis. In prokaryotes, a primosome couples activity of primase with parental DNA unwinding by a hexameric helicase and a single-stranded DNA (ssDNA)-binding protein, largely through dynamic physical associations among the three proteins [3, 119]. In eukaryotes, the core of the primosome is the DNA polymerase α-primase complex (pol-prim), which catalyzes both RNA primer synthesis and extension into RNA-DNA primers [43]. Pol-prim initiates synthesis of both leading and lagging strands at eukaryotic replication origins and is required during elongation to initiate synthesis of each Okazaki fragment on the lagging strand. Pol-prim also plays a vital role in telomere maintenance and intra-S phase checkpoint activity. However, the mechanisms that regulate recruitment and activity of pol-prim in these various settings remain poorly understood.

Pol-prim is a complex of four subunits. Its primase subunits (p48 and p58) initially synthesize an 8-12-nucleotide RNA primer, which is then shifted internally to the active site of the associated p180 DNA polymerase subunit for extension into a 30-35-nucleotide RNA-DNA

* The work of this chapter was published in Huang, H[1]., Weiner, B.E.[1], Zhang, H., Fuller, B,E., Gao, Y., Wile, B.M., Zhao, K., Arnett, D.R., Chazin, W.J., Fanning, E. J Biol Chem. 2010 May 28;285(22):17112-22.
[1] These authors contributed equally to this work.

primer [120, 121]. The fourth subunit of the pol-prim complex, known as p68 or B-subunit, lacks enzyme activity but is essential for S phase entry in yeast [81] and for p180 accumulation and nuclear import [77, 78, 82, 110]. The sequence and structure of the C-terminal domain (CTD) of p68 are conserved in the B-subunits of DNA polymerases δ and ε; the p68CTD is tightly associated with the CTD of the p180 subunit [85, 122, 123] (Fig. 2.1A). In contrast, the N-terminal region of p68 shows little amino acid sequence conservation even with the corresponding pol α-subunits of lower eukaryotes, leading to assumptions that it may be disordered. The N-terminal region of p68 contains a cluster of sites phosphorylated by cyclin-dependent kinase at the G1/S transition (Fig. 2.1A) whose precise role in chromosomal replication has not been established [80, 83, 124]. Indeed, whether the N terminus of p68 is needed for chromosomal replication or cell viability remains questionable [78, 81].

Pol-prim is essential for replication of SV40 DNA in a complete cell-free reaction reconstituted with purified human proteins [5, 6, 37]. Detailed analysis of pol-prim in SV40 DNA replication demonstrated that it primes both leading and lagging strand synthesis [27, 125, 126]. The availability of recombinant human replication proteins and their structures now provides an opportunity to utilize this system to deepen our understanding of the molecular mechanisms underpinning the progression of replication. We have adopted the SV40 model system here to explore the molecular basis for initiation of replication, focusing on the transitions from duplex origin DNA unwinding to priming of the DNA template. As in prokaryotes, transient physical interactions among the helicase, ssDNA-binding protein, and pol-prim enable the SV40 primosome to couple DNA unwinding by the hexameric SV40 T antigen (Tag) helicase to

RNA-DNA primer synthesis. Recently, the interacting surfaces of Tag and RPA were mapped in atomic level detail and shown to orchestrate the assembly and disassembly of RPA-ssDNA complexes in subsequent steps of the initiation process [58, 59, 98]. Moreover, at least three subunits of pol-prim make physical contact with Tag, and these interactions have been implicated in SV40 primosome operation [110, 111, 113]. In the presence of ATP or ATPγS, the Tag hexamer interacts with the pol-prim heterotetramer with nanomolar affinity (*Kd*=~12 nM) [112, 117]. However, definitive evidence for a role of direct pol-prim/Tag contacts in SV40 primosome activity and elucidation of how such contacts might control priming remain elusive.

To develop a better understanding of the role of p68 in the SV40 primosome, we have systematically investigated p68 interaction with Tag using a combination of structural and functional approaches. A78-residue globular domain at the p68 N terminus (p68N) was identified and shown to be sufficient to bind the Tag helicase AAA+ domain (TagHD). Removal of p68N from the pol-prim complex does not diminish its polymerase or primase activity but nearly abolishes its ability to support initiation of replication from the SV40 origin and to cooperate with Tag to synthesize primers and extend them on RPA-coated template. To gain further insight into p68-Tag interactions, the structure of p68N was determined by solution NMR spectroscopy. A putative Tag-interacting surface of p68N was identified by NMR and confirmed by structure-guided p68N mutations that showed a reduced ability to interact with Tag. The corresponding mutations incorporated into pol-prim resulted in reductions in primosome activity in two different assays. Our data suggest a refined model for SV40 replication initiation, with potential roles for p68N in facilitating pol-prim recruitment, correctly positioning pol-prim to

bind and prime the template, and enhancing RNA primer extension into an RNA-DNA primer.

Materials and Methods

Yeast Two-hybrid Assay

Coding sequences of p68 fragments were amplified by PCR and ligated into the NdeI/BamHI sites of pGBKT7 vector containing a *LEU2* selection marker. Coding sequences of Tag fragments were amplified by PCR and ligated into the EcoRI/BamHI sites of pGADT7 vector containing a *TRP1* selection marker (Clontech). All of the coding sequences were verified by DNA sequencing. These plasmids were co-transformed into yeast strain AH109, which contains three reporter genes *HIS3*, *ADE2*, and *LacZ*. The cells were allowed to grow for 4 days on -Leu-Trp plates. Positive colonies were picked and streaked on a -Leu-Trp plate and on a -Leu -Trp -His -Ade plate. The plates were photographed after growth for another 4 days.

Protein Expression and Purification

Pol-prim was expressed in Hi-5 insect cells infected with four recombinant baculoviruses and purified by immunoaffinity chromatography as described previously. The pol-prim mutants were purified using the same protocol except that the WT p68 baculovirus was replaced by p68Δ1-78, p68Δ1-107, or I14A baculovirus during infection. SV40 Tag and topoisomerase I were expressed in insect cells using recombinant baculoviruses and purified as described [58]. Recombinant human RPA was expressed in *Escherichia coli* and purified as described [58].

p68(1-107) fragment and the corresponding mutants I14A, I14V, F15A, and F15V were amplified by PCR and ligated into the BamHI/NotI sites of a modified pET-32a plasmid. Coding sequences of Tag fragments 303-627 and 357-627 were PCR amplified, cloned into the BamHI/EcoRI sites of the pGEX-2T expression vector (GE Healthcare), and verified by DNA sequencing. The proteins were expressed in *E. coli* BL21 (DE3) cells and purified using nickel-nitrilotriacetic acid affinity chromatography or glutathione-agarose affinity chromatography.

GST-Tag 303-627 was purified as previously described [127]. p68 constructs were inserted into the in-house pBG100 vector (L. Mizoue, Center for Structural Biology, Vanderbilt University), which contains an N-terminal His_6 tag. p68N I14A was generated using PCR site-directed mutagenesis and confirmed by DNA sequencing. The constructs were expressed in LB medium for unlabeled samples and M9 minimal medium containing $^{15}NH_4Cl$ and/or [^{13}C] glucose for labeled samples. The cells were lysed and purified by nickel-nitrilotriacetic acid chromatography in buffer containing 50mM Tris-HCl (pH 8.0), 300 mM NaCl, and 20 mM imidazole. The proteins were then further purified by size exclusion chromatography using an S75 column and buffer containing 20 mM sodium phosphate (pH 6.5) and 50 mM NaCl. The NMR samples were then concentrated to ~0.75 mM in the same buffer.

Tag Pull-down Assays

Purified Tag was bound to monoclonal antibody Pab101-coupled Sepharose beads, or GST-tagged Tag fragments (10 μg) were bound to glutathione-agarose beads. The protein-bound

beads were then incubated with His-tagged p68 or p68 mutant proteins (5 μg or as stated in the figure legend) in binding buffer (30 mM HEPES-KOH, pH 7.8, 10mM KCl, 7mM $MgCl_2$) containing 2% nonfat dry milk for 1 h at 4 °C with end-over-end rotation. The beads were washed once with binding buffer, three times with wash buffer (30 mM HEPES-KOH, pH 7.8, 75 mM KCl, 7 mM $MgCl_2$, 0.25% inositol, 0.1% Nonidet P-40), and once with binding buffer. The beads were resuspended in 30μl of 2X SDS-PAGE loading buffer and heated at 100 °C for 5 min. The samples were analyzed by SDS-PAGE and visualized by immunoblotting with monoclonal Pab101 for Tag, monoclonal 2CT25 for pol-prim p180 subunit, rabbit anti-GST (Invitrogen) for Tag fusion proteins, anti-His (9801; Abcam) for His-tagged proteins, and chemiluminescence (GE Healthcare).

DNA Polymerase Assay

The polymerase activities of the WT and mutant pol-prim were assayed on a randomly primed poly (dA)-oligo(dT) template (20:1) as described previously [84]. Specific activity was typically 50 pmol of dTMP/pmol of pol-prim/min.

DNA Primase Assay

The primase activities of the WT and p68 Δ1-107 pol-prim were assayed on single-stranded M13 DNA as described previously [91].

Initiation of SV40 DNA Replication

Monopolymerase assays were carried out as described previously [58]. Briefly, reaction mixtures (20 µl) contained 250 ng of supercoiled pUC-HS plasmid DNA, 200 ng of RPA, 300 ng of topoisomerase I, indicated amounts of Tag and recombinant pol-prim in initiation buffer (30 mM HEPES-KOH, pH 7.9, 7 mM magnesium acetate, 10 µM $ZnCl_2$, 1 mM DTT, 4 mM ATP, 0.2 mM each GTP, UTP and CTP, 0.1 mM each dGTP, dATP, and dTTP, 0.02 mM dCTP, 40 mM creatine phosphate, 40 ug/ml of creatine kinase) supplemented with 3 µCi of [γ-^{32}P]dCTP (3000 Ci/mmol). Reaction mixtures were assembled on ice, incubated at 37 °C for 90 min, and then digested with 0.1 mg of proteinase K/ml in the presence of 1% SDS and 1 mM EDTA at 37 °C for 30 min. Radiolabeled reaction products were purified on G-50 Sephadex columns and precipitated with 2% $NaClO_4$ in acetone. The products were washed, dried, resuspended in alkaline loading buffer (60 mM NaOH, 2 mM EDTA [pH 8.0], 20% [w/v] Ficoll, 0.1% [w/v] bromophenol blue, 0.1% [w/v] xylene cyanol) and electrophoresed on 1.5% agarose gels in running buffer (30 mM NaOH, 1 mM EDTA). The gels were fixed in 10% TCA and dried. The reaction products were visualized by autoradiography and quantified by densitometry or phosphorimaging.

Primer Synthesis and Elongation in the Presence of RPA

Reaction mixtures (20 µl) containing 100 ng of single-stranded M13 DNA were preincubated with 600-1000 ng of RPA, as stated in the figure legends, in initiation buffer [58] at 4 °C for 20 min. The reactions were then supplemented with 3 µCi of [γ-32P]dCTP, 400-600 ng of Tag (or as

indicated), and increasing amounts of WT or mutant pol-prim as indicated; incubated at 37 °C for 45 min; and then digested with 0.1 mg of proteinase K/ml in the presence of 1% SDS and 1mM EDTA at 37 °C for 30 min. Radiolabeled reaction products were then processed and analyzed as described above for the monopolymerase assay.

Isothermal Titration Calorimetry

p68N constructs and Tag 303-627 were buffer exchanged into 25mM Tris-HCl (pH 8.0), 150 mM NaCl, 1 mM EDTA, and either 1 mM dithiothreitol (for NMR) or 5mM β-mercaptoethanol. For these experiments, 400 μM p68N was titrated into 20 μM Tag 303-627 at 25 °C.

NMR Spectroscopy

Structure determination for p68N and analysis of Tag binding were performed using previously published protocols [128]. All of the NMR experiments were carried out at 25 °C on Bruker Avance 500, 600, or 800 MHz spectrometers equipped with a cryoprobe. Backbone resonance assignments were completed using ^{13}C, ^{15}N-labeled p68N in traditional heteronuclear experiments. Side chain resonance assignments were completed using homonuclear COSY and (H)CC(CO)NH and H(CC)(CO)NH total correlation spectroscopy spectra. ^{1}H-^{1}H distance restraints were generated using two-dimensional homonuclear NOESY, three-dimensional ^{15}N-edited NOESY, three-dimensional ^{13}C-edited NOESY, and four-dimensional ^{13}C, ^{13}C-edited NOESY spectra. Dihedral angle restraints were generated using TALOS [129]. NOESY spectra were assigned using CYANA [130] supplemented with manual assignments. CYANA was also

used to generate initial structures using torsion angle dynamics. These structures were then refined using restrained molecular dynamics in AMBER [131]. A summary of structural statistics is listed in Table 2.1. For the differential line broadening NMR experiment, ^{15}N-^{1}H HSQC spectra of 100 μM p68N were recorded before and after the addition of 10 μM unlabeled Tag 303-627.

Results

Identification of a Tag-binding Domain at the N Terminus of p68

To gain more insight into the potential functions of p68 in the SV40 replication model, we sought to determine a minimal Tag-binding fragment of p68 in pull-down assays. A purified p68 fragment containing residues 1-107 co-immunoprecipitated with full-length Tag, whereas a large C-terminal p68 fragment lacking residues 1-107 (p68 (108-598)) did not (Fig 2.1, A and B). Additional fragments of p68 and Tag were screened using yeast two-hybrid and pull-down assays. In screening various fragments, all of the constructs encompassing p68 residues 1-107 and the helicase AAA+ domain (residues 357-627, TagHD) were found to interact (Fig 2.1C).

We next asked whether the p68 (1-107) Tag-binding fragment might constitute a structured domain. However, this protein was found to readily degrade into smaller but stable fragments under the conditions used for NMR spectroscopy. Analysis by two-dimensional 15N-1H HSQC NMR revealed that p68 (1-107) and the smaller fragments contained a well folded globular domain, because each spectrum contained a characteristic set of well dispersed signals (Fig. 2.1D, left panel). The fragments were isolated on SDS gels and mass spectrometry analysis showed that

they were formed through loss of residues from the C terminus (not shown). These observations were supported by computational analysis of the 1-107 sequence, which predicted the presence of four N-terminal helices followed by a disordered region of ~30 residues. To confirm this hypothesis, an additional p68 N-terminal construct, p68 (1-78), was designed based on secondary structural analysis, and an expression vector was generated. The NMR spectrum of the purified protein contained all of the dispersed signals observed in the spectrum of p68 (1-107) (Fig. 2.1D, right panel). Moreover, the protein was stable for extended periods of time. Tests of the ability of the p68 (1-78) construct to bind TagHD revealed that it is as effective as p68 (1-107) (Fig. 2.1C). These results show that the Tag binding site on p68 resides in the p68 (1-78) domain, which is termed p68N.

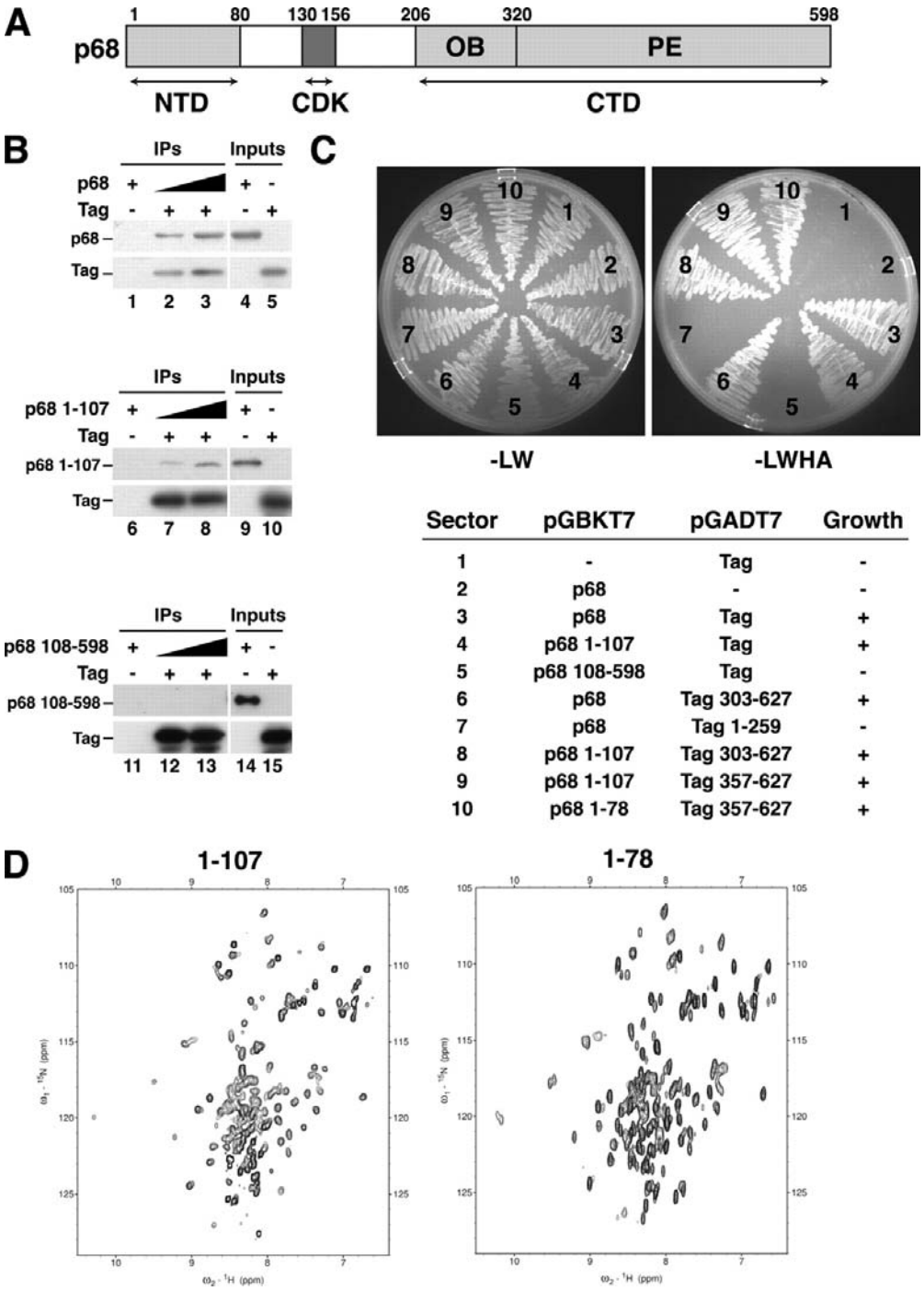

Sector	pGBKT7	pGADT7	Growth
1	-	Tag	-
2	p68	-	-
3	p68	Tag	+
4	p68 1-107	Tag	+
5	p68 108-598	Tag	-
6	p68	Tag 303-627	+
7	p68	Tag 1-259	-
8	p68 1-107	Tag 303-627	+
9	p68 1-107	Tag 357-627	+
10	p68 1-78	Tag 357-627	+

Figure 2.1. The p68 N terminus interacts directly with the Tag AAA+ domain. (A) Diagram of the p68 subunit of human pol-prim. CDK, cluster of sites phosphorylated by cyclin A-dependent kinase; CTD, C-terminal domain composed of an oligonucleotide-oligosaccharide binding (OB) subdomain and a phosphoesterase (PE) subdomain. (B) Purified His-tagged full-length p68 (lanes 1-5), p68(1-107) (lanes 6-10), and p68(108-598) (lanes 11-15) were incubated with anti-Tag beads in the presence (+) or absence (-) of purified Tag.

Figure 2.1, continued. Bound proteins were analyzed by Western blotting with an anti-His or anti-Tag antibody as indicated. (C) Yeast two-hybrid analysis of p68 interaction with Tag. Left panel, control plate -Leu-Trp; right panel, selective plate -Leu, -Trp, -His, -Adenine. The numbered sectors are identified in the table below. (D) p68N contains the structured region of p68 1-107. 15N-1H HSQC spectra were collected for p68 1-107 (left panel) and p68 1-78 (p68N) (right panel). The disperse peaks are present in both spectra, and the peaks absent in the p68N spectrum are all found in the central region of p68 1-107. This indicates that only flexible residues were removed in truncating from 107 to 78 residues, whereas the structured region remains intact. IPs, immunoprecipitates. Data in panel D was collected by Brian E. Weiner.

p68N Forms a Globular Four-helix Bundle Domain

To further elucidate the function of p68N and the molecular basis for its interaction with Tag, the structure of p68N was determined in solution by NMR. Once solution conditions were optimized for p68N, NMR resonance assignments were made using standard double and triple resonance two- and three-dimensional experiments on protein enriched in ^{15}N and/or ^{13}C isotopes. The p68N solution structure was determined using over 1100 distance and dihedral angle restraints in iterative cycles of structure calculations. An ensemble of 20 conformers with the lowest residual violation energies from the final calculations was selected to represent the NMR solution structure (Fig. 2.2A). In the structure, residues Ala3-Glu68 are well defined, with a high precision reflected in a root mean square deviation from the mean structure of 0.60 Å for the backbone atoms and 1.00 Å for all heavy atoms. The quality of the p68N structure is reflected in structural statistics for the ensemble, including no distance violations greater than 0.2Å and no torsion angle violations greater than 5° (Table 2.1). PROCHECK-NMR analysis revealed that 99.1% of the residues contained dihedral angles in the allowed regions of the Ramachandran plot. The solution structure of p68N reveals a compact, anti-parallel four-helical bundle with short

loops between the helical elements (Fig. 2.2B). The helices include residues (I) Ala5-Phe15, (II) Glu21-Tyr34, (III) Glu38-Thr52, and (IV) Ser59-Glu68. A search using the Dali server with the coordinates of the representative p68N conformer returned the closest fit to the structure of RuvB (similarity score, 8.3). Many of the best fits were AAA+ proteins like RuvB. Although not the lowest score, the Dali server also indicated similarity to the N-terminal domain of the pol ε B subunit (Dpoe2NT) [132]. A structure-based alignment between the two N-terminal domains produces a root mean square deviation of 2.4 Å (Fig. 2.2C). Moreover, a Dali search using the Dpoe2NT domain returned the same structures as p68N [132]. Despite the similarity in their architecture, amino acid sequence alignment of p68N and Dpoe2NT reveals little sequence similarity, and the chemical nature of their surfaces diverges considerably (Fig. 2.2D). The p68N structure is characterized by a largely acidic surface with a few small hydrophobic patches, whereas the pol ε domain displays an electrostatic surface with both basic and acidic charge and no significant hydrophobic patches. As will be discussed in more detail below, the surface characteristics of p68N play an important role in mediating interactions with SV40 Tag. The differences in the surfaces of the p68N and Dpoe2NT domains presumably give rise to their functional specificity.

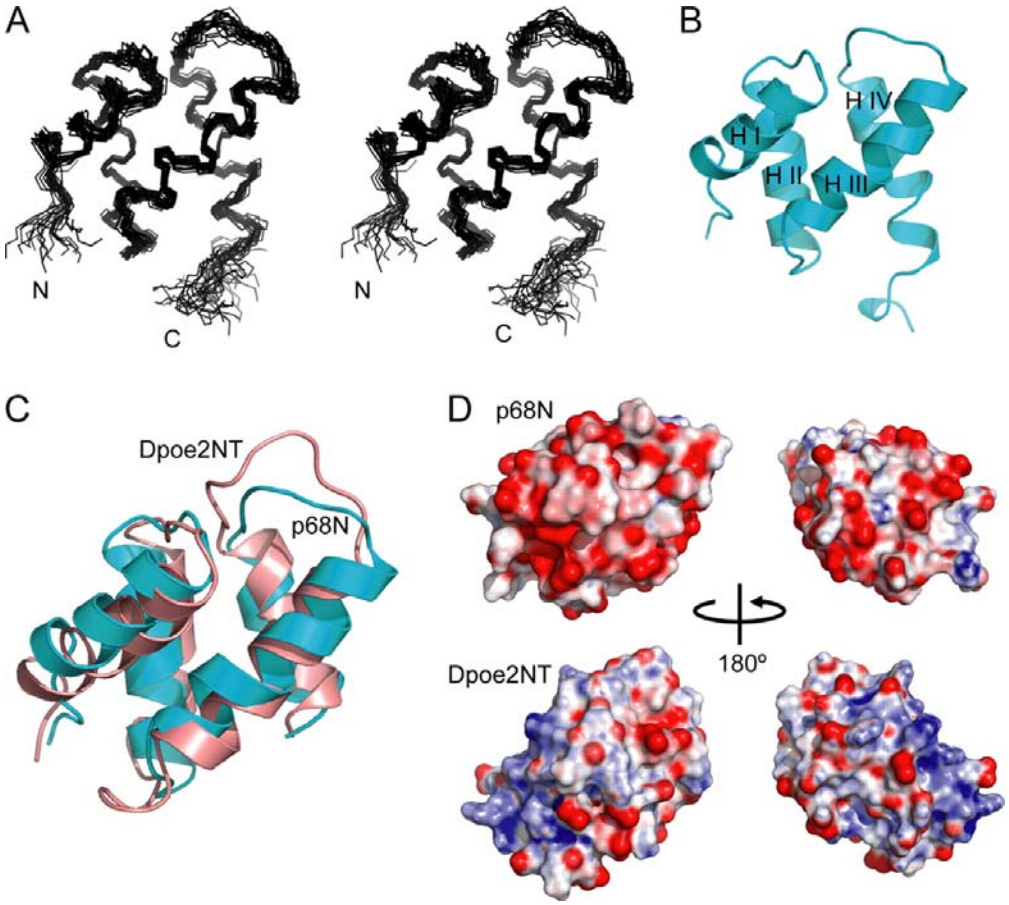

Figure 2.2. p68N adopts a compact, helical fold. (A) Stereo view of the backbone heavy atom trace of the 20 p68N structures with the lowest violation energies. (B) Ribbon diagram of the structure closest to the mean. (C) Structural alignment of p68N (cyan) with residues 1-75 of the pol ε B-subunit, Dpoe2NT (salmon) (Protein Data Bank code 2v6z). (D) Electrostatic surface potential of p68N (top panel) and Dpoe2NT (bottom panel) with red representing negative charge and blue representing positive charge. The orientation on the left is the same as shown in A-C. Data were collected by Brian E. Weiner.

Table 2.1. Structural statistics for p68N. Data were collected by Brian E. Weiner.

p68N Structural Statistics	
Total restraints	1109
NOE restraints	987
Short range	533
Medium range	233
Long range	221
Dihedral angle restraints	122
Restraint violations (mean ± s.d.)	
Distance restraints ≥0.2 Å	0
Dihedral angle restraint violations ≥5º	0
Maximum distance restraint violation	0.13 ± 0.02
Maximum dihedral restraint violation	3.6 ± 0.7
AMBER energies (kcal/mol)	
Restraint energy	3.4 ± 0.4
Total energy	-1314 ± 23
Ramachandran statistics (%)	
Most favored	88
Additionally allowed	10
Generously allowed	2
Disallowed	0
RMSD from mean structure (Å)[1]	
Backbone atoms	0.53
Heavy atoms	1.02
Backbone atoms in helices	0.41
Heavy atoms in helices	0.90

[1]Residues used for RMSD calculations include A3-L74.

Initiation of SV40 DNA Replication and Primosome Activity Require the p68N Terminus

We next investigated whether p68N is needed for viral DNA replication. To this end, purified recombinant pol-prim complexes containing a full-length or a truncated p68 subunit were generated and characterized by denaturing gel electrophoresis and Coomassie staining (Fig. 2.3A). Truncated p68 subunits Δ1-78 and Δ1-107 (lanes 2 and 3) were present in the complex at a stoichiometry equivalent to that of the full-length p68 (lane 1), demonstrating that both truncations retain the ability to stably associate with the p180 polymerase subunit. The polymerase specific activity of the Δ1-107 and WT complexes was identical; the primase specific activity of the Δ1-107 complex was about 2-fold greater than that of the WT (supplemental Fig. S1, A and B). Moreover, truncation of p68 did not compromise the ability of the p180 and primase subunits in the complex to interact with Tag (supplemental Fig. S1C). Two different assays reconstituted with purified proteins were then used to compare the abilities of WT and Δ1-107 pol-prim to initiate SV40 DNA replication. The first assay, a monopolymerase reaction, measured primer synthesis coupled with unwinding of supercoiled DNA containing the SV40 origin [125]. Although accumulation of newly synthesized RNA primers is detectable in this assay in the absence of deoxyribonucleotides, primer-dependent extension into RNA-DNA primers in the presence of radiolabeled dCTP amplifies the signal and is hence a more sensitive measure of primer synthesis [125]. In the monopolymerase reaction performed with WT pol-prim, replication products increased in proportion to the amount of pol-prim in the reaction (Fig. 2.3B, lanes 1-4), and no products were observed in control reactions lacking Tag or pol-prim (lanes 9 and 10). In contrast, little replication was detected with Δ1-107 pol-prim (lanes 5-8).

Quantification of the reaction products revealed that the initiation activity of mutant pol-prim was reduced at least 10-fold (Fig. 2.3B, bottom panel). Similarly, little activity of Δ1-78 pol-prim in initiation of SV40 replication was observed (supplemental Fig. S1D). The results demonstrate a key role for the p68 N terminus in the initiation of replication at the SV40 origin.

In the second assay, natural single-stranded DNA (M13) pre-coated with purified human RPA was used to measure primer synthesis uncoupled from duplex DNA unwinding [58, 133, 134]. On this template, purified pol-prim alone does not efficiently generate RNA primers and extend them into radiolabeled RNA-DNA primers. However, the addition of Tag can overcome the inhibition of priming by RPA to permit priming. If p68N-Tag interactions are required for pol-prim activity on RPA-coated template DNA, the activity of Δ1-107 pol-prim should also be compromised in this second assay.

On naked ssDNA template, the ability of mutant and WT pol-prim to synthesize RNA primers and extend them into labeled RNA-DNA primers was comparable (Fig. 2.3C, lanes 5 and 10), consistent with the similar primase and polymerase enzymatic activity of the two pol-prim complexes. Also as expected, preincubation of the template DNA with saturating amounts of RPA inhibited the activity of all pol-prim complexes (Fig. 2.3C, lanes 4 and 9). In the presence of Tag, WT pol-prim overcame this RPA inhibition, generating RNA primers and extending them into radiolabeled RNA-DNA products as a function of the amount of pol-prim added (Fig. 2.3C, lanes 1-3). In contrast, in reactions containing Δ1-107 pol-prim and Tag, radiolabeled products did not increase beyond the level observed in reactions without Tag (Fig. 2.3C, lanes 6-8). Quantification of the reaction products confirmed that truncation of the p68 N terminus nearly

abolished primosome activity (Fig. 2.3C, bottom panel). The results indicate that the N-terminal region of p68 is vital for SV40 primosome activity.

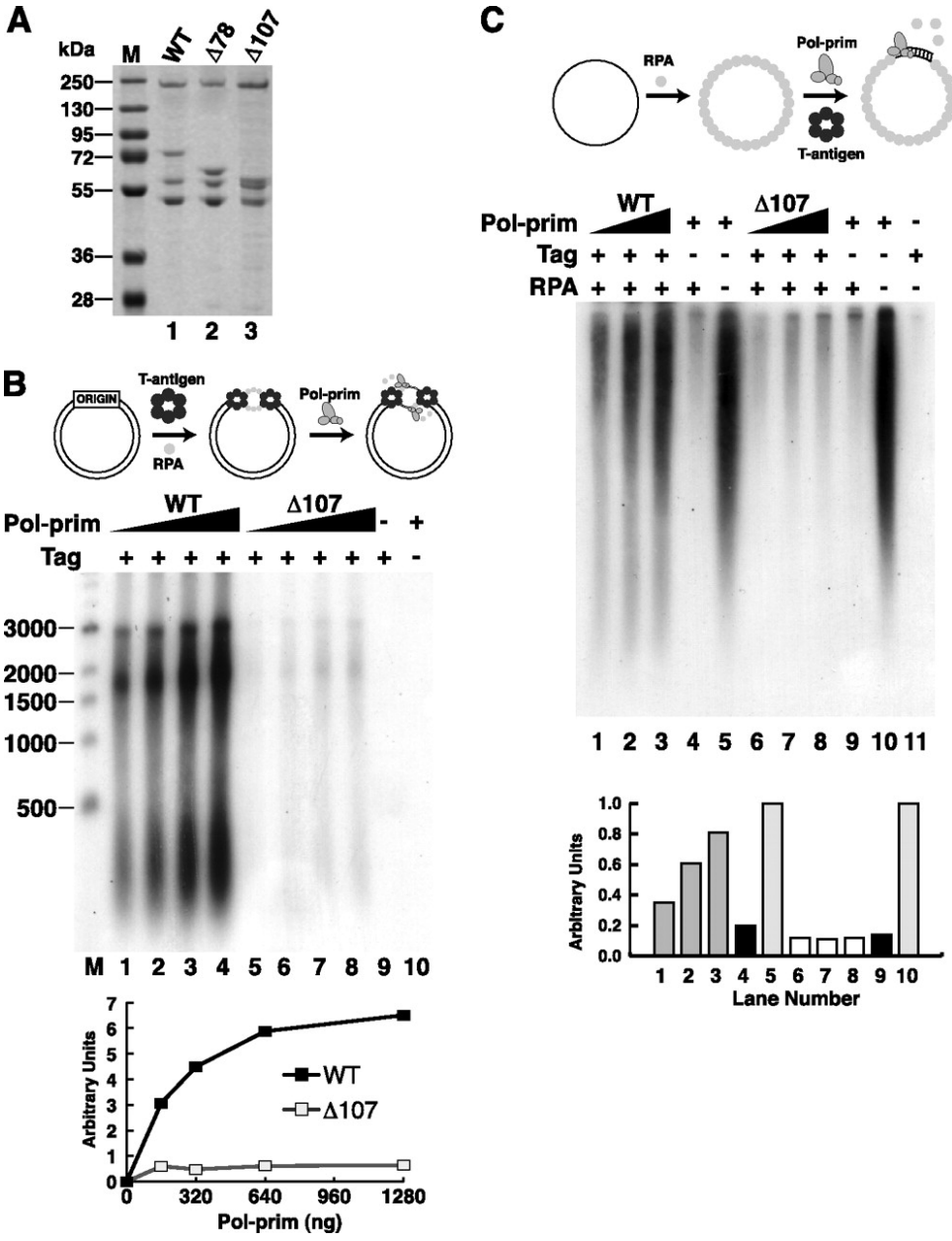

Figure 2.3. Loss of the p68 N terminus abolishes initiation of SV40 DNA replication and primosome activity. (A) Purified WT, Δ1-107, and Δ1-78 pol-prim were separated by SDS-PAGE and Coomassie-stained.M, protein size markers.

Figure 2.3, continued. (B) Initiation of SV40 replication was assayed in monopolymerase reactions containing increasing amounts of WT (lanes 1-4) or Δ1-107 (lanes 5-8) pol-prim. Control reactions lacked pol-prim (lane 9) or Tag (lane 10). The reaction products were resolved by alkaline electrophoresis, visualized by autoradiography, and quantified (lower panel). DNA size markers are indicated (M). (C) Primosome activity of 160, 320, or 640 ng of WT (lanes 1-3) or Δ1-107 pol-prim (lanes 6-8) on ssDNA precoated with RPA was stimulated by Tag. Control reactions lacked Tag (lanes 4 and 9) or both Tag and RPA (lanes 5 and 10). The reaction products were separated by alkaline electrophoresis, visualized by autoradiography, and quantified (lower panel).

The Tag-interacting Surface of p68N

To establish a means to determine the functional role of p68N in the SV40 primosome, we set out to measure the affinity of p68N interaction with Tag and map the p68N surface that interacts with Tag. The technique of isothermal titration calorimetry was used to obtain accurate binding parameters. Fitting of the binding isotherm for the titration of p68N into a solution of a monomeric Tag 303-627 construct [127] provided a dissociation constant of 6 ±1 μM (Fig. 2.4A). An affinity in the micromolar range is consistent with the proposed role for p68N in mediating the interaction between pol-prim and Tag as part of the dynamic assembly/disassembly of proteins in the primosome.

NMR spectroscopy was then applied to identify p68N residues in the binding interface with Tag 303-627. Titration of a stoichiometric amount of unlabeled Tag 303-627 into a solution of ^{15}N-enriched p68N provided a ^{15}N-^{1}H HSQC spectrum in which the resonances were severely broadened. The loss of signals precludes the use of the powerful NMR chemical shift perturbation approach for analysis of binding surface. However, in these situations an alternative approach can be applied based on detection of differential reduction in signal intensity for residues in the

binding interface at substoichiometric ratios [135]. Fig. 2.4B shows the normalized intensities of the NMR signals for the Tag 303-627-p68N complex at a ratio of 0.1:1. When the residues whose intensities are most significantly reduced are mapped onto the p68N structure, they identify a putative Tag-binding surface (Fig. 2.4C). This surface maps to a hydrophobic patch surrounded by negative charge.

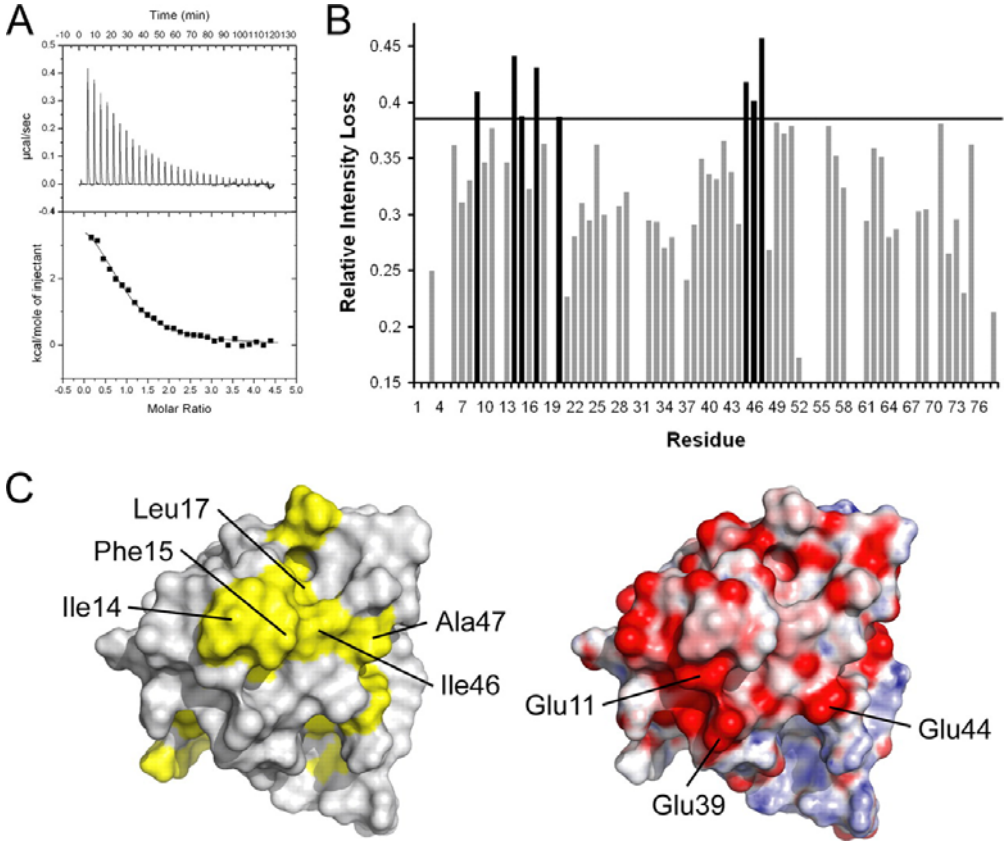

Figure 2.4. p68N interacts with Tag 303-627. (A) Isothermal titration calorimetry titration of p68N into Tag 303-627. The data were fit to a single-site binding model, which provided a Kd of 6±1 µM. (B) NMR differential line broadening assay. Unlabeled Tag 303-627 was added to 15N-labeled p68N. The relative peak intensity after addition was plotted versus residue number to identify selectively broadened residues. The dashed line indicates the mean plus one standard deviation. (C) The selectively broadened residues map to a hydrophobic patch (yellow) surrounded by negative charge (red). This surface represents a potential binding site for Tag. Data were collected by Brian E. Weiner.

The residues in this putative Tag-binding surface are ideal candidates for site-directed mutagenesis experiments to probe the functional role of p68N in the primosome. Toward this end, a series of site-directed substitution mutations in p68N was designed, and yeast two-hybrid assays were performed to screen for their effects on Tag binding. The WT p68N interacted effectively with TagHD, as evidenced by growth in the absence of histidine and adenine, whereas no growth was observed with the empty vector (sectors 1-3) (Fig. 2.5A). In contrast, substitution of p68N Ile^{14} by Ala or Glu (sector 4, not shown) or of Phe^{15} by Arg (not shown) abolished interaction with Tag. Interestingly, the F15A mutation reduced binding to TagHD under physiological conditions, whereas the F15Y substitution still interacted with TagHD (sectors 6, 7). Additional amino acid substitutions at Glu^{11}, Glu^{39}, or Glu^{44} of p68N abolished interaction with TagHD, whereas substitutions at several other residues in p68N had little effect (Fig. 2.5B). Pull-down assays performed at low ionic strength confirmed that Ile^{14} substitution by Ala or Val and Phe^{15} substitution by Ala or Tyr weakened the interaction of p68(1-107) with TagHD (Fig. 2.5C, lanes 3-6). The p68N I14A substitution displayed a similarly reduced interaction with TagHD, compared with that of WT p68N, at KCl concentrations ranging from 10 to 150 mM.

A reduction in mutant p68N interaction with TagHD can arise from the desired perturbation of the interaction surface with TagHD or through perturbation of the structure or loss of structural stability. Therefore, before proceeding to functional analysis, it was imperative to confirm that the effects of amino acid substitutions on the structure of p68N are minimal. To this end, we prepared four ^{15}N-enriched mutant proteins (E11K, E39K, E44K, and I14A) and assayed their structures by ^{15}N-^{1}H HSQC NMR. Indeed, comparisons with the WT p68N revealed that the three Glu to Lys

substitutions led to small but widespread effects on the NMR spectrum, indicating possible structural perturbations (not shown). However, the I14A substitution had much smaller effects on the p68N spectrum (Fig. 2.5D), providing confidence that its structure was not significantly perturbed. To verify the success of the mutant design, the effect of the I14A mutation on Tag interaction was investigated by isothermal titration calorimetry. In contrast to the WT protein, p68N (I14A) showed no detectable heat of reaction upon addition to Tag 303-627 (data not shown). These results led us to select the I14A mutation for subsequent functional analyses.

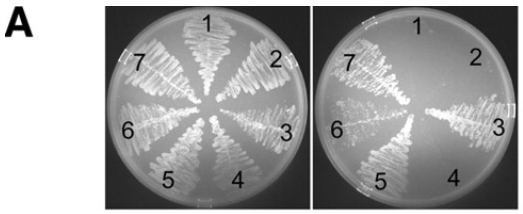

Sector	pGBKT7	pGADT7	Growth
1	-	Tag HD	-
2	p68 1-107	-	-
3	p68 1-107	Tag HD	+
4	p68 1-107 I14A	Tag HD	-
5	p68 1-107 I14V	Tag HD	+
6	p68 1-107 F15A	Tag HD	-
7	p68 1-107 F15Y	Tag HD	+

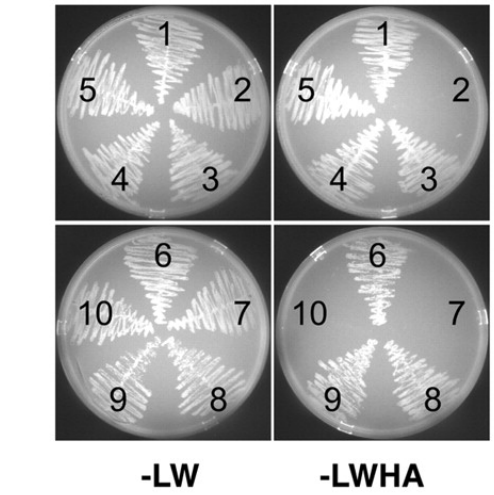

Sector	pGBKT7	pGADT7	Growth
1	p68 1-107	Tag HD	+
2	p68 1-107 E44K	Tag HD	-
3	p68 1-107 S50A	Tag HD	+
4	p68 1-107 T51A	Tag HD	+
5	p68 1-107 H53A	Tag HD	+
6	p68 1-107	Tag HD	+
7	p68 1-107 E11K	Tag HD	-
8	p68 1-107 D18K	Tag HD	+
9	p68 1-107 A47D	Tag HD	+
10	p68 1-107 E39K	Tag HD	-

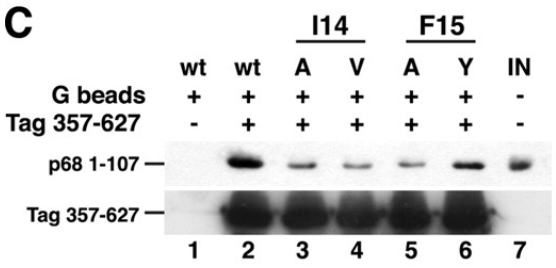

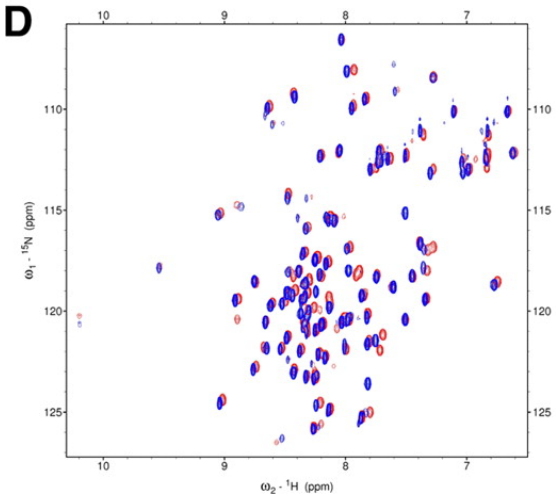

Figure 2.5. Structure-guided mutational analysis of the Tag-binding surface of p68N. (A) and (B), single residue substitutions in p68 (1-107) were screened in yeast two-hybrid assays for interaction with GST-TagHD. Left panel, control plate; right panel, growth on the selective plate indicates interaction. The numbered sectors are identified in the tables below. (C) Glutathione (G) beads were incubated with 10 µg of WT His-tagged p68 (1-107) or mutants I14A, I14V, F15A, and F15Y as indicated in the presence (+) or absence (-) of GST-TagHD (lanes 1-6). Proteins bound to the beads were detected by Western blotting with anti-His or anti-GST antibody.

Figure 2.5, continued. Lane 7, input (IN) p68 (1-107) (200 ng). (D) The p68N I14A domain maintains the WT fold. 15N-1H HSQC spectra were collected for WT (red) and I14A (blue) p68N. The spectra overlay very well, indicating that no major structural perturbation was induced by the I14A mutation. Data in panel D was collected by Brian E. Weiner.

The Tag-interacting Surface of p68 Is Vital for Primosome Activity

If p68-Tag interaction is vital for SV40 DNA replication, the weakened interaction of I14A p68 with Tag would be expected to diminish replication but not abolish it. To test this prediction, a pol-prim with the I14A substitution in p68 was constructed, purified, and characterized (Fig. 2.6A). As expected, the substitution had little effect on the specific activity of pol-prim in polymerase or primase enzyme assays (not shown). However, the single-residue substitution did reduce initiation of SV40 DNA replication in the monopolymerase assay to less than half that of WT pol-prim (Fig. 2.6B). A corresponding decrease in the primosome activity of I14A pol-prim on RPA-ssDNA was observed (Fig. 2.6C). These results provide strong evidence for a crucial role of p68N-Tag interaction in initiation of SV40 replication, specifically in the primosome activity.

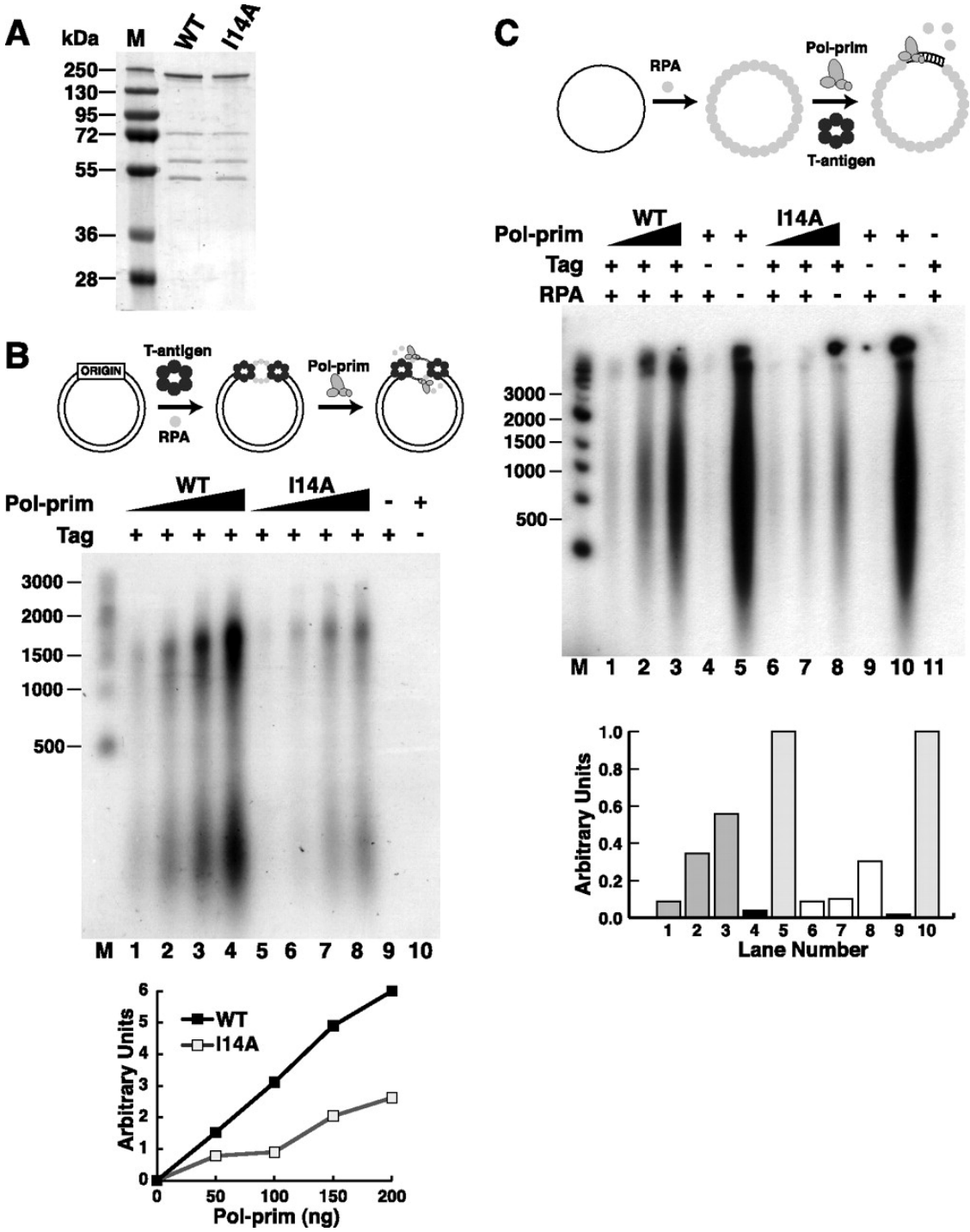

Figure 2.6. A single residue substitution in the Tag-interacting surface of p68N diminishes SV40 primosome activity. (A) Purified pol-prim containing p68 WT or substitution I14A were separated by SDS-PAGE and stained with Coomassie. (B) SV40 initiation was assayed in monopolymerase reactions containing increasing amounts of WT (lanes 1-4) or I14A pol-prim (lanes 5-8) and analyzed by alkaline electrophoresis and autoradiography.

Figure 2.6, continued. DNA size markers are shown (M). Reaction products were quantified; background (lanes 9 and 10) was subtracted from incorporation in lanes 1-8 (lower panel). (C) Primosome activity of 200, 400, or 600 ng of WT (lanes 1-3) or I14A pol-prim (lanes 6-8) was assayed in the presence of 600 ng of Tag on ssDNA precoated with 1 μg RPA. Control reactions lacked Tag (lanes 4 and 9), both Tag and RPA (lanes 5 and 10), or pol-prim (lane 11). The reaction products were analyzed by alkaline electrophoresis and autoradiography. DNA size markers are shown (M). The reaction products were quantified; incorporation in the negative control reaction (lane 11) was subtracted from that in lanes 1-10. Incorporation in lanes 1-4 and 6-9 is graphed as a fraction of that in lanes 5 and 10, respectively.

Discussion

The Interacting Domains of p68 and Tag

Progress in understanding the initiation of eukaryotic replication is currently limited by the lack of knowledge of the structural basis for the recruitment of pol-prim and delivery of the template strand to it for priming. Here we identified a previously unrecognized N-terminal globular domain in the p68 subunit of pol-prim, showed that it binds to the helicase domain of Tag, and demonstrated the functional relevance of this interaction in initiation of replication and in primosome activity. Together, the structural and mutational evidence suggest that a hydrophobic patch on the surface of p68N, centered on Ile^{14} and surrounded by acidic residues, interacts with the AAA+ domain of Tag (Figs. 2.1, 2.2, 2.4, and 2.5). It is common for protein interactions to involve a combination of hydrophobic and electrostatic contacts, *i.e.* as proposed for the assembly of the T7 and *E. coli* replisomes [3, 119, 136]. The attraction through long range electrostatic forces presumably provides an initial guide for docking of the two domains, which is then further stabilized by hydrophobic contacts. The observation of a *Kd* value in the low

micromolar range for p68N binding to TagHD is consistent with the relatively small size of the binding surface determined by NMR. Like many DNA processing proteins, pol-prim is highly modular. Interactions among such proteins typically occur through multiple weak interactions [104], precisely of the nature observed here for p68N-TagHD.

The structure of the p68N domain is closely related to that of the NTD of pol ε Dpoe2 and subdomains of other AAA+ proteins (Fig. 2.2C), reflecting an evolutionary relationship [132]. AAA+ proteins function in multiple steps of DNA replication as origin-binding proteins, helicases, helicase loaders, and clamp loaders [137]. Interestingly, the AAA+ protein DnaC from *E. coli* is needed in conjunction with the hexameric DnaB helicase to enable primer synthesis by DnaG on ssDNA template coated by the *E. coli* SSB protein but not on naked ssDNA template [138]. Thus, docking of p68N with Tag in the SV40 primosome (Figs. 2.3 and 2.6) may play a role analogous to that of DnaC in the prokaryotic primosome [138].

The data presented here are derived from a viral model system, but it seems unlikely that the p68N domain could have been evolutionarily selected solely to enable viral primosome activity. A more likely possibility is that p68N may interact with cellular proteins to enable primer synthesis in chromosomal replication, but to our knowledge this has not been reported. The absence of significant amino acid sequence homology between p68N and Dpoe2 NTD and the distinctly different chemical nature of their surfaces suggest that they have diverged and likely interact with different cellular partner proteins. Powerful precedents for structural and functional conservation of DNA processing proteins without significant amino acid sequence homology are well known, *e.g.* proliferating cell nuclear antigen and β-clamp [139]. The structural similarity of

p68N and Dpoe2 NTD suggests that Dpoe2 NTD also serves as a docking module, directly or indirectly facilitating interaction of polymerase ε with the Mcm2-7 complex at replication origins.

Model for Recruitment of Pol-prim to Initiate Priming on RPA-coated Template DNA

In previous studies, we obtained evidence using reconstituted SV40 replication reactions that the hexameric Tag helicase interacts with two molecular surfaces of RPA [58, 59, 98]. A basic surface of the origin-binding domain (OBD) (residues 131-259) of Tag binds to an acidic surface of RPA70AB; as ssDNA is extruded from the helicase, a ternary complex of OBD-70AB-ssDNA assembles transiently. Upon extrusion of additional ssDNA, formation of the RPA-ssDNA complex leads to release of Tag-OBD for additional RPA loading, thus coupling origin unwinding to RPA-ssDNA filament formation [59]. Conversely, to facilitate priming of RPA-bound template by pol-prim, transient physical interactions between the basic surface of the OBD of one subunit of a Tag hexamer with RPA32C and the same surface of a second Tag subunit with an acidic surface of RPA70AB lead to remodeling of the ssDNA binding mode of RPA [58, 59, 98] (Fig. 2.7, top panel). The remodeled ssDNA binding mode, in which RPA occludes only 8-10 nucleotides, transiently exposes ssDNA template that can be utilized for primer synthesis (Fig. 2.7, middle panel).

This model can be extended based on the data described here, which show that physical interactions of pol-prim with TagHD enable primase recruitment to the exposed ssDNA. Each hexamer of Tag helicase associates with one pol-prim complex [117]. Previous work demonstrated the interaction of Tag with p180 and p68 and suggested their involvement in the

initiation of replication [110, 111]. Our combined structural and functional analysis of these interactions now reveals that the N-terminal domain of p68 (residues 1-78, p68N) docks on the surface of TagHD and is tethered through a long, presumably disordered linker to the conserved CTD of p68 (residues 206-598) (Fig. 2.1A). The C-terminal domain of p68, in turn, associates tightly but flexibly with the C-terminal zinc domain of p180 [85]. The zinc domain of p180 also binds to the primase heterodimer [120].

The data in Figs. 2.3 and 2.6 imply that p68N interaction with TagHD is crucial for pol-prim recruitment to RPA-ssDNA and primer synthesis. Several plausible roles for Tag-p68N interaction in primosome activity can be envisioned. In the simplest model, the weak interactions of both p68N and p180N with TagHD may be needed to form a sufficiently high affinity interaction to allow pol-prim to bind to the naked ssDNA exposed by RPA binding to Tag OBD. In the absence of p68N, the remaining interaction of TagHD with p180 may be too weak and transient to support primosome activity. Although qualitative in nature, pull-down reactions conducted under conditions similar to those in the cell-free replication assay suggest that Tag interaction with Δ1-107 and Δ1-78 pol-prim is similar to that with WT pol-prim (supplemental Fig. S1C). These observations suggest that binding of p180 and primase to Tag are independent of p68N and, in combination, are of sufficient affinity to generate a stable complex [117]. Nonetheless, the decrease in primosome activity of p68 mutant pol-prim in two different assays directly correlates with the decrease in p68NTag interaction affinity (compare Figs. 2.1 and 2.3 with Figs. 2.5 and 2.6). Taken together, these results argue that the role of p68N docking with TagHD in primosome activity is important but probably not solely to increase the affinity of

interaction.

A second potential role for independent docking sites for p68N, p180, and primase on Tag may be to position the primase subunits spatially to access the template DNA exposed through Tag-directed remodeling of the RPA ssDNA binding mode (Fig. 2.7, *middle* and *lower panels*). In this scenario, loss of the p68N contact with TagHD may result in an overly mobile TagHD/pol-prim assembly that is unable to position primase properly to bind to the exposed template or to maintain it in that position long enough to form a primer. Consistent with this possibility, the p68CTD-p180CTD interaction module observed in cryo-electron microscopy [85] displays considerable flexibility that might be constrained by docking the N termini of the two subunits at separate sites on Tag-HD. Similarly, the length of the tethers that link the p68CTD-p180CTD module with p68N and p180 residues 189-313 [111], which dock on Tag, may be important to position primase on the template.

Docking of p68N on TagHD may also be important for temporal coordination of priming with origin DNA unwinding by Tag, as well as strand separation during fork progression. Initial indications of temporally coordinated helicase-primase movement came from the observation that the rate of DNA unwinding by Tag helicase is slowed in the presence of pol-prim [112, 140]. This inhibition was observed using supercoiled SV40 origin DNA, as well as on model fork templates, and depended on pol-prim concentration. Notably,

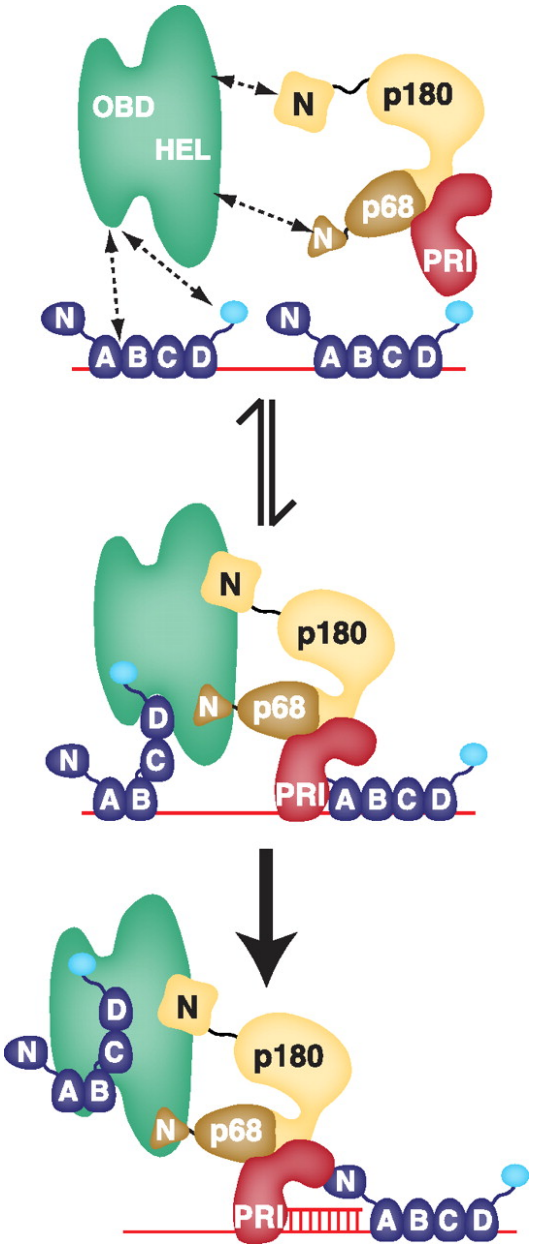

Figure 2.7. A working model for regulation of SV40 primosome activity via p68N docking with Tag. *Top panel*, the three major proteins in the SV40 primosome: Tag hexamer [62] containing the origin DNA- and RPA-binding domains (*OBD*) and helicase domains (*HEL*); RPA (*blue*) with four oligonucleotide- oligosaccharide binding fold domains *A-D* bound with 5' to 3' polarity to ssDNA (*red*) (occluding 28-30 nucleotides) and the RPA32C domain (*cyan*) tethered to oligonucleotide-oligosaccharide binding domain D; pol-prim with the p180 DNA polymerase (*orange*), p68 subunit (*brown*), and p58-p48 primase (*PRI*, *red*). *Wavy solid lines* represent flexible linkers between folded domains. *Dotted lines* with *arrowheads* denote transient physical interactions among protein modules.

Figure 2.7, continued. *Middle panel*, ssDNA is transiently exposed by Tag contacts with RPA that remodel it into a more compact, lower affinity ssDNA binding mode and stabilize it as a ternary complex. The p68N domain of pol-prim is proposed to dock on the AAA+ domain of the Tag hexamer. The N-terminal region of the p180 subunit also docks on TagHD at an unidentified site; the reported interaction of p48/p58 with Tag has not been mapped. A single pol-prim complex binds to a Tag hexamer in solution. The ensemble of these interactions is proposed to position primase on the naked template to synthesize an RNA primer (*red*) and transfer it to p180 for extension (*bottom panel*). Thus, p68N docking on Tag hexamer effectively directs primase activity in the SV40 primosome. Artwork courtesy of Diana R. Arnett.

pol-prim inhibition of Tag helicase was shown to require the p48-p58 complex, the p180-p68 complex, and human RPA, mirroring the requirements for SV40 primosome function, but did not require oligoribonucleotide synthesis [140]. These findings suggest that physical interaction of pol-prim with Tag helicase may pause its translocation, possibly to allow for priming, as reported for prokaryotic helicase-primase assemblies [3][141, 142].

Implications for Pol-prim Function in Chromosomal DNA Processing

The essential helicase at eukaryotic chromosomal replication forks is the Mcm2-7 hexamer in complex with Cdc45 and GINS proteins [143-145]. Like Tag, the Mcm2-7 helicase assembly unwinds duplex DNA as it translocates 3'-5' on the leading strand template, displacing the lagging strand template. Moreover, the concerted head-to-head assembly of two Mcm2-7 hexamers on duplex DNA [146, 147] is strikingly similar to the assembly of Tag helicase on the SV40 origin [65, 148]. Yet how the Mcm2-7 complex, upon activation of DNA unwinding, associates with DNA polymerase α-primase for primosome activity remains poorly understood.

The crucial role for human p68 in the initiation of SV40 DNA replication would be

consistent with the requirement for the corresponding pol α subunit B (Pol12) for the G1/S transition and cell viability in budding yeast [81]. Interestingly, although the N terminus of yeast Pol12 shows little amino acid sequence conservation with human p68N, computational prediction of its structure reveals a similar four-helix bundle (data not shown). However, in-frame deletions within the predicted N-terminal domain of the yeast B-subunit did not reduce cell viability or growth rate [81], raising the question of whether the Pol12 N terminus contributes to initiation of replication in yeast. It remains possible that the Pol12 N terminus docks with an interaction partner in the replisome but that loss of the interaction might not lead to an obvious phenotype in a wild type genetic background. This would be reminiscent of yeast strains lacking Ctf4, which are viable [149, 150], even though binding of And-1 (known as Ctf4 or Mcl1 in yeast) to p180 is now known to serve a vital role in pol-prim recruitment and in replisome progression in organisms from yeast to human [151-157]. Further analysis is needed to explore a potential role for p68N in initiation of chromosomal replication under more stringent conditions. In addition, primosome activity at telomeres [76, 158] and at sites of stalled replication forks [75, 159] is vital for genomic stability but remains poorly understood. Our work suggests that a role for p68N should be investigated.

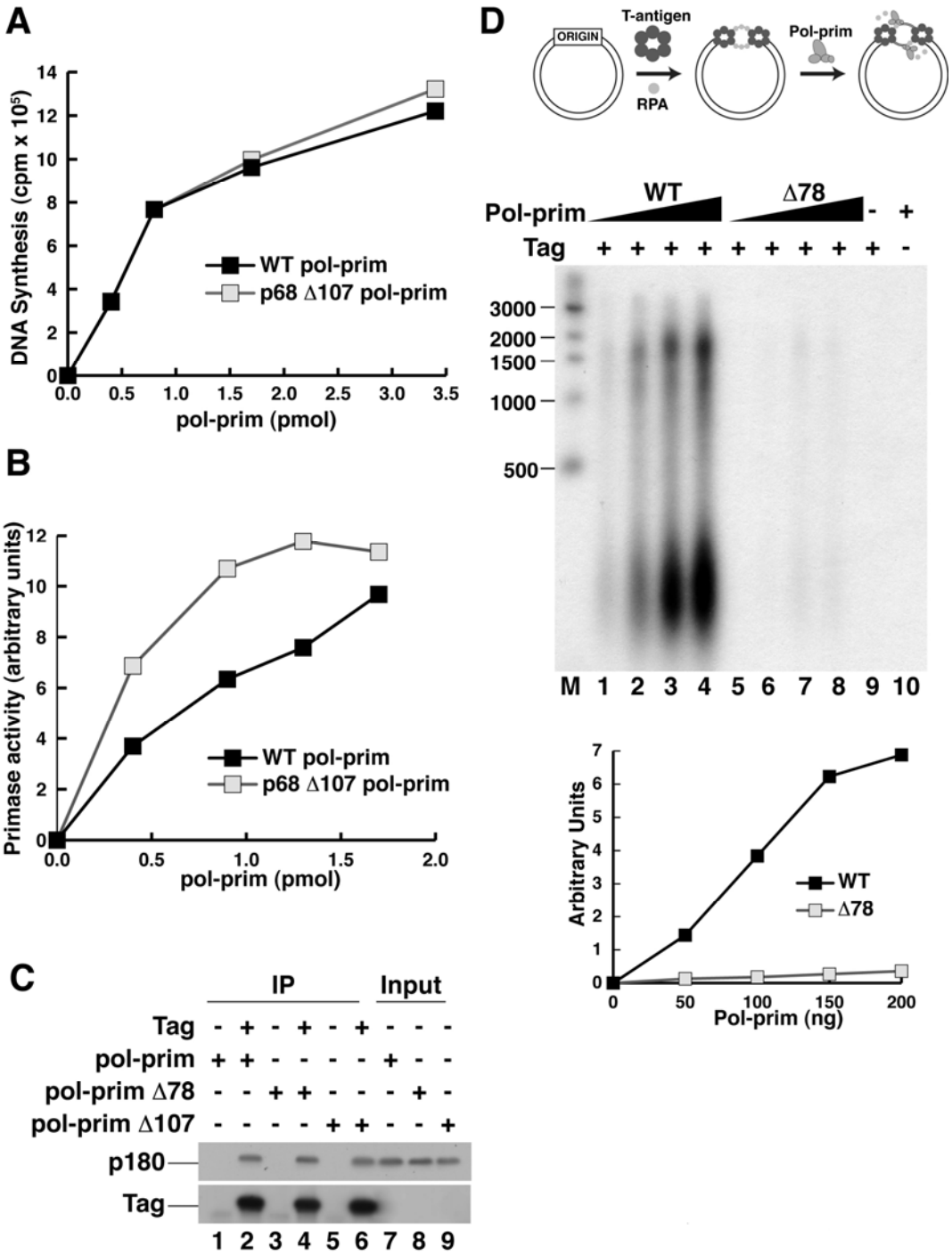

Figure S1. Biochemical activities of wild type and mutant pol-prim. (A) DNA polymerase activity of the indicated molar amounts of wild type and Δ1-107 pol-prim was assayed on poly(dA)-oligo(dT) template. Radiolabeled DNA products were analyzed by scintillation counting. (B) Primase activity of equal molar amounts of WT and Δ1-107 pol-prim was assayed on single-stranded M13 DNA template. Radiolabeled primers synthesized by pol-prim were visualized by denaturing electrophoresis and autoradiography, and quantified by densitometry.

Figure S1, continued. (C) Equal amounts of WT (lanes 1, 2), Δ1-78 (lanes 3, 4), or Δ1-107 (lanes 5, 6) pol-prim were incubated with anti-Tag beads in the presence (+) and absence (-) of Tag. Immunoprecipitated pol-prim and Tag were detected by western blotting. Input: 10% of the pol-prim used in lanes 1-6. (D) Initiation of SV40 replication was assayed in monopolymerase reactionscontaining increasing amounts of WT (lanes 1-4) or Δ1-78 (lanes 5-8) pol-prim. Control reactions lacked pol-prim (lane 9) or Tag (lane 10). Reaction products were resolved by alkaline electrophoresis, visualized by autoradiography, and quantified (lower panel). DNA size markers are indicated (M).

CHAPTER III*

A SPECIFIC DOCKING SITE FOR DNA POLYMERASE α-PRIMASE ON THE SV40 HELICASE IS REQUIRED FOR VIRAL PRIMOSOME ACTIVITY, BUT HELICASE ACTIVITY IS DISPENSABLE

Introduction

De novo DNA replication begins with RNA primer synthesis on single-stranded template DNA, followed by primer extension by a processive DNA polymerase. In prokaryotic replication, the activity of the primase is coordinated with unwinding of duplex DNA by a hexameric replicative helicase and a single-stranded DNA (ssDNA)-binding protein, largely through dynamic physical interactions among the three proteins, which constitute a primosome [3, 116, 119, 160]. In eukaryotes, the DNA polymerase alpha-primase (pol-prim) complex catalyzes both RNA primer synthesis and extension yielding RNA-DNA primers of 30-35 nucleotides [120, 121]. Unlike the single subunit prokaryotic primases, pol-prim is a stable heterotetramer composed of the primase heterodimer p48/p58, the catalytic DNA polymerase subunit p180, and a regulatory subunit (B or p68) [43]. The eukaryotic replicative helicase complex, Cdc45/Mcm2-7/GINS, and the ssDNA-binding protein, replication protein A (RPA), appear to coordinate primer synthesis by pol-prim with parental DNA unwinding, as in prokaryotes [145, 153, 161-163]. However, the nature of the eukaryotic primosome and its operation during chromosome replication, telomere maintenance, and checkpoint signaling at stalled replication

*The work of this chapter was published in Huang, H., Zhao, K., Arnett, D.R., Fanning, E. J Biol Chem. 2010 Oct 22;285(43):33475-84.

forks remain elusive.

Since pol-prim is essential for replication of simian virus 40 (SV40) DNA, we utilize this model system here to investigate the functional architecture of a eukaryotic primosome. SV40 DNA replication can be reconstituted in cell-free reactions with purified recombinant human proteins and the viral large T antigen (Tag) [5]. Tag serves as the replicative helicase and orchestrates the assembly of the viral replisome. Tag monomers first assemble cooperatively into a pre-initiation complex on the viral origin of DNA replication, forming two hexamers oriented head-to-head, akin to the Mcm2-7 hexamer assemblies recently visualized on yeast origins [49, 146, 147]. To initiate replication, the pre-initiation complex rearranges into a bidirectional mini-replication factory [49, 55, 68, 71, 164]. As Tag unwinds parental DNA, it interacts physically with two different surfaces of RPA and actively loads it onto the emerging template via a transient ternary complex with RPA-ssDNA, thereby coupling DNA unwinding with RPA deposition [54, 58, 59, 117]. Tag also interacts physically with at least three subunits of pol-prim [84, 110-113, 117, 118]. These interactions led to a model of SV40 primosome activity in which Tag contacts with RPA-ssDNA remodel RPA into a weaker ssDNA-binding mode, transiently affording local access to the template (Fig. 3.1A). Tag can then load its associated pol-prim onto RNA-ssDNA in a molecular handoff reaction that enables primer synthesis [37, 58, 98, 133, 134]. Thus, physical interactions among pol-prim, Tag, and RPA are proposed to contribute to primosome activity in the SV40 replisome.

To gain greater insight into the operation of the SV40 primosome, we recently identified a previously unrecognized domain of the pol-prim p68 subunit (p68N) that docks on Tag,

determined its solution structure, and identified the surface of p68N that docks on Tag [165]. Structure-guided mutagenesis of p68N was used to confirm its Tag-docking surface. Substitutions in this surface that specifically reduced its affinity for Tag were then introduced into the intact pol-prim complex and shown to diminish SV40 primosome activity. The results demonstrated that p68-Tag docking is vital for primosome activity, even in the presence of p180 and primase docking on Tag, supporting a working model in which this network of contacts may position pol-prim to access the exposed template. This model implies the existence of a corresponding docking site for p68N on the surface of Tag. Localization of pol-prim docking sites on Tag would provide new insight into the architecture of the primosome and coordination of its activity with that of the helicase.

Here we report the identification of the predicted p68N-docking site on the C-terminal face of the Tag helicase domain, show that a Tag variant unable to bind to p68 retains binding to p180 and primase, and demonstrate the importance of p68-Tag interaction in primosome activity. In addition, we report that the ATPase/translocase activity (and hence helicase activity) of Tag is dispensable for primosome activity in vitro. Potential implications of our data for the overall architecture of the SV40 primosome and the coordination of priming with parental DNA unwinding are discussed.

Materials and Methods

Yeast Two-hybrid Assay

Coding sequences of Tag fragments were amplified by PCR and ligated into the EcoRI/BamHI sites of pGADT7 vector containing a *TRP* selection marker (Clontech). Coding sequences of p68 fragments were amplified by PCR and ligated into the NdeI/BamHI sites of pGBKT7 vector containing a *LEU* selection marker. These plasmids were cotransformed into yeast strain AH109, which contains three reporter genes *HIS3, ADE2* and *LacZ*. The cells were allowed to grow four days on -Leu -Trp plates. Positive colonies were picked and streaked on a -Leu -Trp plate and on a -Leu -Trp -His -Ade plate. Plates were photographed after growth for another four days.

Protein Expression and Purification

Wild type (WT) and mutant SV40 Tag and topoisomerase I were expressed in insect cells using recombinant baculoviruses and purified as described [58]. Pol-prim was expressed in Hi-5 insect cells infected with four recombinant baculoviruses and purified by immunoaffinity chromatography as described previously [84]. Bacterially expressed His-p68 [84] and p48/p58 human primase [88, 91] were prepared as described. Recombinant human RPA was expressed in *Escherichia coli* and purified as described [166].

The DNA encoding pol-prim p68 1-107 was amplified by PCR, verified by DNA sequencing, and ligated into the BamHI/NotI sites of a modified pET-32a plasmid [165]. Thioredoxin

(Trx)-His-tagged pol-prim p68 1-107 and p180 1-323 fragments were purified using nickelnitrilotriacetic acid affinity chromatography. Coding sequences of Tag fragments 131-259, 251-627, 303-627 and 357-627 were PCR amplified, cloned into the BamHI/EcoRI sites of the pGEX-2T expression vector (GE Healthcare), and verified by DNA sequencing. Glutathione *S*-transferase [119] fusion proteins were expressed in *E. coli* BL21 (DE3) cells and purified using glutathione-agarose affinity chromatography.

Tag Pull-down Assays

Purified Tag was bound to monoclonal antibody Pab101-coupled Sepharose beads or GST-tagged Tag fragments (10 μg) were bound to glutathione-agarose beads. The protein-bound beads were then incubated with His-p68, His-p68 1-107, His-p180 1-323, or primase (as stated in figure legends) in binding buffer (30 mM HEPES-KOH, pH 7.8, 10 mM KCl, 7 mM $MgCl_2$) containing 2% nonfat dry milk for 1 h at 4 °C with end-over-end rotation. The beads were washed once with binding buffer, three times with wash buffer (30 mM HEPES-KOH, pH 7.8, 25 mM KCl, 7 mM $MgCl_2$, 0.25% inositol, 0.01% NP-40), and once with binding buffer. For Pab101 pulldowns, binding and wash buffers were supplemented with 10 μM $ZnCl_2$. The beads were resuspended in 30 μl of 2x SDS-PAGE loading buffer and heated at 100 °C for 5 min. Samples were analyzed by SDS-PAGE and visualized by immunoblotting with monoclonal Pab101 for Tag [167], rabbit anti-GST (Invitrogen) for Tag fusion proteins, anti-His (Abcam 9801 or Genscript A00186) for His-tagged proteins, rat PRI-8G10 for p48 [112], and chemiluminescence (Perkin Elmer).

Tag Helicase Assay

To prepare the helicase substrate, a 33-nt oligonucleotide (5'TCGACTCTAGAGGATCCCCGGGTACCGAG CTCG) was labeled at the 5' end with [γ-^{32}P]ATP by T4 polynucleotide kinase (NEB) and annealed to M13mp18 ssDNA (USB). Approximately 10 fmol of substrate was incubated with WT or mutant Tag (2, 4, or 6 pmol) for 45 min at 37 °C in a 15 µl reaction consisting of 20 mM Tris (pH 7.5), 10 mM $MgCl_2$, 4 mM ATP, 0.1 µg/µl bovine serum albumin, and 1 mM DTT. Reactions were terminated by addition of SDS to 0.25% and EDTA to 50 mM, separated by electrophoresis in 12% native acrylamide gels in 0.5x Tris-borate EDTA buffer, and visualized using a PhosphorImager (Molecular Dynamics).

Tag ATPase Assay

WT or mutant Tag (0.5, 1.0 or 1.5 µg) was added to a reaction mixture (20 µl) containing 50 pmol of ATP and 1 µCi of [α-^{32}P]ATP (3000 Ci/mmol; Perkin Elmer) in 50 mM Tris-HCl [pH 8], 10 mM NaCl, 7 mM $MgCl_2$, 0.05% NP-40, 1 mM DTT. After 10 min at 37 °C, 1 µl of 1% SDS, 40 mM EDTA was added to terminate the reaction. 1 µl of the reaction mixture was spotted onto polyethyleneimine-cellulose F thin layer chromatography plates (EMD Chemicals), and the plates were developed in 1 M formic acid, 0.5 M LiCl. After the plates dried, released phosphate and remaining ATP were visualized by autoradiography.

Initiation of SV40 DNA Replication

Monopolymerase assays [125] were carried out as described previously [58]. Briefly, reaction

mixtures (20 µl) contained 250 ng of supercoiled pUC-HS plasmid DNA, 200 ng of RPA, 300 ng of topoisomerase I, 600 ng Tag and 50-200 ng of recombinant pol-prim in initiation buffer (30 mM HEPES-KOH, pH 7.9, 7 mM magnesium acetate, 10 µM $ZnCl_2$, 1 mM DTT, 4 mM ATP, 0.2 mM each GTP, UTP and CTP, 0.1 mM each dGTP, dATP, and dTTP, 0.02 mM dCTP, 40 mM creatine phosphate, 40 µg/ml of creatine kinase) supplemented with 3 µCi of [α-^{32}P]dCTP (3000 Ci/mmol). Reaction mixtures were assembled on ice, incubated at 37 °C for 90 min, and then digested with 0.1 mg of proteinase K/ml in the presence of 1% SDS and 1 mM EDTA at 37 °C for 30 min. Radiolabeled reaction products were purified on G-50 Sephadex columns and precipitated with 2% $NaClO_4$ in acetone. The products were washed, dried, resuspended in alkaline loading buffer (60 mM NaOH, 2 mM EDTA [pH 8.0], 20% [w/v] Ficoll, 0.1% [w/v] bromophenol blue, 0.1% [w/v] xylene cyanol) and electrophoresed on 1.5% agarose gels in running buffer (30 mM NaOH, 1 mM EDTA). The gels were fixed in 10% TCA and dried. The reaction products were visualized by autoradiography and quantified by densitometry or phosphorimaging.

Primer Synthesis and Elongation in the Presence of RPA

Reaction mixtures (20 µl) containing 100 ng of single-stranded M13 DNA were preincubated with 1000 ng of RPA in initiation buffer (see above) at 4 °C for 20 min. The reactions then were supplemented with 3 µCi of [α-^{32}P]dCTP, 200-600 ng of Tag, and 600 ng of pol-prim as indicated in the figure legends, incubated at 37 °C for 45 min, and then digested with 0.1 mg of proteinase K/ml in the presence of 1% SDS and 1 mM EDTA at 37 °C for 30 min. Radiolabeled reaction

products were then processed and analyzed as described above for the monopolymerase assay.

Results

The AAA+/D3 Subdomains of Tag Interact with the p68 Subunit of Pol-prim

Tag is a modular protein composed of three major domains linked through flexible peptides, and a C-terminal region of unknown structure (Fig. 3.1B). Using yeast two-hybrid assays, we recently demonstrated that the N-terminal domain of p68 (residues 1-78 and 1-107) interacts physically with the helicase domain of Tag [165]. To confirm the Tag-p68 mapping data, bacterially expressed, purified GST-Tag constructs were tested for their ability to bind to purified p68 1-107 in pulldown assays. No p68 interaction was detected with the origin DNA binding domain of Tag (residues 131-259) (Fig. 3.1C, lanes 2, 3), but all three GST-Tag fragments containing the AAA+/D3 region (residues 357-627) pulled down the p68 fragment in a concentration-dependent manner (lanes 4-9). The results demonstrate that the AAA+/D3 subdomains of Tag bind specifically and directly to the N-terminus of p68.

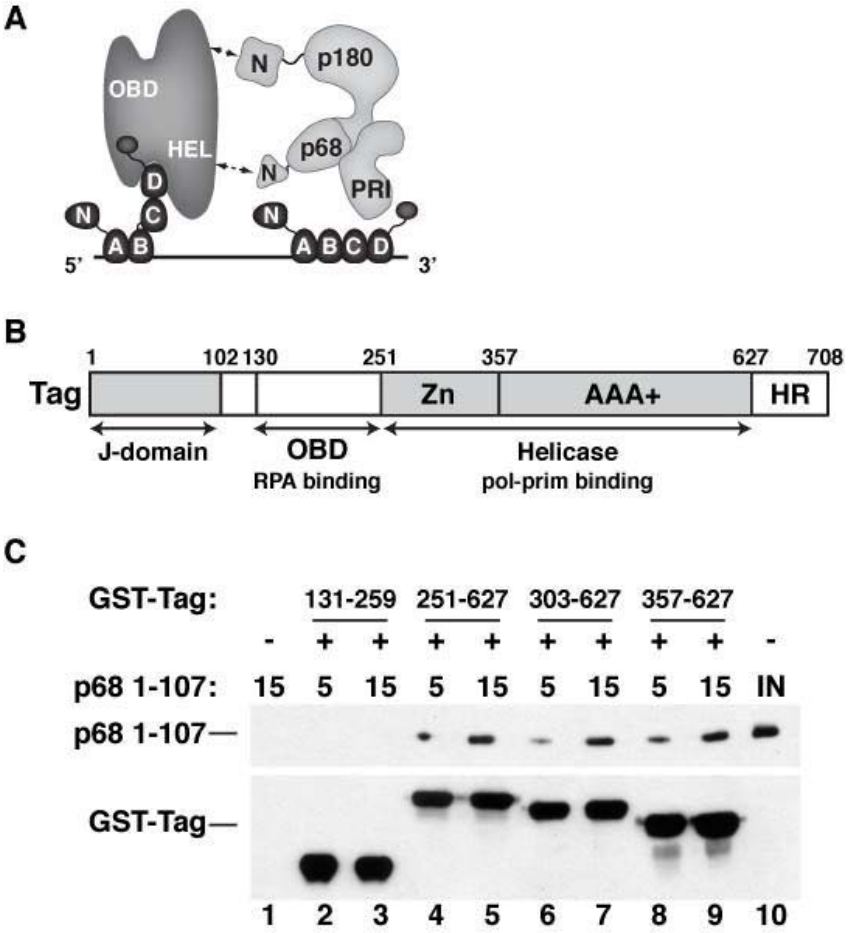

Figure 3.1. Tag357-627 is sufficient to bind to pol-prim p68 1-107. (A) A molecular handoff model for SV40 primosome activity on RPA-coated ssDNA. The four ssDNA-binding domains (A-D) of RPA (*dark gray*) occlude up to 30 nucleotides of ssDNA (*straight line*). Flexible linkers (*wavy lines*) join the N-terminal domain of RPA70 and the C-terminal domain of RPA32 to the RPA-ssDNA. Tag contacts with RPA32C and RPA70AB remodel it into a more compact, lower affinity ssDNA-binding mode and stabilize it as a ternary complex [58, 59, 98], transiently exposing the template ssDNA. Pol-prim (*light gray*) contacts the Tag helicase domains (HEL) through p68N [165], the N-terminus of p180 DNA polymerase, and through unknown surfaces of primase p58/p48 (PRI) [111, 112, 117]. The ensemble of these interactions is proposed to position primase on the exposed template to synthesize an RNA primer (*not shown*). (B) Domain architecture of SV40 Tag. The DnaJ chaperone domain [46], SV40 origin-DNA-binding domain (OBD) [47], and helicase domain [66, 127] are depicted. The structure of the host-range (HR) domain is not known [168]. (C) GST-tagged Tag fragments 131-259 (lanes 2 and 3), 251-627 (lanes 4 and 5), 303-627 (lanes 6 and 7), or 357-627 (lanes 8 and 9) adsorbed to glutathione beads were incubated with increasing amounts of His-tagged p68 1-107 as indicated. Proteins bound to the beads were separated by SDS-PAGE and visualized by Western blotting with anti-His antibody (upper panel) or anti-GST antibody (lower panel).

Figure 3.1, continued. Glutathione beads lacking GST-Tag protein (lane 1) are shown as negative control. Lane 10 shows 200 ng of input p68 1-107.

Mapping the p68-interacting Surface of the Tag Helicase Domain

Crystal structures of the hexameric Tag helicase domain reveal a "double donut" structure consisting of the six zinc subdomains (residues 251-356) in a smaller ring and the six AAA+ (ATPases associated with a variety of cellular activities) subdomains and the surrounding helices of the D3 subdomains (residues 357-627) in a larger ring [48, 61, 169] (Fig. 3.2A). These structures provide a foundation for mapping the binding sites of pol-prim subunits on the surface of Tag.

Based on the hydrophobic and acidic character of the Tag-binding surface of p68N [165], we reasoned that the p68N-binding surface of Tag would be likely to display some positive charge. To search for such a surface on the helicase domain, we utilized a recently generated panel of amino acid substitutions in conserved, surface-exposed residues, which was designed using structural models of the hexameric helicase domain [48, 61, 170]. Use of the hexamer structure to identify surface residues for mutagenesis should minimize substitutions that would cause gross structural perturbations of the protein or interfere with its oligomerization. Clusters of charged surface residues were grouped to generate a panel of five "patch mutants", each containing four charge-reverse substitutions [170] (Fig. 3.2A). Four patch mutants were screened in yeast two-hybrid assays for interaction with p68 1-107. The initial screen demonstrated that p68 1-107 interacted with WT and patch mutants 1-3, but failed to interact with the patch 4 cluster containing K425E, R483E, K535E, and K543E substitutions (Fig. 3.2B, sector 5). A second

round of screening was conducted using a series of Tag constructs, each with one of the substitutions from patch 4. In this screen, the p68 fragment interacted well with WT Tag357-627 and all of the single charge-reverse proteins except K425E (Fig. 3.2C, sector 6). To validate the two-hybrid results, pulldown experiments were conducted with purified GST-Tag357-627 constructs and p68 1-107. The WT GST-Tag construct pulled down the p68 fragment, but the patch 4 mutant (P4) and the K425E mutant constructs displayed little or no interaction with the p68 N-terminus (Fig. 3.2D, compare lanes 2, 3 with 4-7). These results indicate that a direct interaction between Tag and p68 1-107 is disrupted by the K425E substitution in Tag. Pulldown experiments also showed that K425E, but not K425R, substantially reduced Tag357-627 binding to p68 1-107 (Fig. 3.2E, compare lanes 4, 5 with 6, 7), confirming that the charge swap was responsible for the weakened interaction.

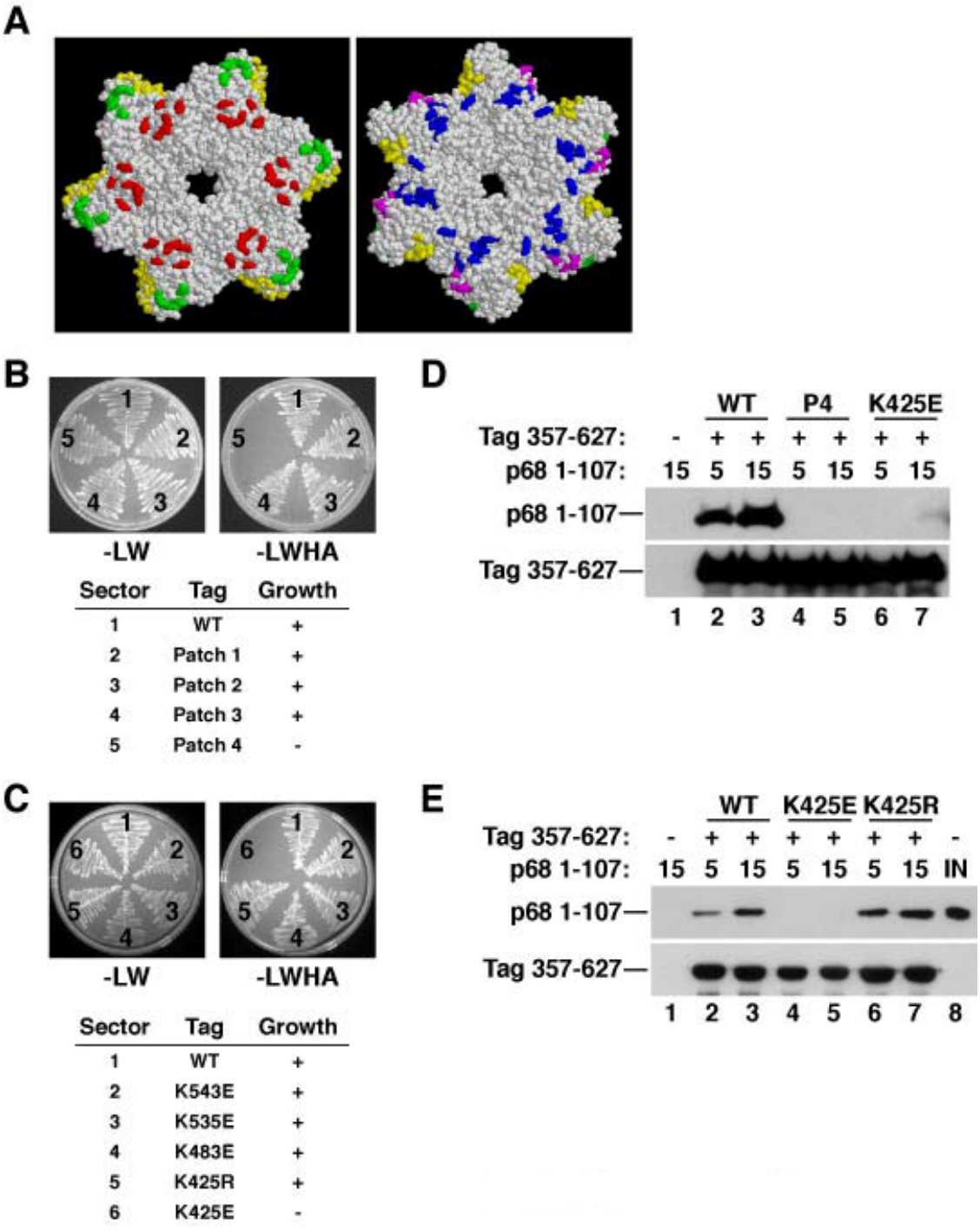

Figure 3.2. Structure-guided mutagenesis of Tag surface residues to map the p68N-docking site. (A) Diagram of conserved patches of charged surface residues of the Tag hexamer (residues 266-627) ((Ahuja, 2009 #104); reprinted with permission). In the left view, the six zinc subdomains face the reader; the right view is rotated 180^{o} so that the AAA+ subdomains face the reader. Patch 1, green; 2, yellow; 3, red; 4, blue; 5, magenta.

Figure 3.2, continued. (B) Patch mutants and (C) single residue substitutions of pGADT7-fused Tag were screened in yeast two-hybrid assays for interaction with pGBKT7-fused p68 1-107. The numbered sectors are identified in the tables below. (D) Glutathione beads alone (lane 1), or adsorbed to WT (lanes 2, 3), patch 4 (P4) mutant (lanes 4, 5), or K425E GST-Tag357-627 (lanes 6, 7) were incubated with 5 or 15 μg His-tagged p68 1-107 as indicated. Bound proteins were analyzed by western blotting with anti-His (upper panel) or anti-GST antibody (lower panel). (E) Glutathione beads alone (lane 1) or adsorbed to GST-Tag357-627 WT (lanes 2 and 3), K425E (lanes 3 and 4), or K425R (lanes 6 and 7) were incubated with 5 or 15 μg of p68 1-107 as indicated. Bound proteins were analyzed by western blotting with anti-His (upper panel) or anti-GST antibody (lower panel). Lane 8 shows 200 ng of input p68 1-107.

Mutation of the p68-interacting Surface of Full-Length Tag Does Not Significantly Reduce Binding to p180 or Primase, but Nearly Abolishes Primosome Activity

The mapping results in Figures 3.1 and 3.2 suggest that the K425E substitution compromises Tag interaction with the p68 subunit of pol-prim. Together with evidence that p68 docking on Tag is vital for primosome activity [165], these findings predict that Tag K425E should display defective primosome activity. In order to test this prediction, we first generated the full-length recombinant K425E protein and characterized it. The purified mutant Tag was stable and obtained in yields comparable to that of WT Tag (Fig. 3.3A), suggesting that K425E Tag is folded reasonably well. First, to rule out the possibility that the K425E substitution perturbs the interaction between Tag and other subunits of pol-prim [111, 112, 117], we compared the ability of K425E and WT Tag to interact physically with primase and the N-terminal region of p180. Purified heterodimeric human primase or His-tagged p180 1-323 was incubated with anti-Tag antibody beads alone, or in the presence of increasing amounts of WT or mutant Tag. After the beads were washed, bound proteins were detected by denaturing gel electrophoresis and immunoblotting. The amounts of primase bound to WT and K425E Tag were very similar (Fig.

3.3B, compare lanes 2, 3 with lanes 4, 5). Moreover, the amounts of p180 1-323 bound to WT and K425E Tag were very similar (Fig. 3.3C, compare lanes 2, 3 with lanes 4, 5). Taken together, the results support the interpretation that p68 binding to Tag is specifically reduced by the K425E charge-reversal.

To verify this finding in the context of the intact pol-prim complex, increasing amounts of purified pol-prim were incubated with anti-Tag beads in the absence or presence of WT or K425E Tag. Bound pol-prim was detected by immunoblotting with anti-p180 antibody (Fig. 3.3D). No detectable pol-prim was bound to the beads in the absence of Tag (lane 1). K425E Tag (lanes 4, 5) bound nearly as much pol-prim as did WT Tag (lanes 2, 3), consistent with loss of only the low affinity p68-Tag docking [165] and retention of the contacts with primase and p180. Taken together, the results suggest that the K425E substitution specifically abrogates p68 docking without gross perturbation of Tag binding to other pol-prim subunits.

Since mutations in the p68N domain of pol-prim that weakened or prevented its physical interaction with Tag diminished or abolished SV40 primosome activity on RPA-coated ssDNA [165], we expected that primosome activity of K425E Tag should also be compromised. To assay primosome activity of K425E Tag independently of origin DNA unwinding, we utilized natural ssDNA saturated with RPA as the template. RPA inhibits the ability of pol-prim to generate RNA primers on the template and extend them into RNA-DNA products [37, 133, 134]. RNA primer synthesis can be monitored directly by polymerization of radiolabeled ribonucleotides. However, extension of unlabeled RNA primers into dCTP-radiolabeled RNA-DNA primers amplifies the signal significantly and was therefore adopted as a more sensitive measure of primosome activity

[58, 125, 165].

As expected, the ability of pol-prim to synthesize primers on naked ssDNA and extend them into radiolabeled RNA-DNA products was substantially inhibited when the template was precoated with RPA (Fig. 3.3E, compare lanes 7 and 8). Also as expected, addition of WT Tag to the reaction relieved the inhibition of pol-prim, stimulating the production of radiolabeled RNA-DNA in a concentration-dependent manner (Fig. 3.3E, lanes 1-3). In contrast, K425E Tag failed to relieve the RPA inhibition (Fig. 3.3E, lanes 4-6). Quantification of the products confirmed that the primosome activity of K425E Tag was reduced to essentially background level (Fig. 3.3F, compare lanes 4-6 with lane 7). These results are consistent with the interpretation that physical interaction of Tag with p68 is vital for primosome activity on RPA-ssDNA.

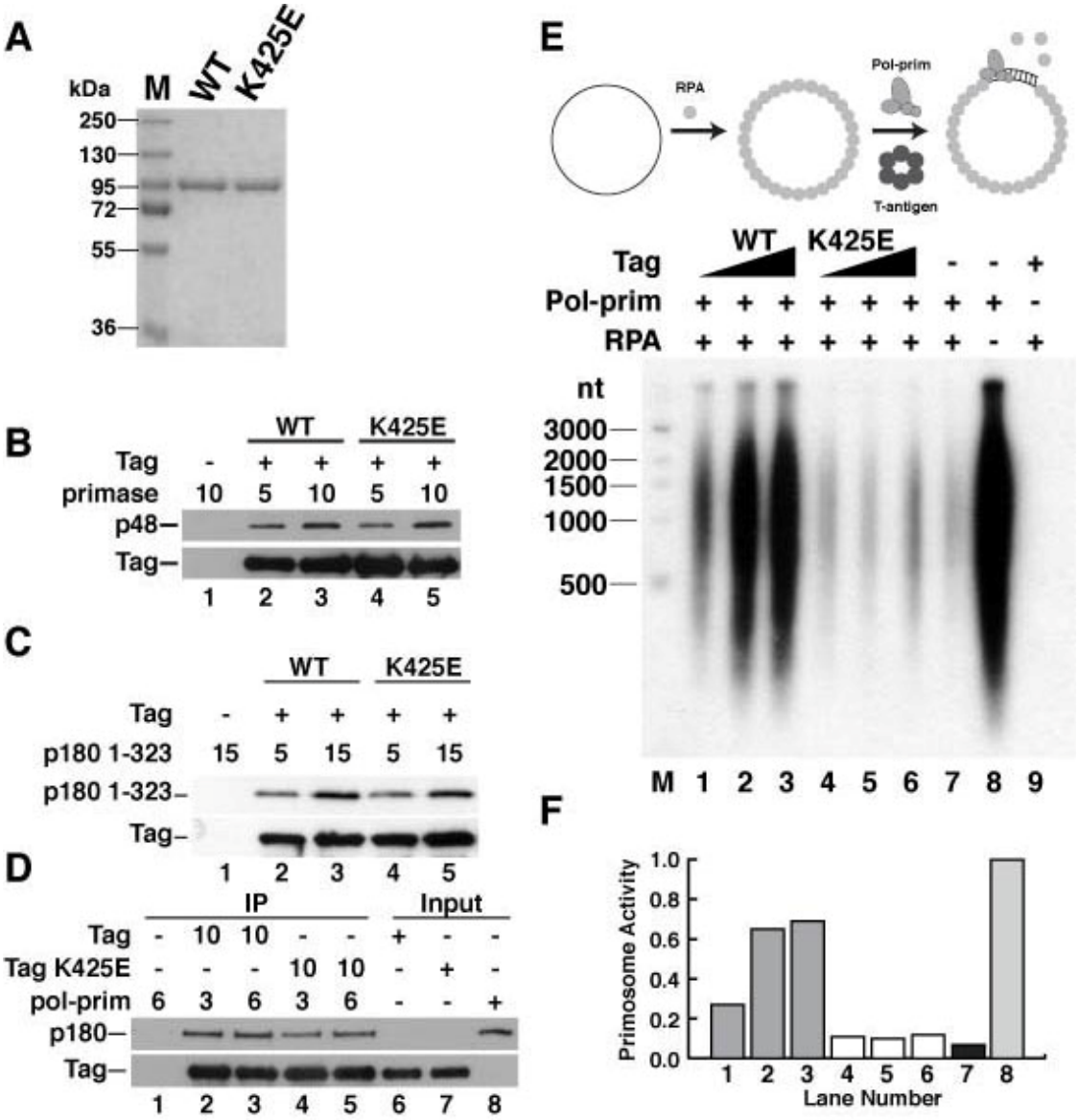

Figure 3.3. K425E Tag binds to primase and p180 pol-prim, but lacks primosome activity. (A) Purified WT and K425E Tag were separated by SDS-PAGE and stained with Coomassie. M: protein size-markers. (B, C) Pab101 beads alone (lane 1) or bound to WT (lanes 2 and 3) or K425E Tag (lanes 4 and 5) was incubated with increasing amounts of primase dimer (B) or His-p180 1-323 (C) as indicated. Bound proteins were detected by SDS-PAGE and immunoblotting with anti-p48, anti-His (Genscript, A00186), or Pab101 against Tag. (D) Anti-Tag beads alone (lane 1), or adsorbed to 10 μg WT (lanes 2, 3) or K425E Tag (lanes 4, 5) were incubated with 3 or 6 μg of pol-prim as indicated. Bound proteins analyzed by western blotting with anti-Tag and anti-p180 antibody as indicated. Input: 100 ng. (E, F) Primosome activity of 200, 400 or 600 ng of Tag WT (lanes 1-3) or K425E (lanes 4-6) was assayed on 100 ng ssDNA pre-coated with 1 μg RPA in the presence of 600 ng of pol-prim. Control reactions lacked Tag (lane 7), Tag and RPA (lane 8), or pol-prim (lane 9).

Figure 3.3, continued. Reaction products were analyzed by alkaline electrophoresis and visualized by autoradiography (E). DNA size-markers are shown (M). (F) Reaction products were quantified; signal in the negative control reaction (lane 9) was subtracted from that in lanes 1-8. Incorporation in lanes 1-7 is expressed as a fraction of that in lane 8.

The K425E Substitution Inhibits Tag Helicase Activity and Origin DNA Unwinding-dependent Initiation of SV40 Replication

To determine whether the K425E substitution might also affect enzymatic functions of the Tag helicase domain, the ATPase activity of K425E Tag was assayed by monitoring radiolabeled inorganic phosphate released from labeled ATP (Fig. 3.4A). Indeed, the ATPase activity of K425E Tag was strongly reduced compared to that of WT Tag (compare lanes 5-7 with lanes 2-4). Additionally, K425E Tag helicase activity was markedly lower than that of WT Tag (Fig. 3.4B, compare lanes 8-10 to lanes 4-6). Since the ATPase/helicase activity of Tag is required to unwind SV40 origin DNA to generate the template, K425E Tag would be expected to display a defect in origin-dependent initiation of replication. This prediction was tested in a monopolymerase reaction [125] using supercoiled DNA containing the SV40 origin and four purified proteins; T antigen, RPA, pol-prim, and topoisomerase I, with unlabeled ribo- and deoxyribonucleoside triphosphates and labeled dCTP. In the presence of WT Tag, radiolabeled RNA-DNA products accumulated in proportion to the amount of pol-prim present in the reaction (Fig. 3.4C, lanes 1-3), as expected, and no products were generated in the absence of Tag or pol-prim (lanes 7, 8). Conversely, radiolabeled replication products were barely detectable in reactions containing K425E Tag, regardless of the amount of pol-prim present (lanes 4-6). These observations confirm that origin unwinding dependent-replication activity of K425E Tag is defective.

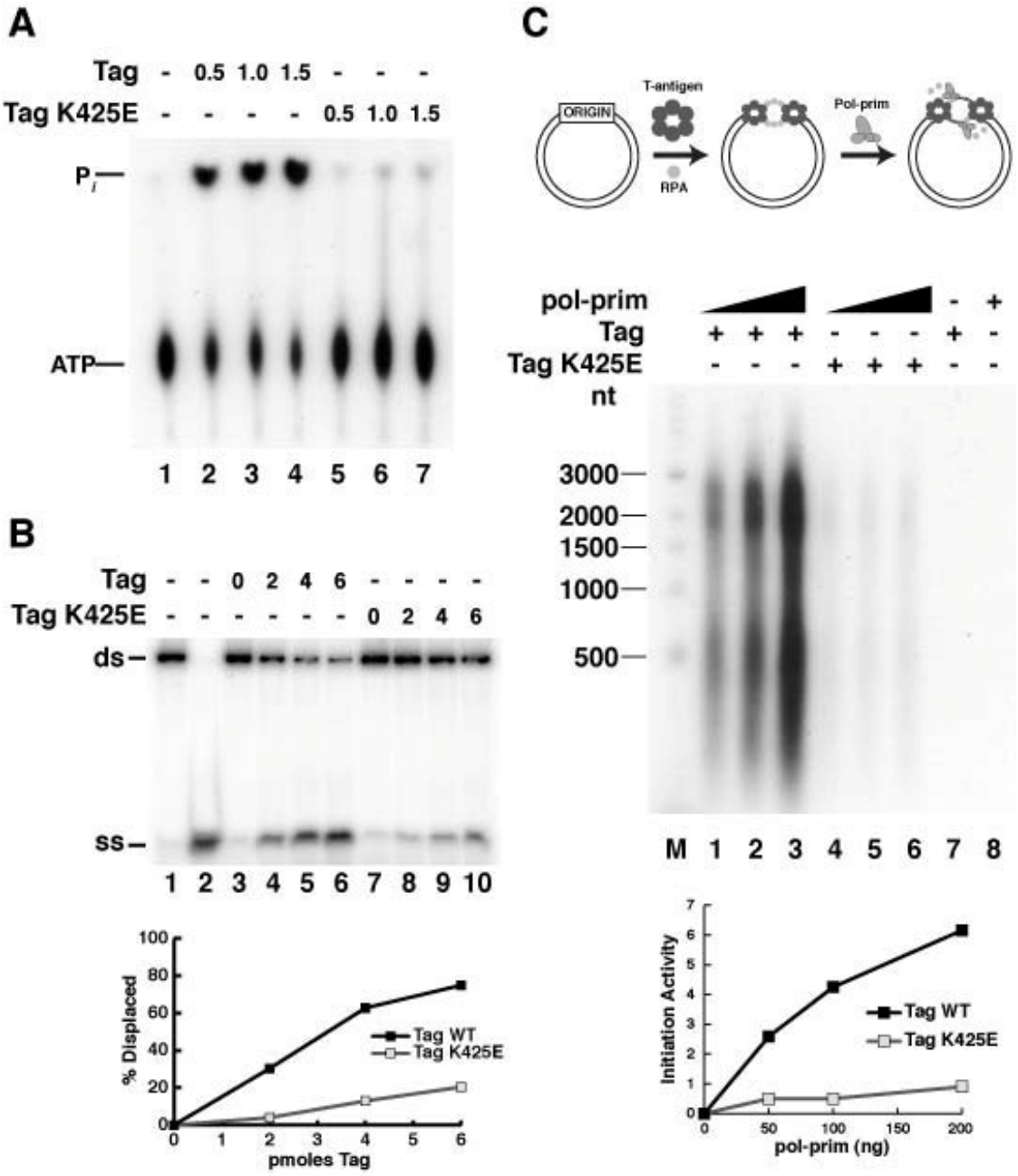

Figure 3.4. K425E Tag is defective in ATPase activity and initiation of SV40 replication. (A) ATPase reactions were carried out without Tag (lane 1), or with increasing amounts of Tag WT (lanes 2-4) or K425E (lanes 5-7) as indicated. After 10 min, the reaction products were separated by ascending thin-layer chromatography and visualized by autoradiography. (B) To assess helicase activity, 10 fmol of DNA substrate was incubated without Tag (lanes 3 and 7) or with increasing amounts (2, 4, or 6 pmoles) of WT (lanes 4-6) or K425E (lanes 8-10) Tag. Lanes 1 and 2 contain DNA substrate or boiled substrate alone.

Figure 3.4, continued. (C) SV40 initiation activity of Tag WT (lanes 1-3) or K425E (lanes 4-6) (600 ng) was assayed in monopolymerase reactions with 50, 100, or 200 ng of pol-prim. Radiolabeled DNA products were visualized by alkaline agarose electrophoresis and autoradiography. Products from control reactions without pol-prim (lane 7) or Tag (lane 8) are shown as indicated (-). End-labeled DNA fragments of the indicated sizes are shown at the left (M). Reaction products were quantified; background (lanes 7 and 8) was subtracted from incorporation in lanes 1-6 (*lower panel*). Data in panel B were collected by Diana R. Arnett.

Is Tag ATPase/helicase Activity Needed for Primosome Activity Independently of Origin DNA Unwinding?

The results from the monopolymerase assay (Fig. 3.4C) cannot distinguish whether the defective ATPase and helicase activities of K425E Tag (Fig. 3.4A, B), its poor binding to p68 and defective primosome activity (Figs. 3.2, 3.3), or a combination of these defects is responsible for the initiation defect. Therefore, it remains conceivable that ATPase/helicase activity of Tag contributes to primosome activity even when RPA-ssDNA is used as the template to bypass the requirement for origin DNA unwinding, as in Figure 3. In that case, the ATPase defect of K425E Tag, rather than its defect in p68 docking, could be responsible for the loss of primosome activity observed in Figure 3.3.

In order to evaluate the possibility that the ATP hydrolysis activity of Tag might play a vital role in primosome activity independently of origin DNA unwinding, we sought to inactivate Tag ATPase activity without affecting its interaction with pol-prim. Toward this end, we generated recombinant Tag with a substitution in the Walker B motif. The purified mutant protein D474N was stable and obtained in wild type yield (Fig. 3.5A). As expected, the D474N protein displayed very little ATPase activity (Fig. 3.5B, compare lanes 2 and 3) and no helicase activity (Fig. 3.5C). Also as expected, D474N Tag displayed little activity in an origin unwinding-dependent SV40

initiation assay (Fig. 3.5D, compare lanes 1-3 with lanes 4-6).

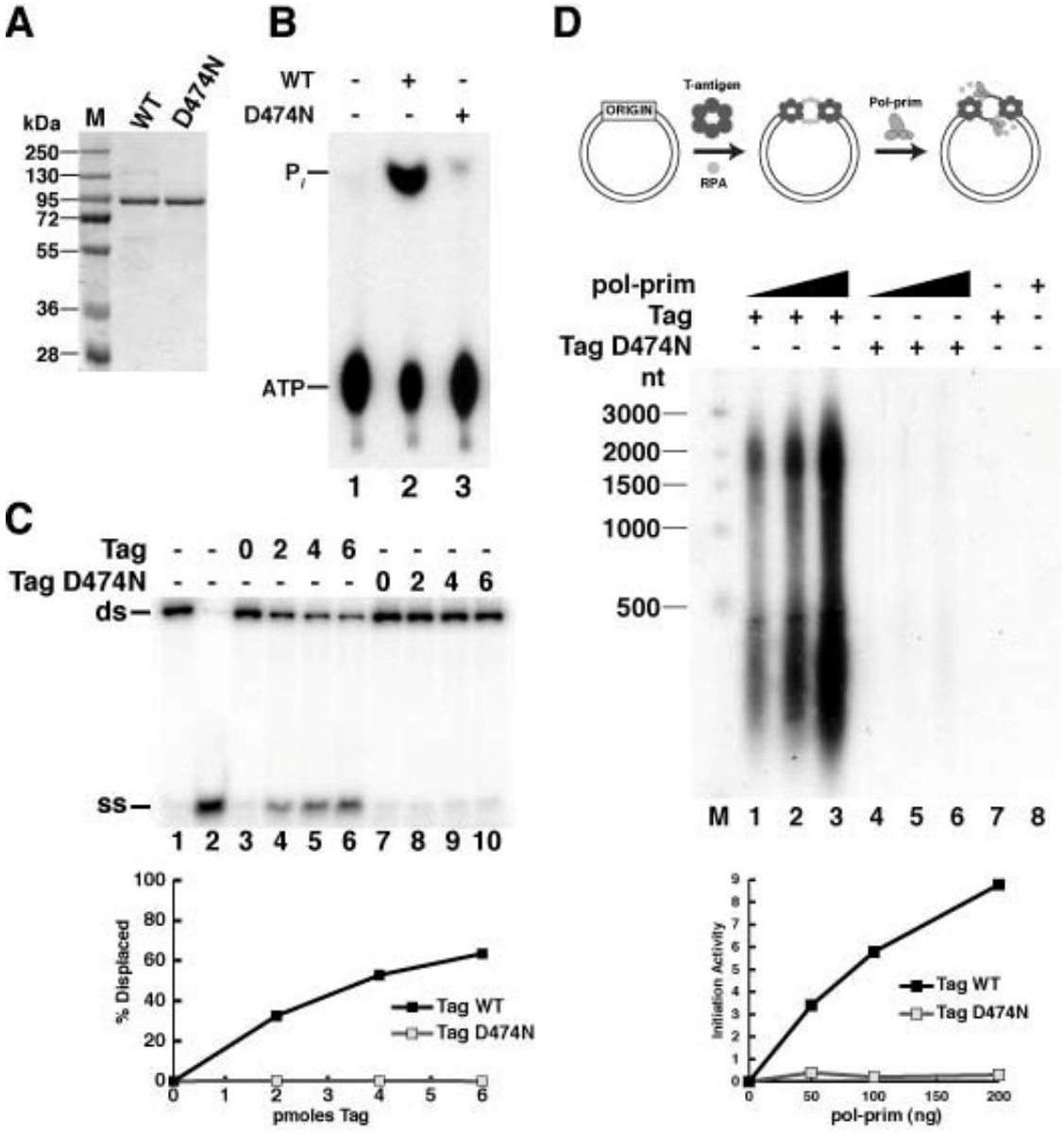

Figure 3.5. A single residue substitution in the Walker B motif of Tag abolishes ATPase/helicase activity and initiation of SV40 replication. (A) Purified WT and D474N Tag were separated by SDS-PAGE and stained with Coomassie. M: protein size-markers. (B) ATPase reactions were carried out without Tag (lane 1), or with 1 μg of Tag WT (lane 2) or D474N (lane 3). The reaction products were separated by ascending thin-layer chromatography and visualized by autoradiography.

Figure 3.5, continued. (C) To assess helicase activity, 10 fmol of DNA substrate was incubated without Tag (lanes 3 and 7) or with increasing amounts (2, 4, or 6 pmoles) of WT (lanes 4-6) or D474N (lanes 8-10) Tag. Lanes 1 and 2 contain DNA substrate or boiled substrate alone. (D) SV40 initiation activity of 600 ng Tag WT (lanes 1-3) or D474N (lanes 4-6) was assayed in monopolymerase reactions with 50, 100, or 200 ng of pol-prim. Radiolabeled DNA products were visualized by alkaline agarose electrophoresis and autoradiography. Products of control reactions without pol-prim (lane 7) or Tag (lane 8) are shown as indicated (-). End-labeled DNA fragments of the indicated sizes are shown at the left (M). Reaction products were quantified; background (*lanes 7 and 8*) was subtracted from incorporation in *lanes 1-6* (*lower panel*). Data in panel C was collected by Diana R. Arnett.

To detect possible changes in the interaction of D474N with pol-prim subunits, binding of p180 1-323, primase, and p68 to anti-Tag beads in the presence and absence of Tag was tested in pulldown assays. Both p180 1-323 (Fig. 3.6A) and primase (Fig. 3.6B) bound to the antibody beads in a Tag-dependent manner, with no significant difference between WT and D474N Tag (compare lane 1 with lanes 2, 3 and with lanes 4, 5). Lastly, p68 association with Tag D474N resembled that with WT Tag (Fig. 3.6C), indicating that ATPase/helicase activity is dispensable for physical interaction of Tag with the p68 subunit of pol-prim. Thus Tag D474N appears to be a suitable protein to distinguish a potential role for Tag ATPase in primosome function independently of Tag docking with p68.

We then tested the activity of D474N Tag in the primosome assay. Importantly, D474N Tag relieved RPA-mediated inhibition of primer synthesis and extension on RPA-ssDNA template in a concentration-dependent manner, closely resembling the activity of the WT protein at equal concentrations (Fig. 3.6D and E; compare lanes 1-3 with lanes 4-6). This result demonstrates that Tag ATPase and helicase activity are dispensable for primosome activity on a pre-existing RPA-ssDNA template.

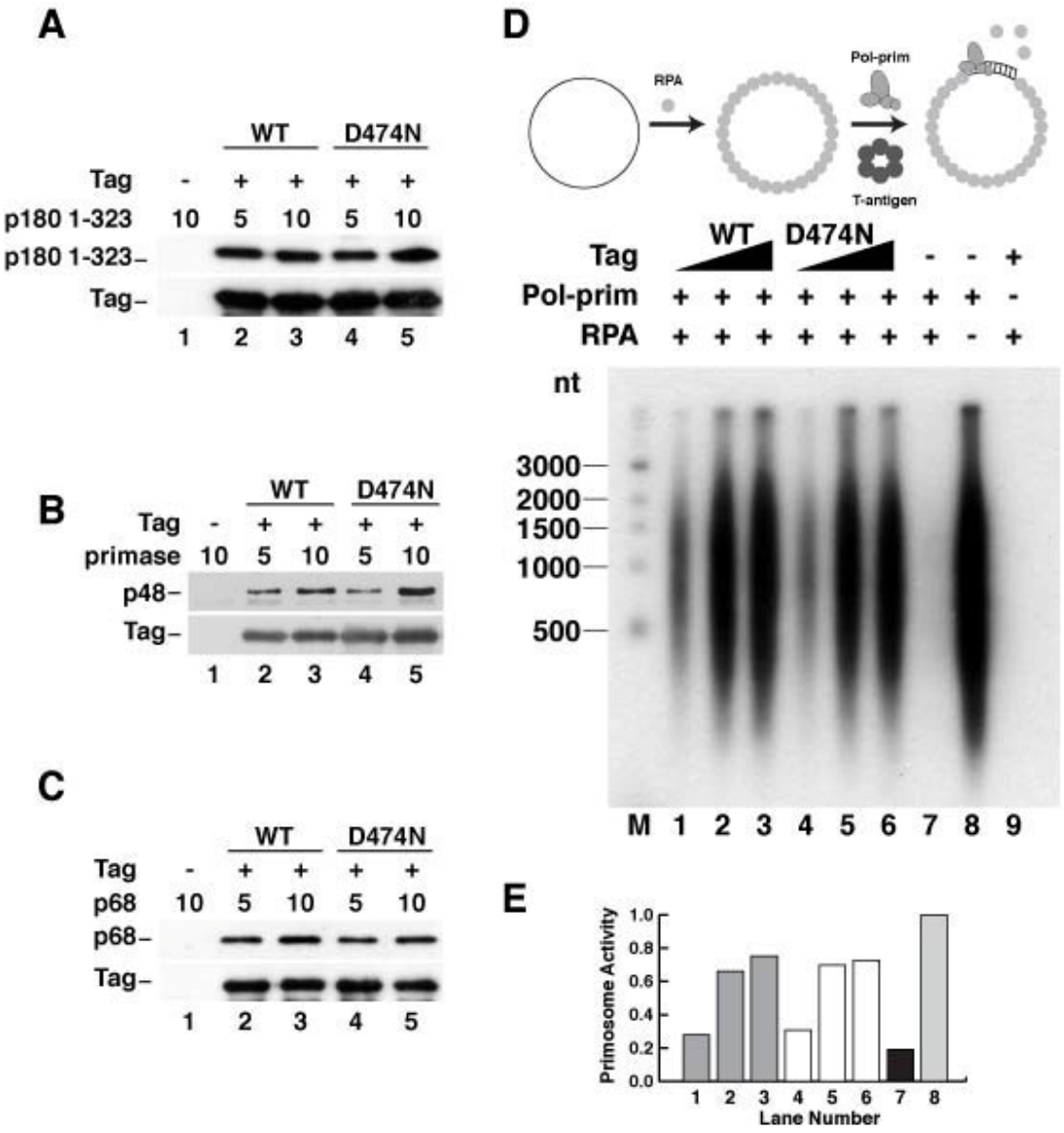

Figure 3.6. ATPase activity of Tag is not required for pol-prim binding or primosome activity on RPA-coated ssDNA. (A, B, C) Purified Tag WT or D474N bound to Pab101-coupled sepharose beads was incubated with increasing amounts of His-p180 1-323 (A), primase dimer (B), or His-p68 (C) as indicated (in μg). Proteins bound to the beads were separated by SDS-PAGE and visualized by Western-blotting with anti-His (Genscript, A00186) for p180, anti-p48, or anti-His (Abcam 9801) for p68, and Pab101 against Tag. (D) Primosome activity of 200, 400 or 600 ng of Tag WT (lanes 1-3) or D474N (lanes 4-6) was assayed on 100 ng ssDNA pre-coated with 1 μg RPA in the presence of 600 ng of pol-prim. Control reactions lacking Tag (lane 7), Tag and RPA (lane 8), or pol-prim (lane 9) are indicated. Reaction products were analyzed by alkaline electrophoresis and autoradiography. DNA size-markers are shown (M).

Figure 3.6, continued. (E) Reaction products were quantified; signal in the negative control reaction (lane 9) was subtracted from that in lanes 1-8. Incorporation in lanes 1-7 is expressed as a fraction of that in lane 8.

Discussion

A Specific p68N-Docking Site on Tag is Vital for SV40 Primosome Activity

We have mapped a p68-docking site on Tag that is disrupted by a charge-reverse substitution K425E, but not by a basic substitution K425R (Fig. 3.1, 3.2). The positive charge of Lys425 is consistent with the expected electrostatic interaction with an acidic surface of p68N [165]. Isothermal titration calorimetry of the binding interaction between the WT Tag and p68N indicated a low micromolar affinity typical of modular proteins, with both electrostatic and hydrophobic components [104, 165]. The overall affinity of the pol-prim/Tag interaction (Kd 12 nM) is more than 100-fold greater than that of Tag/p68 (Kd 6 μM), consistent with additional contacts between the Tag hexamer and other subunits of pol-prim [112, 117, 165]. The K425E substitution in Tag does not appear to disrupt p180 or primase docking on Tag, suggesting that the substitution specifically weakens p68N binding (Figs. 3.2, 3.3). Thus p180 and primase probably contact distinct sites on the surface of the Tag hexamer, giving rise to the robust interaction with the four-subunit polprim.

A recent alanine-scanning analysis of Tag provided additional evidence for an important functional role for Lys 425. In a panel of 61 alanine substitutions in conserved, charged surface residues of the hexameric helicase domain, K425A was one of only six substitutions that, when

individually tested in genomic SV40 DNA transfected into monkey cells, failed to generate viral progeny [170]. Notably, alanine substitutions in each of the other three residues in the patch 4 mutant Tag did not reduce plaque formation. Moreover, the patch 4 mutant Tag retained the ability to transform rodent cells, in contrast with patch 1 and 2 mutant Tag variants that lost p53 or p300/CBP binding activity, respectively, as well as cell transformation activity [170].

Lys 425 appears to be essential for Tag docking on p68N and SV40 primosome function (Figs. 3.2, 3.3), confirming and extending the evidence for p68 docking on Tag in primosome function [165]. Although an obvious potential role for p68-Tag docking in primosome function would be to recruit pol-prim, contacts of Tag with other pol-prim subunits are sufficient to maintain a strong interaction in the absence of p68N-Tag docking. Neither deletion of the N terminus of p68 [165] nor the Tag K425E charge reversal greatly diminished the interaction between Tag and pol-prim (Fig. 3.3B, C, D). Thus, we postulate that p68-Tag docking, together with the interactions of p180 and primase with Tag, may be needed to properly position pol-prim in order to allow primase access to template DNA exposed by Tag-OBD contacts with RPA [165] (Fig. 1A). This would be consistent with the extreme species-specificity of pol-prim in cell-free SV40 DNA replication. For example, although mouse and human pol-prim are highly conserved overall and Tag interacts physically with both enzymes, the degree of conservation of the N-termini of p68 is much lower and only primate pol-prim is active in the SV40 primosome [4, 171-173]. Moreover, although Lys425 is conserved among primate polyomavirus Tag proteins [170], it is not conserved among related viral helicases, e.g. papilloma virus E1 proteins, which also physically interact with and utilize pol-prim for viral DNA replication [174-176].

Architecture of the SV40 Primosome.

The working model that pol-prim docking with the Tag helicase domain enables pol-prim to access the template exposed by local Tag-RPA remodeling implies that Tag is essentially a scaffold that positions the primosomal proteins for a molecular handoff reaction. Upon assembly with pol-prim, the relatively symmetric Tag hexamer would be transformed into an asymmetric primosome. In the primosome assay used here, the availability of RPA-ssDNA template bypasses the need for unwinding and allows stepwise dissection of the protein interactions required to assemble the primosome. The dispensability of Tag ATPase/helicase activity in this assay (Figs. 3.5, 3.6), together with the requirement for Tag docking with RPA and pol-prim (Figs. 3.2, 3.3), suggests that the interactions among these primosomal proteins may be sufficient to support primer synthesis and extension in vitro. Interestingly, the ATPase activity of the *E. coli* PriA fork restart helicase is also dispensable for PriA-catalyzed primosome assembly in vitro [177, 178].

The identification of Lys425 as the first pol-prim docking site mapped on Tag provides some clues to the overall architecture of the viral primosome. Analysis of several hexameric helicases indicates that as the helicase tracks along one strand at the fork, either 5'-3' in prokaryotes or 3'-5' in archaea and eukaryotes, displacing the other strand, the motor domains face the duplex DNA [116, 160, 179-183]. In prokaryotic primosomes, the primase docks on (or is fused to) the N-terminal domain of the helicase and thus follows behind as the helicase tracks on the lagging strand template. In contrast, the p68-docking site at Lys425 resides on the C-terminal face of the AAA+ domains in the Tag hexamer (Fig. 3.2A, blue residues), facing the duplex DNA as Tag tracks on the leading strand template (Fig. 3.7). If pol-prim docks at the leading face of the Tag

helicase, as our data suggest, how might the SV40 primosome initiate Okazaki fragments on the lagging strand template? When the p68N domain docks at Lys425, it is tethered through an apparently unstructured linker (residues ~80-205) to the C-terminal p68 domain (residues 206-598), which in turn is tightly complexed with the C-terminal zinc domain of the p180 subunit [85, 165] (Fig. 3.7). The p58 subunit of the primase heterodimer is also complexed with the p180 zinc domain [77, 120]. Cryo-electron micrographs of a complex containing the structured C-terminal domains of yeast p68 (or B-subunit) and p180 indicate that the human p180/p68 complex is comparable in size to the hexameric Tag helicase domain [49, 85]. Based on these structures, and the current Tag/p68-docking data, we speculate that the catalytic domains of p180 and primase may be positioned at some distance from the helicase surface where the p68 N-terminus docks [165]. This flexible spatial relationship between Tag and pol-prim might facilitate pol-prim access to the lagging strand template, as suggested by a hypothetical model depicted in Figure 3.7. Clearly, the p180 and primase docking sites on Tag remain to be determined. Competition of p53 with pol-prim for binding to Tag [171, 184, 185] suggests that one of these docking sites may overlap with the p53-binding surface at the outer edge of each AAA+/D3 domain [169]. Since other aspects of the model may also be tested experimentally, we anticipate that it may prove useful in developing a better understanding of eukaryotic primosomes.

Coordination of DNA Unwinding and Primosome Functions at the Fork

In the replisome, the primosome handoff reaction is coupled with ATP hydrolysis and parental strand separation [3]. In prokaryotes, several mechanisms that coordinate primosome activity with DNA unwinding, and lagging with leading strand replisome movement, have been elucidated [3, 141, 142, 186-188]. However, it is not known whether or how such mechanisms might operate in eukaryotic replisomes. SV40 primosome activity appears to require interactions of a pol-prim heterotetramer with a Tag hexamer [84, 117, 125, 140, 165]. These interactions are stabilized in the presence of ATP or a nonhydrolyzable ATP analog [117]. Here we present evidence that ATPase/helicase activity is dispensable for primosome activity when RPA-ssDNA template is supplied (Figs. 3.5, 3.6). Thus SV40 primosome activity can be mutationally and biochemically uncoupled from DNA unwinding in vitro, raising the question of whether such uncoupling may occur transiently in the viral replisome during primer synthesis. Consistent with this possibility, pol-prim has been reported to substantially inhibit Tag helicase activity in the presence of RPA [140]. The requirements for this inhibition were essentially identical to those for primosome activity, except that primer synthesis was dispensable. Thus, it is tempting to speculate that docking of pol-prim subunits on Tag may reduce or inhibit its helicase activity, perhaps pausing 3'-5' helicase progression on the leading strand template to promote primosome activity on the lagging strand (Fig. 3.7). Dissociation of one or more subunits of pol-prim from the helicase after primer synthesis, extension into an RNA-DNA primer, or the switch to pol delta might "release the brakes" [6, 37]. However, this is clearly speculative and future work will be needed to understand how SV40 primosome activity is coordinated with DNA unwinding.

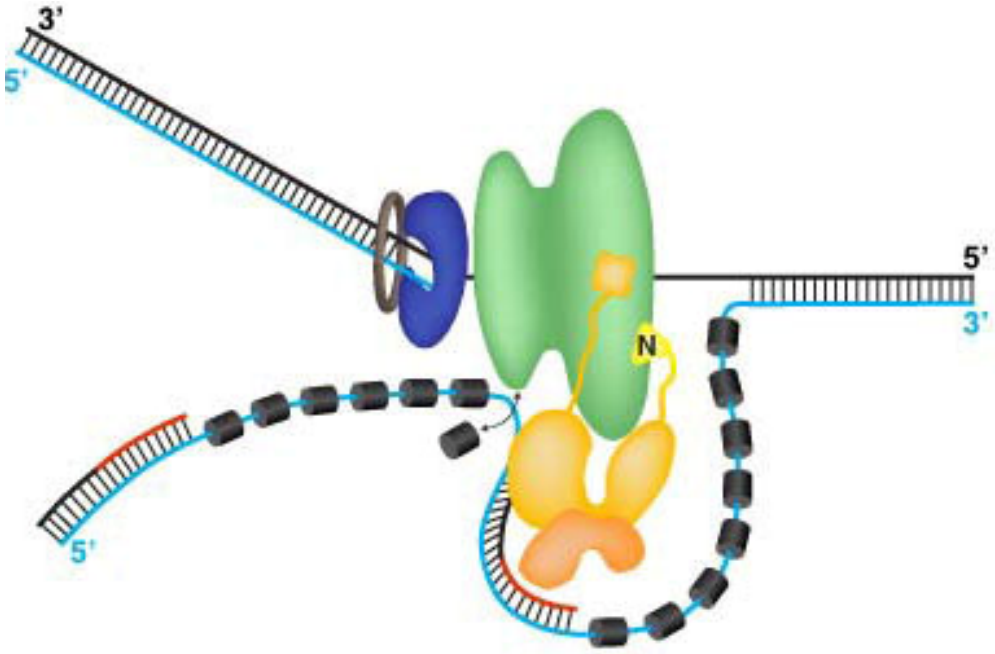

Figure 3.7. Speculative model of the SV40 primosome at a replication fork. A single Tag hexamer [62] tracking 3'-5' on the leading strand template (*black*) is followed by DNA polymerase delta (*blue*)-PCNA (*brown*) holoenzyme. The lagging strand template is displaced as Tag unwinds the duplex, but its point of exit from the helicase and its path after exit are controversial [48, 55, 61, 68, 71, 164]. Hence the path depicted here is the simplest possibility. RPA (*dark gray cylinders*) bound to the lagging strand template (*cyan line*) is remodeled by specific contacts with the OBDs of the Tag hexamer into a weaker ssDNA-binding mode [58, 59, 118] that is easily displaced [105], exposing the template. The p180/p68 (*gold*) subunits of pol-prim contact the helicase domains of Tag through p68N [165]; and the N-terminus of p180, which we propose are flexibly tethered to the pol-prim complex [111, 112, 117]. The primase p58/p48 (*orange*) interaction surfaces with Tag are not known [112]. Pol-prim correctly positioned on Tag is postulated to access the template exposed upon RPA remodeling, synthesize an RNA primer (*red line*) and extend it (*black line*), yielding an RNA-DNA primer. The subsequent PCNA clamp-loading and switch to DNA polymerase delta holoenzyme are not depicted [6, 37]. Artwork courtesy of Diana R. Arnett.

CHAPTER IV

CONCLUSION AND FUTURE DIRECTIONS

The Tag-p68 Interaction is Essential for SV40 Primosome Activity

This thesis contains a systematic characterization of the interaction between the SV40 helicase Tag and the p68 subunit of DNA pol-prim, using a combination of biochemical, structural, and functional approaches. Tag is at the core of the SV40 replisome and orchestrates SV40 primosome assembly. p68 had been previously shown to be required for SV40 primosome activity and to bind directly to Tag. We aimed to explore a functional link between Tag-p68 interaction and primosome activity.

In Chapter II, we mapped the interacting domains of Tag and p68 using yeast two-hybrid and pull-down assays. A previously unrecognized N-terminal domain of p68 (p68N，residues 1-78) was identified to interact with the helicase domain (residues 357-627) of Tag. The solution structure of p68N was determined by NMR spectroscopy in the Chazin lab. It adopts a compact, four-helical fold. The p68N deletion mutant of pol-prim was shown to be defective in primosome activity at the origin of SV40 replication in the monopolymerase assay as well as on RPA-coated ssDNA in the primosome assay. The putative Tag-interacting surface on p68N was further mapped by NMR spectroscopy to a hydrophobic patch surrounded by negative charges. This hydrophobic patch is mainly composed of Ile^{14} and Phe^{15} of p68N. A series of site-directed substitutions of Ile^{14} and Phe^{15} were made and tested for their binding with Tag. The I14A

substitution was finally chosen for functional studies as it decreases Tag binding, but does not alter the structural integrity of p68N. The p68 I14A mutant pol-prim decreases primosome activity in proportion to its binding deficiency for Tag.

In Chapter III, we further mapped the p68N-docking site on Tag by using structure-guided mutagenesis of the Tag helicase surface. A charge-reversal substitution in Tag K425E disrupted p68N-binding and primosome activity, but did not affect docking with other pol-prim subunits. Unexpectedly, this substitution also disrupted Tag ATPase and helicase activity, suggesting a potential link between p68N docking and ATPase/helicase activity. To assess this possibility, we generated the Tag D474N mutant protein, in which the helicase Walker B motif is disrupted. Although the D474N substitution abolished ATPase and helicase activities as expected, it did not affect pol-prim docking on Tag or primosome activity on RPA-coated ssDNA, indicating that Tag helicase activity is dispensable for primosome activity on the lagging strand *in vitro*. These data collectively provide strong evidence for a crucial role of p68-Tag interaction in the SV40 primosome activity. They also suggest a potential mechanism for coordination of helicase and primosome functions of Tag during lagging strand synthesis, which will be discussed further in this chapter.

A model is proposed for how p68-Tag interaction regulates the SV40 primosome activity (Fig. 2.7). Based on this model, the p68-Tag interaction plays at least two important roles in SV40 primosome. First, this interaction increases the overall affinity of the Tag/pol-prim complex, which probably enhances pol-prim recruitment to ssDNA template. Second but most important, it cooperates with other pol-prim subunits to position the primase appropriately for priming on

ssDNA exposed via Tag-mediated conformational remodeling of RPA. In this view, loss of p68N docking with Tag would result in an excessively mobile Tag/pol-prim assembly which fails to position primase properly for priming. The importance of p68 positioning the primase is supported by the cryo-EM studies showing that the p68CTD-p180CTD interaction module displays extensive flexibility [85]. In both p68 and p180, the N-terminus is connected to the C-terminal domain through a long and flexible linker. Independent docking of the two N-termini with Tag would constrain the flexibility of the Tag/pol-prim assembly, and thereby enable proper positioning of the primase subunits on the template.

This model could be further validated through structural and biochemical approaches. Toward this end, we have begun a collaboration to determine the structure of Tag/pol-prim complex by cryo-EM. Previous EM studies of pol-prim indicated that the primase subunits likely produce excess noise, which made data processing challenging. To overcome this impediment, initial experiments will be done with the p180-p68 heterodimer to reduce structural complexity. Both Tag and p180-p68 heterodimer can be purified at milligram levels in our laboratory. The cryo-EM structures of the Tag/pol-prim complex are expected to display less flexibility than the pol-prim itself, and deletion of either p68N or p180N is predicted to increase the flexibility to some extent.

Also in this model, the p68CTD-p180CTD interaction is predicted to be an important anchor and p68N is connected to it via a flexible linker. If the stability of p68CTD-p180CTD is disrupted to some extent but their association is still retained, the primosome activity of pol-prim should be affected. Based on the co-crystal structure of p68CTD-p180CTD [85], we are able to identify the

interface between the two proteins. As p180CTD also interacts with primase, mutations in p180CTD may affect its association with primase as well. In this case, it will be interesting to mutate residues of p68CTD that make contacts with p180CTD. These mutations should not affect the primase and polymerase activities of pol-prim as p68 is not required for either activity. Mutations that decrease the stability of p68CTD-p180CTD interaction but still retain the association can be incorporated into pol-prim and purified to test for their primosome activities. Since the interface between p68 and p180 involves at least two independent regions, finding such mutants seems feasible. If our hypothesis is correct, the primosome activities of these mutants should decrease without reducing polymerase or primase activity or interaction with Tag.

The Tag-p68 interaction displays common features of other interactions involved in DNA processing. This interaction involves modular domains with moderate affinity (Kd~6 μM), which allows dynamic regulation [104]. Previous studies in our lab showed that phosphorylation of p68 by cyclin A/E-Cdk2 inhibits the primosome activity of pol-prim *in vitro*[84], but the underlying mechanism remains elusive. It is interesting to note that the phosphorylation sites are located in the linker region that connects the p68N and p68CTD. Thus, one possible explanation for the observation that phosphorylation of p68 inhibits primosome activity is that phosphorylation of p68 induces some conformational change that affects proper docking of p68N on Tag, and therefore disrupts the primosome activity.

What activities of Tag are required for the SV40 primosome operation has been an intriguing question for a long time. These activities were previously proposed to include DNA helicase activity to unwind the duplex DNA and protein-protein interactions with pol-prim and RPA that

mediate recruitment [189]. This should be true for primosome assembly at the SV40 origin, but our data of Tag D474N suggest that protein-protein interactions of Tag cxsfwith pol-prim and RPA are sufficient to orchestrate primosome assembly on the lagging strand and that helicase activity is dispensable.

In prokaryotes, transient uncoupling of the helicase and primosome function on the lagging strand has been proposed to coordinate DNA unwinding with primosome assembly, thus preventing leading stand synthesis from outpacing lagging strand synthesis [3, 141, 186-188]. The finding that SV40 primosome assembly on RPA-coated ssDNA does not require helicase activity suggests that SV40 might employ a similar mechanism to coordinate DNA unwinding with primosme function, which will be discussed in detail later. The modular and moderate affinity properties of Tag-p68 interaction actually might facilitate such regulation. In addition, the fact that the p68N docking site on Tag is close to the ATP binding site might provide additional insight into how such regulation might be achieved.

The Tag/pol-prim Interaction: Implications for Eukaryotic Replisome

Data in this dissertation together with previous findings collectively suggest that the Tag/pol-prim interaction is essential to orchestrate the SV40 primosome assembly. This finding raises a more challenging question: how might pol-prim recruitment and primosome assembly be achieved in eukaryotic genomic DNA replication?

Eukaryotic DNA replication is a highly complex process. Replication in eukaryotic cells depends on the formation of a pre-replicative complex (pre-RC), which is composed of the origin

recognition complex [85], Cdc6, Cdt1 and the Mcm2-7 helicase, at origins of replication [190]. Activation of the pre-RC through a series of phosphorylation events by cyclin- and Dbf4-dependent kinases [191, 192] and concurrent recruitment of key factors including Mcm10, cdc45 and the GINS complex to the origin lead to origin unwinding [143, 144, 161, 193, 194]. Replication initiates following RPA and DNA pol-prim loading onto ssDNA. The association of RFC, PCNA, the leading strand pol ε and the lagging strand pol δ completes the replisome [38].

Initiation of DNA replication at a cellular origin requires recruitment of pol-prim to assemble a functional primosome. In SV40, the helicase Tag directly binds to pol-prim and loads it onto the origin of replication. Although the Mcm2-7 helicase shares similarity with Tag in terms of the 3'-5' translocation direction and head-to-head assembly mode [146, 147], recruitment of pol-prim in eukaryotes is likely mediated by several accessory proteins. In *S.cerevisiae*, Mcm10 has been shown to physically interact with and stabilize the p180 subunit of pol-prim and to recruit the complex to origins of replication [195-198]. Ctf4, another replication factor that associates with Mcm10, has been reported to physically interact with and stabilize p180 on chromatin in human cells [152]. Interaction between Ctf4 and Mcm10 has been shown to be important for pol-prim loading onto chromatin during initiation of replication in extracts of *Xenopus* eggs [152]. In this view, recruitment of pol-prim to origins of replication in eukaryotes likely occurs through physical interaction of the p180 subunit with Mcm10 and/or Ctf4. However, it is noteworthy that recruitment itself is not sufficient for assembly of a functional primosome, based on what we have learned from the SV40 model system. Multiple interactions between Tag and pol-prim are required to place the primase subunits on an appropriate template for priming. Indeed, physical

interactions between other subunits of pol-prim with initiation factors haven been observed. The human GINS protein has been shown to physically interact with the primase subunits [199] and human Cdc45 has been reported to bind directly to the p68 subunit [200]. Thus, multiple and dynamic linkages between pol-prim and the Mcm 2-7 helicase that may be achieved indirectly through regulatory proteins such as Mcm10, Ctf4, Cdc45 and GINS, and these may drive the assembly of a functional eukaryotic primosome at an origin of DNA replication.

During the elongation phase, the Mcm2-7 helicase, surrounded by many regulatory proteins, migrates along with the replication fork (Fig. 1.1B). These regulatory proteins assemble around the Mcm2-7 helicase to form the replisome progression complex (RPC) [144]. RPC proteins include GINS, Cdc45, Ctf4, Mcm10, Mrc1, Tof1-Csm3, FACT and topoisomerase I. The consequences of RPC formation are likely to keep the Mcm2-7 helicase in an active form and to connect the helicase to other components within the replisome such as DNA polymerases. Linkage between the helicase and polymerase is necessary for maintaining genome stability. Functional uncoupling of the helicase and the polymerase would result in accumulation of RPA-coated ssDNA that leads to checkpoint activation [201]. Consistent with this idea, the RPC protein Mrc1 has been shown to associate with the leading strand pol ε throughout the cell cycle and plays an important role in determining the progression rate of the replication fork [202]. An analogous link is expected between the helicase Mcm2-7 and pol-prim, as pol-prim is repeatedly required for priming on the lagging strand. RPC proteins including Mcm10, Ctf4, Cdc45 and GINS are likely candidates to serve as such links, similar to the case at the origin of replication. Indeed, both Ctf4 and Mcm10 have been shown to play important roles in coupling the Mcm2-7

helicase to pol-prim at the replication fork [153, 203].

In summary, multiple and dynamic linkages between the Mcm2-7 helicase and the primase-containing pol-prim can be established through regulatory proteins that associate with both of them, and hence enable proper priming at the origin of replication, as well as on the lagging strand. Future insight into the architecture of the eukaryotic primosome will require systematic characterization of the interactions between subunits of pol-prim with RPC proteins. The modular strategy that we used for characterizing the interaction of Tag/RPA or Tag/pol-prim can be applied.

Roles of Pol-prim at Stalled Replication Forks

Besides its essential role in DNA replication, the activity of pol-prim is also required for activation of ATR checkpoint signaling by generating the 5' recessed ssDNA-dsDNA junction to load the Rad9-Rad1-Hus1 (9-1-1) complex at stalled replication forks [75]. Accumulating evidence suggests that pol-prim and the 9-1-1 complex are recruited onto chromatin in a TopBP1-dependent manner [151]. In this view, it might be interesting to test whether TopBP1 interacts with subunits of pol-prim, and thus loading pol-prim onto sites of stalled replication forks. In addition, accumulation of RPA-coated ssDNA also serves as a platform to recruit checkpoint proteins [75]. Unpublished data in our lab suggests that human DNA helicase B (HDHB) gets recruited to stalled replication forks by RPA (Guler and Fanning, unpublished data), and HDHB has been shown to interact with pol-prim [204]. So, it might also be interesting to test whether HDHB recruits pol-prim to stalled replication forks to provide the primosome activity.

The Helicase-primase Interaction: Lessons from Prokaryotic Replisomes

The interaction between helicase and primase has been well characterized in prokaryotic *E.coli* and phage T7 replisomes (Fig. 4.1). In *E.coli,* the DnaB helicase is a two-domain protein with an N-terminal interaction domain and a C-terminal helicase domain. The N-terminal domain, together with the linker, mediates interaction with the DnaG primase. DnaG contains three independent domains connected by flexible linkers. An N-terminal zinc-binding domain plays a critical role in recognizing the trinucleotide initiation sequence on ssDNA template. An RNA polymerase domain carries out primer synthesis. A C-terminal interaction domain interacts with the helicase (Fig. 4.1) [116]. Through this, DnaB and DnaG regulate each other's activities. DnaG increases both the ATPase and the helicase activities of DnaB [205], while DnaB stimulates primer synthesis and affects the size of the primer, as well as initiation specificity by DnaG [206-208]. A co-crystal structure of the DnaB helicase in complex with the C-terminal DnaB interaction domain of DnaG has been determined [179]. The structure showed that three monomers of the C-terminal domain of DnaG bound to the dimer interface of the N-terminal domain of the hexameric DnaB, in agreement with previous observations that DnaG primases form a complex with the hexameric DnaB in a stoichiometry of 3:1 [205].

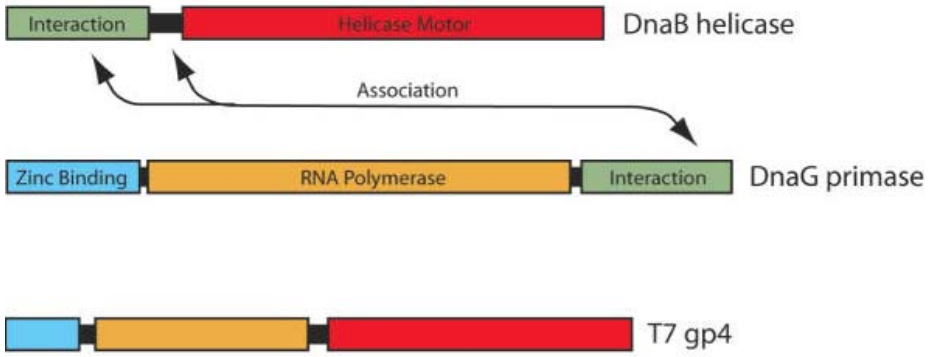

Figure 4.1. Domain organization of *E.coli* and phage T7 helicase/primase systems. Bacterial DnaB is a two-domain protein with an N-terminal interaction domain and a C-terminal helicase domain. DnaG is a three-domain protein with an N-terminal regulatory Zinc Binding Domain, central RNA Polymerase Domain and C-terminal Interaction Domain. Known areas of interaction between the two proteins are shown as arrows. The phage T7 gp4 protein, on the other hand, fuses DnaB- and DnaG-related domains into a single polypeptide [116].

In bacteriophage T7, the gp4 protein fuses the DnaG-like primase with the Dna B-related helicase domain into a single polypeptide by deletion of the interaction domains [3]. The gp4 protein therefore has three functional domains connected by flexible linkers: the N-terminal zinc-binding domain, the RNA polymerase domain, and the helicase domain. Thus, the primase and helicase are covalently connected in T7. Two forms of gp4 co-exist in T7-infected cells [209]. The full-length 63 kDa protein contains all three domains and has both primase and helicase activities, while the 56 kDa form lacks the zinc-binding domain, and consequently loses its primase activity. A mixture of the two isoforms assembles into mixed oligomers with full primase and helicase activities [210]. The crystal structure of the 56 kDa gp4 has been determined in a heptamer form [211]. But a hexameric form of the 63 kDa protein was seen by electron microscopy [211] and the structure of the helicase domain alone has been determined and a hexamer is found [63]. Given that the two isoforms exist in equal amounts in T7-infected cells, a

stoichiometry of three functional primases per helicase hexamer can also be achieved if the two forms alternate within a helicase hexamer.

Template-directed primer synthesis by prokaryotic primase requires an interaction between the zinc-binding motif and the RNA polymerase domain [116]. Association of primase with helicase is likely to increase the local concentration of ssDNA template relative to primase. This interaction could occur within the same primase monomer (*cis* mode) or between the two adjacent primase monomers (*trans* mode) within the hexameric helicase. A stoichiometry of three primases per helicase hexamer might be an optimal spatial arrangement for the *trans* mode interaction (Fig. 4.2). Single-molecule measurements of enzymatic kinetics of the T7 replisome suggested that the *trans* mode of primer synthesis could stop the helicase movement and hence the leading-strand synthesis [186]. This pause would save time for slower synthesis by primase and thus prevent leading-strand synthesis from outpacing lagging strand synthesis. Similarly, single-molecule studies of the dynamics of the *E.coli* replisome showed that cooperative binding of two or three DnaG monomers to DnaB halts helicase activity and decreases leading strand synthesis [187]. This pausing, however, is dependent on cooperative DnaG-DnaB protein-protein interaction rather than on primer synthesis. In both systems, cross-talk between adjacent primase monomers, either *trans* mode interaction between DnaG monomers in *E.coli* or *trans* mode primer synthesis by gp4 in T7, is necessary to signal the helicase to stop and consequently prevents leading-strand synthesis from outpacing lagging strand synthesis. Nonetheless, association of multiple primases with a helicase hexamer is a prerequisite.

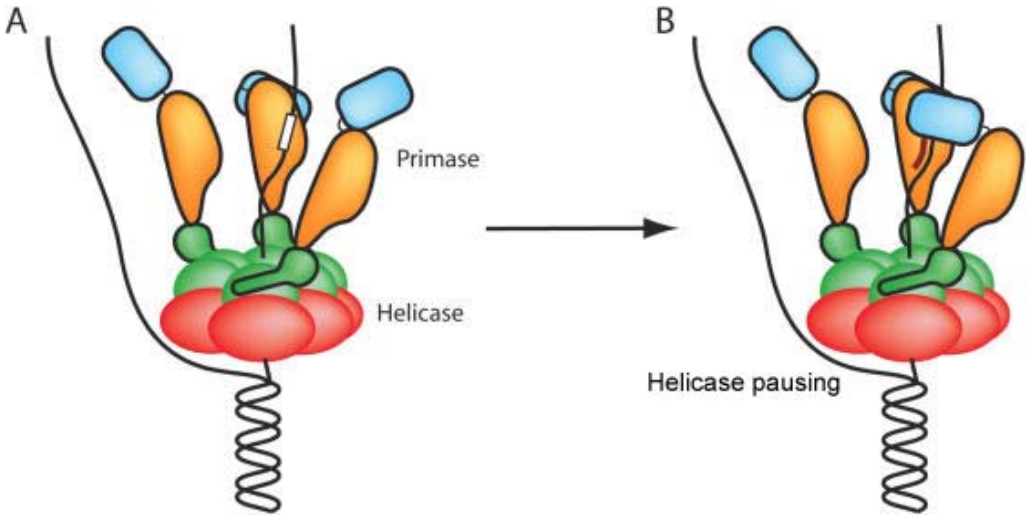

Figure 4.2. Model for the functional coordination of multiple primases bound to the replicative helicase. Domains of the DnaG primase are outlined in black, while those of the DnaB helicase are not. Domains are colored as in Fig. 4.1. (A) Three primases associate with a helicase hexamer. As the helicase unwinds the parental strands, ssDNA containing a trinucleotide primer initiation site (white rectangle) is extruded from the helicase ring. (B) The Zinc binding domain of one primase molecule may form a complex with a second primase's RNA polymerase domain (*trans* mode), resulting in an active complex that allows primer synthesis and sigals the helicase to pause. Adapted from [116].

Summary

Primase has evolved from a monomer in prokaryotes to a heterotetramer in eukaryotes. Instead of just synthesizing small RNA primers, the eukaryotic primase pol-prim synthesizes a chimeric DNA-RNA primer as it possesses both primase and polymerase activities [31]. The SV40 replication system has been used as a model to study eukaryotic replication. In this system, the helicase Tag interacts with pol-prim and stimulates the priming activity of pol-prim. Work presented in this thesis demonstrates that the p68 subunit of pol-prim directly binds to the SV40 helicase Tag and p68-Tag interaction is vital for viral primosome activity. The p180 subunit and the primase have been shown to bind to Tag as well. Taken together, at least three subunits of pol-prim are involved in Tag binding [110, 111, 118]. The pol-prim heterotetramer interacts with

the Tag hexamer in a stoichiometry of 1:1 [117], suggesting that three subunits of one pol-prim contacts Tag within a hexamer. This scenario appears to mimic association of three primase monomers with a helicase hexamer in *E.coli* and T7. Whether this association mode plays a similar role in pausing helicase activity and coordinating the leading-strand synthesis with the lagging-strand synthesis at the SV40 replication fork becomes very intriguing.

The model proposed in chapter II (Fig. 2.7) suggested that multiple interactions with Tag are necessary to enable pol-prim recruitment to ssDNA template and position it appropriately for primer synthesis. Pol-prim was shown to be able to inhibit the origin unwinding activity of Tag in the presence of RPA and the requirements for this inhibition are the same as those for primer synthesis, except that primer synthesis is dispensable [140]. This observation is reminiscent of the observation that helicase halting at the *E.coli* replication fork, which depends on DnaB-DnaG interaction rather than primer synthesis. In this view, it is reasonable to envision that full association of pol-prim with Tag could play at least two important roles besides recruitment. First, it may enable pol-prim to initiate primer synthesis on ssDNA template. Second, it may function as a brake to stop the helicase movement and hence coordinate the leading-strand synthesis with lagging-strand synthesis, analogous to the function in T7 and *E.coli*. Dissociation of one or more subunits of pol-prim from Tag after primer synthesis might release the brake. The modular and moderate affinity properties of the Tag/pol-prim interaction would facilitate such regulation.

It is also noteworthy that the p68 docking site on Tag that was identified in Chapter III is close to the ATP binding pocket. Association of pol-prim with Tag helicase is then likely to inhibit the helicase activity through blocking ATP binding or inhibiting ATP hydrolysis. To test

whether multiple contacts between pol-prim and Tag are required for pausing the helicase activity, the first task is to map out each of these contacts. Then mutant pol-prim proteins that attenuate interaction with Tag need to be made and tested to see whether they are able to inhibit the Tag helicase activity. Application of single-molecule techniques in SV40 replication system is also feasible as its replisome can be reconstituted with just a few purified proteins like that of T7 and *E.coli*. Analysis of enzymatic kinetics at the SV40 replication fork would directly show us whether the association of pol-prim with Tag can act as a brake to stop replication fork progression and to coordinate leading-strand synthesis with the lagging-strand synthesis. Tag and pol-prim might represent a novel helicase-primase interaction that acts as a brake to stop helicase movement, and thereby achieve coordination of DNA unwinding with primosome function.

APPENDIX A

This chapter presents a brief synopsis of the experimental work that I contributed to a collaborative publication on DNA primase: Weiner, B. E., Huang, H., Dattilo, B. M., Nilges, M. J., Fanning, E., Chazin, W. J. An iron-sulfur cluster in the C-terminal domain of the p58 subunit of human DNA primase. J Biol Chem. 2007 Nov 4; 282(46): 33444-51.

Introduction

DNA primase is a specialized DNA-dependent RNA polymerase that can synthesize short RNA molecules used as primers for DNA polymerase during DNA replication [31]. Eukaryotic primase is a heterodimer consisting of p48 and p58 subunits, and is normally associated with DNA polymerase alpha through the interaction of p58 with p180 [31]. The p48 subunit contains the catalytic active site. Three aspartates, Asp 109, Asp111, and Asp 306, have been proposed to coordinate metal binding in the p48 active site [87]. The p58 subunit does not have enzymatic activity, but it is crutial for primase activity. p58 stabilizes p48 and stimulates p48 activity *in vitro* [88]. The p58 subunit has been shown to be important for primer initiation, elongation and primer length counting [89]. In addition, the ability of p58 to interact with both primer and template suggests a potential role of p58 to mediate the transfer of RNA primer to the active site of DNA polymerase alpha [90].

Primer synthesis involves steps of template binding, NTP binding, initiation, extension and transfer of the RNA primer to DNA polymerase alpha catalytic subunit [31]. The rate-limiting

step of initiation is the dinucleotide formation from the first two individual ribonucleotides [95]. The primase synthesizes a 7-10 nucleotide RNA primer, without dissociation, the RNA primer is then handed to DNA polymerase alpha and extended to a chimeric RNA-DNA primer of about 30 nucleotides [96].

Although primase is essential for DNA replication, very little is known about its structural information. The only available structure for a heterodimeric primase is from the archaeal *Sulfolobus solfataricus* (*Sso*) [212] , and this primase does not associate with DNA polymerase alpha. The *Sso* core primase is formed by its small (PriS) subunit, which has homology with p48, and the N-terminal half of the large (PriL) subunit, which shares homology with the N-terminal region of p58. But this structure does not include the C-terminal domain of PriL. The structure suggests that PriL is unlikely to be directed involved in the catalytic steps of primer synthesis as it is away from the enzymatic active site of PriS. However, for human primase, both the N- and C-terminal regions of p58 contact p48 [88]. Particularly, a region in the C-terminal half of p58 has homology to an 8 kDa domain of DNA polymerase β, and this region is suggested to be important for primer initiation, elongation and counting [89].

Given the important function of p58 during primer synthesis, it is vital to elucidate its structure. The human p58 and p48 subunits can be expressed and purified as a heterodimer that retains primase activity. In the Chazin laboratory, limited proteolytic digestion, together with mass spectrometry and N-terminal sequence identified a structured domain in the C-terminus of the p58 subunit (p58C, residues 266-509). When either the primase dimer or p58C was purified, the protein solution displayed a golden-brown color. The color intensified as the protein was

concentrated, becoming very dark at high concentrations. The absorption spectrum of p58C showed a broad shoulder around 400 nanometers [142], similar to spectra from proteins containing iron-sulfur clusters. The primase dimer also had this property, whereas isolated p48 did not. EPR analysis of p58C under oxidation condition produced a spectrum that is consistent with the presence of a HiPIP like $[4Fe\text{-}4S]^{3+}$ cluster [91].

To identify the iron-sulfur ligands in p58C, we performed multiple sequence alignment of p58 across five different species and identified four conserved cysteines that are most likely to coordinate the cluster binding. To investigate the role of the iron-sulfur cluster in primase activity, we generated a mutant human primase heterodimer, in which one of the conserved cysteines ligands (C367) in p58 was replaced by serine. UV visible spectroscopy analysis of this mutant showed no broad peak at 400 nm, suggested that this mutant primase does not contain an iron-sulfur cluster. This mutant displayed reduced primase activity in an *in-vitro* assay, suggesting that the iron-sulfur cluster is essential for the primase activity.

Materials and Methods

Primase Construct Design

The recombinant human p48/p58 primase expression plasmids, pET21a-Hp48 and pACYC184-Hp58, have been previously described (18). The C367S mutation was generated in the p58C expression plasmid pET15b by site-directed mutagenesis (QuikChange, Stratagene), and verified by DNA sequencing. A SphI-BglII fragment of p58C containing the C367S mutation

was then used to replace the corresponding wild-type fragment in pACYC184-Hp58 to produce p48/p58 C367S.

Protein Expression and Purification

Each construct was expressed in BL21 (DE3) cells. Cells were grown at 37 °C in LB to an A_{600} of ~0.6. The temperature was then lowered to 22 °C, and the cells were allowed to equilibrate for 30 min. Expression was induced using 1mM isopropyl thio-β-D-galactopyranoside. Cells were harvested by centrifugation 4 h postinduction. Pelleted cells were resuspended in lysis buffer containing 50 mM Tris-HCl (pH 8), 300mM NaCl, 20mM imidazole, 3mM 2-mercaptoethanol (BME), 1% Nonidet P-40, 0.5 mg/ml lysozyme, ~10 mg of DNase I, and one Complete Mini EDTA-Free protease inhibitor mixture tablet (Roche Applied Science). Cells were lysed by sonication at 4 °C. Insoluble material was removed by centrifugation. The primase polypeptides were purified using nickel-nitrilotriacetic acid affinity chromatography. The bound proteins were eluted using a linear imidazole gradient ranging from 20mM to 250 mM. Fractions containing the primase polypeptides were pooled and dialyzed overnight at 4 °C into buffer containing 30 mM MES (pH 6.5), 50 mM NaCl, and 3 mM BME. The sample was then further purified using a Mono S column (Amersham Biosciences) equilibrated in the same buffer and eluted with a linear gradient to 1 M NaCl.

Multiple Sequence Alignment

Amino acid sequences of p58 from *Homo sapiens*, *Mus musculus*, *Drosophila melanogaster*,

Caenorhabditis elegans, and *Saccharomyces cerevisiae* were aligned using ClustalX.

UV-visible Spectrophotometry

Spectra were recorded using a Varian Cary 100 Bio spectrophotometer. Samples were scanned from 550 to 250 nm at room temperature in buffer containing 20 mM Tris (pH 7.5), 50 mM NaCl, and 3 mM BME.

Primase Assay

The activity of wild-type and mutant primases was tested on M13mp18 ssDNA (USB Corp., Cleveland, OH). Reactions (20 ul) contained 0-8 pmol of primase, 100 ng of M13 DNA, in reaction buffer (30mM HEPES-KOH (pH 7.9), 1 mM dithiothreitol, 7 mM magnesium acetate, 4 mM ATP, 0.2mM UTP, 0.2mM GTP, 0.01 mM CTP) and 20 uCi of [γ^{-32}P]CTP (3000 Ci/mmol, PerkinElmer Life Sciences, Boston,MA). Reactions were assembled on ice and incubated at 37 °C for 90 min. Reaction products were precipitated with 2% $NaClO_4$ in acetone, washed with acetone, and dried. Reaction products were dissolved in formamide loading buffer (45% v/v formamide, 5 mM EDTA) at 65 °C for 10 min and resolved by denaturing 20% polyacrylamide gel electrophoresis for 4-5 h at 500 V, monitored using 0.08% w/v xylene cyanol and 0.08% bromphenol blue as markers. The reaction products were visualized and quantified by phosphorimaging.

Results

Identification of Iron-Sulfur Ligands in p58C

Iron-sulfur clusters are typically bound to proteins via four cysteine residues, and p58C contains six cysteine residues. Following the strategy used for other DNA-processing proteins that contain an iron-sulfur cluster, potential cysteine ligands were identified from a multiple sequence alignment of p58 from five different species using ClustalX. The alignment in Fig. A.1a reveals that four of the cysteine residues (Cys-287, Cys-367, Cys-384, and Cys-424) are conserved. These are residues most likely responsible for cluster binding. To test this hypothesis, each of the four cysteine residues in p58C was individually mutated to serine. Although the mutant constructs expressed well, they were poorly soluble and degraded rapidly (data not shown). Consequently, an alternate strategy was used involving mutation in the context of the p48/p58 dimer. Data are shown here for the C367S mutant primase dimer, which was expressed at levels comparable to the wild-type primase, remained soluble, and co-purified with the p48 subunit (Fig. A.1b). Analysis of this mutant primase dimer by UVvisible spectroscopy provided a spectrum in which the broad peak at 400 nm was clearly absent (Fig. A.1c), confirming this mutant primase does not contain an iron-sulfur cluster.

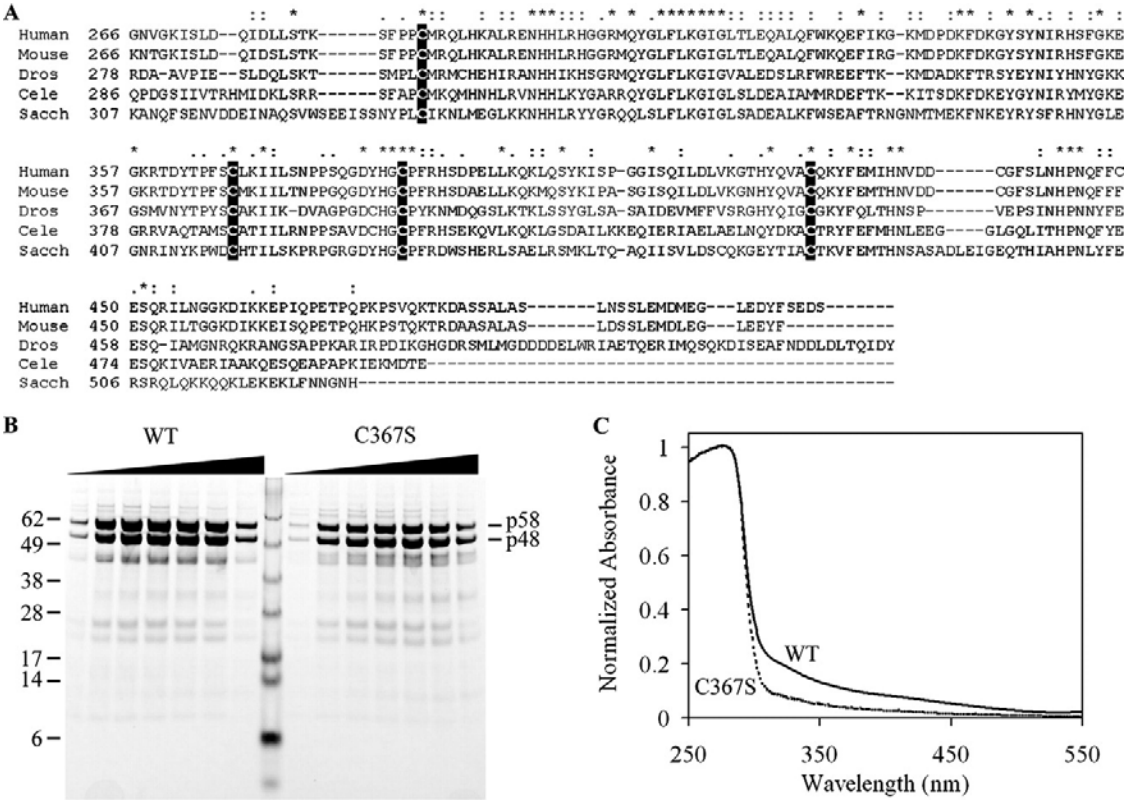

Figure A.1. The p58C iron-sulfur cluster is coordinated by four conserved cysteines. (a) Multiple sequence alignment of p58 proteins. Sequences are shown for: *H. sapiens* (*Human*), *M. musculus* (*Mouse*), *D. melanogaster* (*Dros*), *C. elegans* (*Cele*), and *S. cerevisiae* (*Sacch*). The four *highlighted* cysteine residues are conserved, suggesting they serve as ligands for the iron-sulfur cluster. (b) Ni-purified p48/p58 WT (*left*) and p48/C367S-p58 mutant (*right*) were visualized by SDS-PAGE and Coomassie staining. Lanes represent fractions collected during nickel-nitrilotriacetic acid purification as the concentration of imidazole is increased using a linear gradient. (c) UV-visible spectrum of WT p48/p58 (*solid line*) and p48/C367S-p58 (*dashed line*) p48/p58 primase. Data were collected by Brian E. Weiner.

A Role for the Iron-Sulfur Cluster in Primase Function

To initially assess the functional relevance of the iron-sulfur cluster in p58, the primase activity of wild-type and p48/C367S-p58 primase dimers on a natural ssDNA template was assayed as a function of protein concentration. Radiolabeled CTP was incorporated into RNA

primers of 8-10 nucleotides by the wild-type primase (Fig. A.2a, *lanes 1-3*), and small amounts of larger products were detectable, as observed previously. No RNA primers were observed in the absence of enzyme (Fig. A.2a, *lane 7*). Products of the mutant primase that lacks the iron-sulfur cluster were barely detectable above background (Fig. A.2a, *lanes 4-6*), and the level of reaction product was not proportional to the amount of mutant primase in the reaction. Quantification of the products as a function of primase concentration revealed that the specific activity of the mutant primase was reduced at least 5-fold (Fig. A.2b). These data suggest that the iron-sulfur cluster in p58 is crucial for the primase activity of p48/p58 in this assay.

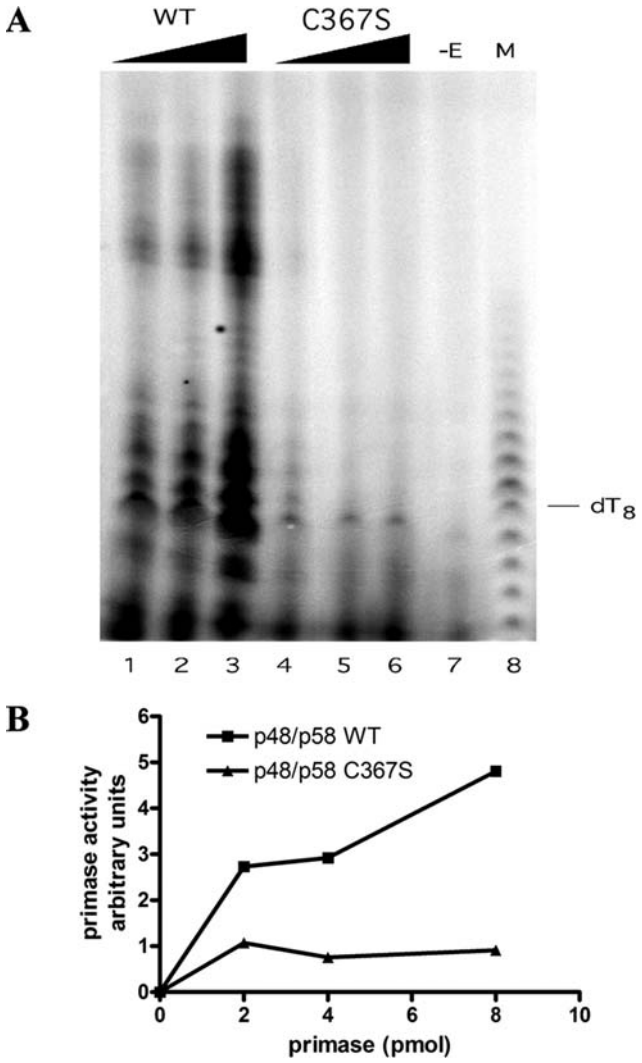

Figure A.2. Primase activity of p48/p58 requires the iron-sulfur cluster. (a) Radiolabeled primers synthesized by wild-type (*WT*) p48/p58 (*lanes 1-3*) or mutant C367S (*lanes 4-6*) on M13 ssDNA template were visualized by denaturing gel electrophoresis and phosphorimaging. Products of a control reaction without enzyme (*-E*) are shown in *lane 7*. *M*, radiolabeled dT4-22 markers (*lane 8*). (b) Primase products were quantified using PhosphorImager software. Incorporation in the negative control reaction (*a*, *lane 7*) was subtracted from those in *lanes 1-6* and graphed as a function of primase concentration.

Discussion

The work described in this chapter showed that the iron-sulfur cluster in human p58C that is coordinated by four conserved cysteines is essential for the primase activity. However, the specific function of the cluster remains unclear. The decreased solubility and stability of the cysteine-to-serine mutants in p58C suggest that the cluster does provide some level of structural stability to the protein [91]. However, full-length p58 is still sufficiently structured in the absence of the iron-sulfur cluster to bind p48. Furthermore, disruption of the iron-sulfur cluster by cysteine-to-alanine mutations (C336A, C474A) only causes a partial, rather than a complete, unfolding of the yeast p58C [92]. The observations that both the C367S mutant of human p58 and the C336A, C474A double mutant in yeast p58 have severe defects in RNA primer synthesis suggest that the cluster may also serve a regulatory as opposed to a purely structural function [92].

Primase can initiate *de novo* DNA synthesis by assembling short RNA primers from individual ribonucleotides, it is also capable of extending an existing primer-template substrate. Disruption of the iron-sulfur cluster in both human and yeast primase compromised its ability to initiate RNA primer synthesis [92]. However, yeast primase mutants with the cluster disrupted still retained extension ability on a pre-existing primer-template substrate, suggesting that the essential role of the Fe-S cluster is specific to the initiation of RNA primer synthesis. Primase is thought to have two nucleotide-binding pockets, the initiation and elongation sites, which are simultaneously occupied for formation of the initial dinucleotide during the initiation phase [95]. The findings that the iron-sulfur cluster is essential for synthesis of the RNA primer, but not for

its elongation, point toward a specific role of the cluster in dinucleotide formation.

Recently, the crystal structure of yeast p58C was determined. The structure folds into two largely independent alpha-helical domains joined at their interface by a [4Fe-4S] cluster [93]. Yeast p58C binds to both ssDNA and dsDNA with micromolar affinity [93]. Surprisingly, the N-terminal domain of yeast p58C shares a striking structural similarity with the active site region of members of the DNA photolyase /cryptochrome family of DNA repair proteins. A potential model for the essential role of yeast p58C in initiation of RNA primer synthesis was proposed based on structural comparison with cryptochrome Cry3 [93]. In this model, the iron-sulfur containing p58C would assist the catalytic subunit p48 in binding of the two initial ribonucleotides and promoting dinucleotide base-pairing with template DNA at the initiation site. This model is consistent with the observations that both p58 and p48 subunits participated in the formation of the catalytic active sites and single-point mutations in p58 can dramatically reduced the RNA primer synthesis by primase. This model is very promising, but high-resolution structures of human p58C are still needed to confirm whether this intriguing model can be applied to human primase.

APPENDIX B

This chapter presents the experimental work that I contributed to a collaborative publication on Mcm10: Warren EM, Huang H, Fanning E, Chazin WJ, Eichman BF, Physical interactions between Mcm10, DNA, and DNA polymerase alpha. J Biol Chem. 2009 Sep 4; 284(36):24662-72.

Introduction

Mcm10 is an essential eukaryotic replication factor required for replication activation and progression [144, 198, 201]. Mcm10 is recruited onto chromatin in early S phase and associated with it throughout S phase. Chromatin association of Mcm10 is required for loading of Cdc45 and GINS, which function together with Mcm2-7 as a Cdc45/Mcm2-7/GINS (CMG) replicative helicase [143, 144, 161]. A number of genetic and physical interactions have been observed between Mcm10 and components of the replication machinery, including the origin recognition complex (ORC), Cdc45, Mcm2-7, and DNA polymerase α (pol α) [152-154, 156, 198]. These interactions are essential for establishing an active replication fork [193]. Particularly, interaction between Mcm10 and pol α is critical as pol α is the only enzyme that is capable of initiating *de novo* DNA synthesis. This interaction stabilizes pol α and helps its recruitment onto chromatin [195, 197, 198]. The ability of Mcm10 to interact with both the CMG complex and pol α suggests that it may function as a physical linker between helicase and polymerase machineries within a replisome [198, 203]. Consistent with this idea, Mcm10 and pol α dissociate from the CMG

helicase complex in response to damage-induced replication fork stalling [201].

Mcm10 is composed of three structural domains, the N-terminal (NTD), internal (ID), and C-terminal (CTD) domains [197]. The NTD is thought to be an oligomerization domain. The ID is highly conserved among all eukaryotes, whereas CTD exists in higher eukaryotes but not yeast. The crystal structure of ID revealed that this domain is composed of an oligonucleotide/oligosaccharide binding (OB)-fold and a zinc motif, which form a unified DNA binding platform. The CTD contains two zinc motifs, of which only one is involved in DNA binding. Both the ID and CTD interact with pol α [197].

Previous work in collaboration with the Eichman lab showed that Mcm10-ID binds to the N-terminal 323 residues of the catalytic p180 subunit of pol α [197]. This region is highly conserved but lacks appreciable predicted secondary structure or sequence complexity. To map the Mcm10-p180 interaction in detail, $p180^{1-323}$ was subjected to limited proteolysis in the Eichman lab. The resulting stable fragments were identified by mass spectrometry. Proteolytically sensitive sites were found at residues 145 and 189. Consequently, $p180^{1-145}$ and $p180^{189-323}$ were subcloned, purified, and tested for physical interaction with Mcm10-ID. However, the $p180^{1-145}$ protein was not sufficiently stable in solution to test for a putative interaction. GST pull-down assay results showed that $p180^{189-323}$, as well as an even smaller region $p180^{243-310}$, is sufficient to bind to Mcm10-ID.

Materials and Methods

Protein Expression and Purification

Mcm10-ID was prepared as described previously. Briefly, the protein was overexpressed from a modified pET-32a vector (Novagen) in *E. coli* BL21 (DE3) cells for 16 h at 16 °C and purified using nickel-nitrilotriacetic acid affinity chromatography. $p180^{189-323}$ and $p180^{243-310}$ were amplified by PCR on a cDNA template pBR322-p180 and cloned into the BamHI/EcoRI sites of a pGEX-2T expression vector (GE Healthcare). GST fusion proteins were expressed and purified by glutathione-agarose affinity chromatography as described previously.

GST Pull-down Assay

10 ug of GST-tagged $p180^{189-323}$ and $p180^{243-310}$ were absorbed on glutathione-agarose beads (Sigma-Aldrich). The protein-bound beads were then incubated with either 5 or 10 ug of Trx-His_6-Mcm10-ID in binding buffer (30 mM HEPES-KOH, pH 7.8, 10 mM KCl, 7 mM $MgCl_2$) containing 2% nonfat dry milk for 1 h at 4 °C with end-over-end rotation. The beads were washed once with binding buffer, three times with wash buffer (30 mM HEPESKOH, pH 7.8, 75 mM KCl, 7 mM $MgCl_2$, 0.25% inositol, 0.1% Nonidet P-40), and once with binding buffer. The beads were resuspended in 30 ul of 2X SDS-PAGE loading buffer and heated at 100 °C for 5 min. The samples were analyzed by 10% SDS-PAGE and visualized by immunoblotting with anti-His (9801; Abcam) for His-tagged Mcm10-ID and anti-GST (Invitrogen) for p180N fragments.

Results

$p180^{189-323}$ and $p180^{243-310}$ Bind to Mcm10-ID

The N-terminal 323 residues of p180 have previously been shown to bind to the Mcm10-ID. To further narrow down the interaction region in p180, limited proteolysis, together with mass spectrometry was used by the Eichman lab to identify $p180^{189-323}$ as a stable and structured domain. $p180^{189-323}$ was then expressed and purified as a GST fusion protein to test its interaction with Mcm10-ID. GST-tagged $p180^{189-323}$ immobilized on glutathione-Sepharose was able to capture His-tagged Mcm10-ID from solution (Fig B.1), demonstrating that this region of p180 is sufficient to bind to Mcm10-ID. To map the minimal region of $p180^{189-323}$ needed to interact with Mcm10-ID, the p180 sequence was aligned and examined for conservation and predicted secondary structure. In combination with data from NMR chemical shift perturbation experiment, two candidate peptides $p180^{243-256}$ and $p180^{286-310}$ were identified as minimal regions within $p180^{189-323}$ that were required for Mcm10-ID binding. Due to the potential difficulty of working with a peptide of ~20 residues, we expressed and purified the GST fusion protein $p180^{243-310}$ spanning both peptides and tested its interaction with Mcm10-ID. Indeed, glutathione-immobilized GST-tagged $p180^{243-310}$ was able to capture Mcm10-ID from solution in pull-down assay (Fig. B.1), supporting the hypothesis that the minimal region pf p180 that is required for Mcm10-ID binding is within residues 243-310.

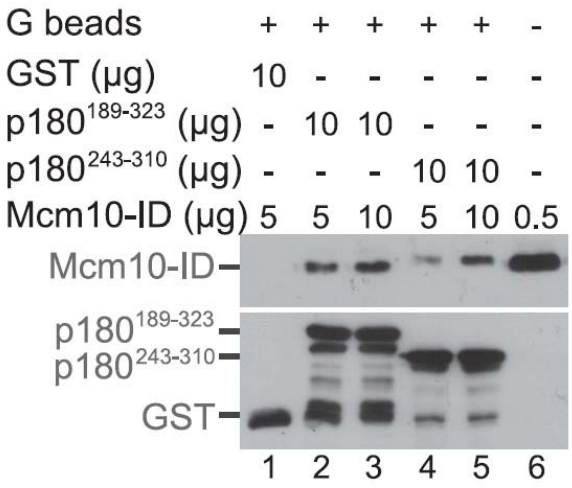

Figure B.1. p180$^{189\text{-}323}$ and p180 $^{243\text{-}310}$ physically interact with Mcm10-ID. GST pull-down experiments between His-taggedMcm10-ID and GST-tagged p180 fragments. p180 fragments 189-323 and 243-310 were adsorbed on glutathione (*G*) beads and mixed with Mcm10-ID in the amounts indicated. Bound Mcm10-ID was detected by Western blotting with anti-His antibody (*upper blot*), whereas retention of p180 fragments was detected by Western blotting with anti-GST antibodies (*lower blot*).

Discussion

The work described in this chapter showed that p180$^{189\text{-}323}$, as well as p180$^{243\text{-}310}$, is sufficient to bind to Mcm10-ID. This result is consistent with results from fluorescence anisotropy and NMR chemical shift perturbation experiments [213]. Coincidentally, preliminary data showed that p180$^{189\text{-}323}$ and p180$^{243\text{-}310}$ are able to bind to Tag as well (Huang, unpublished data), suggesting that p180 may utilize a common surface to interact with other replication factors, like Tag and Mcm10. Since the N-terminus of p180 is dispensable for polymerase activity and is not required for assembly of the pol α-primase complex, the interaction of Mcm10 or Tag with p180 could help the association of pol α complex with DNA without interfering with primer synthesis. Further detailed analysis of interaction of Tag with p180 is in progress in the lab.

On the other hand, fluorescence anisotropy and NMR chemical shift perturbation experiments demonstrated that both ssDNA and the N-terminal region of p180 compete for binding to a relatively hydrophobic surface within the OB-fold cleft of Mcm10-ID [213]. In addition, Mcm10-CTD interacts with both ssDNA and p180 as well [214]. This observation suggests that Mcm10 may transition between interaction with DNA and p180, helping load and stabilize the pol α complex at the replication fork via a hand-off mechanism. Three possible hand-off modes have been proposed [213], so additional studies are required to fully understand how Mcm10 utilizes the hand-off mechanism.

REFERENCES

1. Benkovic, S.J., A.M. Valentine, and F. Salinas, *Replisome-mediated DNA replication.* Annu Rev Biochem, 2001. **70**: p. 181-208.

2. Yao, N.Y. and M. O'Donnell, *SnapShot: The replisome.* Cell, 2010. **141**(6): p. 1088, e1.

3. Hamdan, S.M. and C.C. Richardson, *Motors, switches, and contacts in the replisome.* Annu Rev Biochem, 2009. **78**: p. 205-43.

4. Bullock, P.A., *The initiation of simian virus 40 DNA replication in vitro.* Crit Rev Biochem Mol Biol, 1997. **32**(6): p. 503-68.

5. Waga, S. and B. Stillman, *Anatomy of a DNA replication fork revealed by reconstitution of SV40 DNA replication in vitro.* Nature, 1994. **369**(6477): p. 207-12.

6. Waga, S. and B. Stillman, *The DNA replication fork in eukaryotic cells.* Annu Rev Biochem, 1998. **67**: p. 721-51.

7. Fanning, E. and R. Knippers, *Structure and function of simian virus 40 large tumor antigen.* Annu Rev Biochem, 1992. **61**: p. 55-85.

8. Fiers, W., et al., *Complete nucleotide sequence of SV40 DNA.* Nature, 1978. **273**(5658): p. 113-20.

9. Reddy, V.B., et al., *The genome of simian virus 40.* Science, 1978. **200**(4341): p. 494-502.

10. Stehle, T., et al., *The structure of simian virus 40 refined at 3.1 A resolution.* Structure, 1996. **4**(2): p. 165-82.

11. Levine, A.J., *The common mechanisms of transformation by the small DNA tumor viruses: The inactivation of tumor suppressor gene products: p53.* Virology, 2009. **384**(2): p. 285-93.

12. Ahuja, D., M.T. Saenz-Robles, and J.M. Pipas, *SV40 large T antigen targets multiple cellular pathways to elicit cellular transformation.* Oncogene, 2005. **24**(52): p. 7729-45.

13. Daniels, R., D. Sadowicz, and D.N. Hebert, *A very late viral protein triggers the lytic release of SV40.* PLoS Pathog, 2007. **3**(7): p. e98.

14. Sullivan, C.S., et al., *SV40-encoded microRNAs regulate viral gene expression and reduce susceptibility to cytotoxic T cells.* Nature, 2005. **435**(7042): p. 682-6.

15. Borowiec, J.A., et al., *Binding and unwinding--how T antigen engages the SV40 origin of DNA replication.* Cell, 1990. **60**(2): p. 181-4.

16. Damm, E.M., et al., *Clathrin- and caveolin-1-independent endocytosis: entry of simian virus 40 into cells devoid of caveolae.* J Cell Biol, 2005. **168**(3): p. 477-88.

17. Norkin, L.C. and D. Kuksin, *The caveolae-mediated sv40 entry pathway bypasses the golgi complex en route to the endoplasmic reticulum.* Virol J, 2005. **2**: p. 38.

18. Pelkmans, L., J. Kartenbeck, and A. Helenius, *Caveolar endocytosis of simian virus 40 reveals a new two-step vesicular-transport pathway to the ER.* Nat Cell Biol, 2001. **3**(5): p. 473-83.

19. Ishizu, K.I., et al., *Roles of disulfide linkage and calcium ion-mediated interactions in assembly and disassembly of virus-like particles composed of simian virus 40 VP1 capsid protein.* J Virol, 2001. **75**(1): p. 61-72.

20. Li, P.P., et al., *Importance of Vp1 calcium-binding residues in assembly, cell entry, and nuclear entry of simian virus 40.* J Virol, 2003. **77**(13): p. 7527-38.

21. Nakanishi, A., et al., *Minor capsid proteins of simian virus 40 are dispensable for nucleocapsid assembly and cell entry but are required for nuclear entry of the viral genome.* J Virol, 2007. **81**(8): p. 3778-85.

22. Nakanishi, A., et al., *Interaction of the Vp3 nuclear localization signal with the importin alpha 2/beta heterodimer directs nuclear entry of infecting simian virus 40.* J Virol, 2002. **76**(18): p. 9368-77.

23. Sullivan, C.S. and J.M. Pipas, *T antigens of simian virus 40: molecular chaperones for viral replication and tumorigenesis.* Microbiol Mol Biol Rev, 2002. **66**(2): p. 179-202.

24. Li, J.J. and T.J. Kelly, *Simian virus 40 DNA replication in vitro.* Proc Natl Acad Sci U S A, 1984. **81**(22): p. 6973-7.

25. Ishimi, Y., et al., *Complete enzymatic synthesis of DNA containing the SV40 origin of replication.* J Biol Chem, 1988. **263**(36): p. 19723-33.

26. Tsurimoto, T., M.P. Fairman, and B. Stillman, *Simian virus 40 DNA replication in vitro: identification of multiple stages of initiation.* Mol Cell Biol, 1989. **9**(9): p. 3839-49.

27. Weinberg, D.H., et al., *Reconstitution of simian virus 40 DNA replication with purified proteins.* Proc Natl Acad Sci U S A, 1990. **87**(22): p. 8692-6.

28. Yang, L., et al., *Roles of DNA topoisomerases in simian virus 40 DNA replication in vitro.* Proc Natl Acad Sci U S A, 1987. **84**(4): p. 950-4.

29. Wold, M.S. and T. Kelly, *Purification and characterization of replication protein A, a cellular protein required for in vitro replication of simian virus 40 DNA.* Proc Natl Acad Sci U S A, 1988. **85**(8): p. 2523-7.

30. Kuchta, R.D., B. Reid, and L.M. Chang, *DNA primase. Processivity and the primase to polymerase alpha activity switch.* J Biol Chem, 1990. **265**(27): p. 16158-65.

31. Frick, D.N. and C.C. Richardson, *DNA primases.* Annu Rev Biochem, 2001. **70**: p. 39-80.

32. Prelich, G., et al., *Functional identity of proliferating cell nuclear antigen and a DNA polymerase-delta auxiliary protein.* Nature, 1987. **326**(6112): p. 517-20.

33. Tsurimoto, T. and B. Stillman, *Purification of a cellular replication factor, RF-C, that is required for coordinated synthesis of leading and lagging strands during simian virus 40 DNA replication in vitro.* Mol Cell Biol, 1989. **9**(2): p. 609-19.

34. Tsurimoto, T. and B. Stillman, *Replication factors required for SV40 DNA replication in vitro. II. Switching of DNA polymerase alpha and delta during initiation of leading and lagging strand synthesis.* J Biol Chem, 1991. **266**(3): p. 1961-8.

35. Tsurimoto, T. and B. Stillman, *Functions of replication factor C and proliferating-cell nuclear antigen: functional similarity of DNA polymerase accessory proteins from human cells and bacteriophage T4.* Proc Natl Acad Sci U S A, 1990. **87**(3): p. 1023-7.

36. Lee, S.H., et al., *Studies on the activator 1 protein complex, an accessory factor for proliferating cell nuclear antigen-dependent DNA polymerase delta.* J Biol Chem, 1991. **266**(1): p. 594-602.

37. Yuzhakov, A., et al., *Multiple competition reactions for RPA order the assembly of the DNA polymerase delta holoenzyme.* Embo J, 1999. **18**(21): p. 6189-99.

38. Burgers, P.M., *Polymerase dynamics at the eukaryotic DNA replication fork.* J Biol Chem, 2009. **284**(7): p. 4041-5.

39. Huang, L., et al., *Structure-specific cleavage of the RNA primer from Okazaki fragments by calf thymus RNase HI.* J Biol Chem, 1994. **269**(41): p. 25922-7.

40. Turchi, J.J., et al., *Enzymatic completion of mammalian lagging-strand DNA replication.* Proc Natl Acad Sci U S A, 1994. **91**(21): p. 9803-7.

41. Weaver, D.T., S.C. Fields-Berry, and M.L. DePamphilis, *The termination region for SV40 DNA replication directs the mode of separation for the two sibling molecules.* Cell, 1985. **41**(2): p. 565-75.

42. Nick McElhinny, S.A., et al., *Division of labor at the eukaryotic replication fork.* Mol Cell, 2008. **30**(2): p. 137-44.

43. Kunkel, T.A. and P.M. Burgers, *Dividing the workload at a eukaryotic replication fork.* Trends Cell Biol, 2008. **18**(11): p. 521-7.

44. Shi, Y., et al., *Ataxia-telangiectasia-mutated (ATM) is a T-antigen kinase that controls SV40 viral replication in vivo.* J Biol Chem, 2005. **280**(48): p. 40195-200.

45. Zhao, X., et al., *Ataxia telangiectasia-mutated damage-signaling kinase- and proteasome-dependent destruction of Mre11-Rad50-Nbs1 subunits in Simian virus 40-infected primate cells.* J Virol, 2008. **82**(11): p. 5316-28.

46. Kim, H.Y., B.Y. Ahn, and Y. Cho, *Structural basis for the inactivation of retinoblastoma tumor suppressor by SV40 large T antigen.* Embo J, 2001. **20**(1-2): p. 295-304.

47. Luo, X., et al., *Solution structure of the origin DNA-binding domain of SV40 T-antigen.* Nat Struct Biol, 1996. **3**(12): p. 1034-9.

48. Li, D., et al., *Structure of the replicative helicase of the oncoprotein SV40 large tumour antigen.* Nature, 2003. **423**(6939): p. 512-8.

49. Cuesta, I., et al., *Conformational rearrangements of SV40 large T antigen during early replication events.* J Mol Biol, 2010. **397**(5): p. 1276-86.

50. Fanning, E., Pipas, J.M., *Polyomavirus*, in *DNA replication and Human Disease*. 2006, Cold Spring Harbor Laboratory Press: New York. p. 627-644.

51. Weisshart, K., et al., *An N-terminal deletion mutant of simian virus 40 (SV40) large T antigen oligomerizes incorrectly on SV40 DNA but retains the ability to bind to DNA polymerase alpha and replicate SV40 DNA in vitro.* J Virol, 1996. **70**(6): p. 3509-16.

52. Spence, S.L. and J.M. Pipas, *Simian virus 40 large T antigen host range domain functions in virion assembly.* J Virol, 1994. **68**(7): p. 4227-40.

53. Simmons, D.T., G. Loeber, and P. Tegtmeyer, *Four major sequence elements of simian virus 40 large T antigen coordinate its specific and nonspecific DNA binding.* J Virol, 1990. **64**(5): p. 1973-83.

54. Bochkareva, E., et al., *Structure of the origin-binding domain of simian virus 40 large T antigen bound to DNA.* Embo J, 2006. **25**(24): p. 5961-9.

55. Meinke, G., et al., *The crystal structure of the SV40 T-antigen origin binding domain in complex with DNA.* PLoS Biol, 2007. **5**(2): p. e23.

56. Meinke, G., P.A. Bullock, and A. Bohm, *Crystal structure of the simian virus 40 large T-antigen origin-binding domain.* J Virol, 2006. **80**(9): p. 4304-12.

57. Simmons, D.T., K. Wun-Kim, and W. Young, *Identification of simian virus 40 T-antigen residues important for specific and nonspecific binding to DNA and for helicase activity.* J Virol, 1990. **64**(10): p. 4858-65.

58. Arunkumar, A.I., et al., *Insights into hRPA32 C-terminal domain--mediated assembly of the simian virus 40 replisome.* Nat Struct Mol Biol, 2005. **12**(4): p. 332-9.

59. Jiang, X., et al., *Structural mechanism of RPA loading on DNA during activation of a simple pre-replication complex.* Embo J, 2006. **25**(23): p. 5516-26.

60. Neuwald, A.F., et al., *AAA+: A class of chaperone-like ATPases associated with the assembly, operation, and disassembly of protein complexes.* Genome Res, 1999. **9**(1): p. 27-43.

61. Gai, D., et al., *Mechanisms of conformational change for a replicative hexameric helicase of SV40 large tumor antigen.* Cell, 2004. **119**(1): p. 47-60.

62. Shen, J., et al., *The roles of the residues on the channel beta-hairpin and loop structures of simian virus 40 hexameric helicase.* Proc Natl Acad Sci U S A, 2005. **102**(32): p. 11248-53.

63. Singleton, M.R., et al., *Crystal structure of T7 gene 4 ring helicase indicates a mechanism for sequential hydrolysis of nucleotides.* Cell, 2000. **101**(6): p. 589-600.

64. Enemark, E.J. and L. Joshua-Tor, *Mechanism of DNA translocation in a replicative hexameric helicase.* Nature, 2006. **442**(7100): p. 270-5.

65. Valle, M., et al., *Large T-antigen double hexamers imaged at the simian virus 40 origin of replication.* Mol Cell Biol, 2000. **20**(1): p. 34-41.

66. Gomez-Lorenzo, M.G., et al., *Large T antigen on the simian virus 40 origin of replication: a 3D snapshot prior to DNA replication.* Embo J, 2003. **22**(23): p. 6205-13.

67. Valle, M., et al., *Structural basis for the cooperative assembly of large T antigen on the origin of replication.* J Mol Biol, 2006. **357**(4): p. 1295-305.

68. Reese, D.K., et al., *Analyses of the interaction between the origin binding domain from simian virus 40 T antigen and single-stranded DNA provide insights into DNA unwinding and initiation of DNA replication.* J Virol, 2006. **80**(24): p. 12248-59.

69. Kumar, A., et al., *Model for T-antigen-dependent melting of the simian virus 40 core origin based on studies of the interaction of the beta-hairpin with DNA.* J Virol, 2007. **81**(9): p. 4808-18.

70. Wang, W., D. Manna, and D.T. Simmons, *Role of the hydrophilic channels of simian virus 40 T-antigen helicase in DNA replication.* J Virol, 2007. **81**(9): p. 4510-9.

71. Wessel, R., J. Schweizer, and H. Stahl, *Simian virus 40 T-antigen DNA helicase is a hexamer which forms a binary complex during bidirectional unwinding from the viral origin of DNA replication.* J Virol, 1992. **66**(2): p. 804-15.

72. Hubscher, U., G. Maga, and S. Spadari, *Eukaryotic DNA polymerases.* Annu Rev Biochem, 2002. **71**: p. 133-63.

73. Loeb, L.A. and R.J. Monnat, Jr., *DNA polymerases and human disease.* Nat Rev Genet, 2008. **9**(8): p. 594-604.

74. Foiani, M., G. Lucchini, and P. Plevani, *The DNA polymerase alpha-primase complex couples DNA replication, cell-cycle progression and DNA-damage response.* Trends Biochem Sci, 1997. **22**(11): p. 424-7.

75. Cimprich, K.A. and D. Cortez, *ATR: an essential regulator of genome integrity.* Nat Rev Mol Cell Biol, 2008. **9**(8): p. 616-27.

76. Gilson, E. and V. Geli, *How telomeres are replicated.* Nat Rev Mol Cell Biol, 2007. **8**(10): p. 825-38.

77. Mizuno, T., et al., *Molecular architecture of the mouse DNA polymerase alpha-primase complex.* Mol Cell Biol, 1999. **19**(11): p. 7886-96.

78. Mizuno, T., et al., *The second-largest subunit of the mouse DNA polymerase alpha-primase complex facilitates both production and nuclear translocation of the catalytic subunit of DNA polymerase alpha.* Mol Cell Biol, 1998. **18**(6): p. 3552-62.

79. Nasheuer, H.P., et al., *Cell cycle-dependent phosphorylation of human DNA polymerase alpha.* J Biol Chem, 1991. **266**(12): p. 7893-903.

80. Voitenleitner, C., et al., *Cell cycle-dependent regulation of human DNA polymerase alpha-primase activity by phosphorylation.* Mol Cell Biol, 1999. **19**(1): p. 646-56.

81. Foiani, M., et al., *The B subunit of the DNA polymerase alpha-primase complex in Saccharomyces cerevisiae executes an essential function at the initial stage of DNA replication.* Mol Cell Biol, 1994. **14**(2): p. 923-33.

82. Eichinger, C.S., et al., *Aberrant DNA polymerase alpha is excluded from the nucleus by defective import and degradation in the nucleus.* J Biol Chem, 2009. **284**(44): p. 30604-14.

83. Foiani, M., et al., *Cell cycle-dependent phosphorylation and dephosphorylation of the yeast DNA polymerase alpha-primase B subunit.* Mol Cell Biol, 1995. **15**(2): p. 883-91.

84. Ott, R.D., et al., *Role of the p68 subunit of human DNA polymerase alpha-primase in simian virus 40 DNA replication.* Mol Cell Biol, 2002. **22**(16): p. 5669-78.

85. Klinge, S., et al., *3D architecture of DNA Pol alpha reveals the functional core of multi-subunit replicative polymerases.* Embo J, 2009. **28**(13): p. 1978-87.

86. Kirk, B.W. and R.D. Kuchta, *Arg304 of human DNA primase is a key contributor to catalysis and NTP binding: primase and the family X polymerases share significant sequence homology.* Biochemistry, 1999. **38**(24): p. 7727-36.

87. Copeland, W.C. and X. Tan, *Active site mapping of the catalytic mouse primase subunit by alanine scanning mutagenesis.* J Biol Chem, 1995. **270**(8): p. 3905-13.

88. Copeland, W.C., *Expression, purification, and characterization of the two human primase subunits and truncated complexes from Escherichia coli.* Protein Expr Purif,

1997. **9**(1): p. 1-9.

89. Zerbe, L.K. and R.D. Kuchta, *The p58 subunit of human DNA primase is important for primer initiation, elongation, and counting.* Biochemistry, 2002. **41**(15): p. 4891-900.

90. Arezi, B., et al., *Interactions of DNA with human DNA primase monitored with photoactivatable cross-linking agents: implications for the role of the p58 subunit.* Biochemistry, 1999. **38**(39): p. 12899-907.

91. Weiner, B.E., et al., *An iron-sulfur cluster in the C-terminal domain of the p58 subunit of human DNA primase.* J Biol Chem, 2007. **282**(46): p. 33444-51.

92. Klinge, S., et al., *An iron-sulfur domain of the eukaryotic primase is essential for RNA primer synthesis.* Nat Struct Mol Biol, 2007. **14**(9): p. 875-7.

93. Sauguet, L., et al., *Shared active site architecture between the large subunit of eukaryotic primase and DNA photolyase.* PLoS One, 2010. **5**(4): p. e10083.

94. Vaithiyalingam, S., et al., *Insights into eukaryotic DNA priming from the structure and functional interactions of the 4Fe-4S cluster domain of human DNA primase.* Proc Natl Acad Sci U S A, 2010. **107**(31): p. 13684-9.

95. Sheaff, R.J. and R.D. Kuchta, *Mechanism of calf thymus DNA primase: slow initiation, rapid polymerization, and intelligent termination.* Biochemistry, 1993. **32**(12): p. 3027-37.

96. Sheaff, R.J., R.D. Kuchta, and D. Ilsley, *Calf thymus DNA polymerase alpha-primase: "communication" and primer-template movement between the two active sites.* Biochemistry, 1994. **33**(8): p. 2247-54.

97. Wold, M.S., *Replication protein A: a heterotrimeric, single-stranded DNA-binding protein required for eukaryotic DNA metabolism.* Annu Rev Biochem, 1997. **66**: p. 61-92.

98. Fanning, E., V. Klimovich, and A.R. Nager, *A dynamic model for replication protein A (RPA) function in DNA processing pathways.* Nucleic Acids Res, 2006. **34**(15): p.

4126-37.

99. Mer, G., et al., *Structural basis for the recognition of DNA repair proteins UNG2, XPA, and RAD52 by replication factor RPA.* Cell, 2000. **103**(3): p. 449-56.

100. de Laat, W.L., et al., *DNA-binding polarity of human replication protein A positions nucleases in nucleotide excision repair.* Genes Dev, 1998. **12**(16): p. 2598-609.

101. Blackwell, L.J. and J.A. Borowiec, *Human replication protein A binds single-stranded DNA in two distinct complexes.* Mol Cell Biol, 1994. **14**(6): p. 3993-4001.

102. Blackwell, L.J., J.A. Borowiec, and I.A. Mastrangelo, *Single-stranded-DNA binding alters human replication protein A structure and facilitates interaction with DNA-dependent protein kinase.* Mol Cell Biol, 1996. **16**(9): p. 4798-807.

103. Bastin-Shanower, S.A. and S.J. Brill, *Functional analysis of the four DNA binding domains of replication protein A. The role of RPA2 in ssDNA binding.* J Biol Chem, 2001. **276**(39): p. 36446-53.

104. Stauffer, M.E. and W.J. Chazin, *Structural mechanisms of DNA replication, repair, and recombination.* J Biol Chem, 2004. **279**(30): p. 30915-8.

105. Bochkareva, E., et al., *Single-stranded DNA mimicry in the p53 transactivation domain interaction with replication protein A.* Proc Natl Acad Sci U S A, 2005. **102**(43): p. 15412-7.

106. Ball, H.L., et al., *Function of a conserved checkpoint recruitment domain in ATRIP proteins.* Mol Cell Biol, 2007. **27**(9): p. 3367-77.

107. Xu, X., et al., *The basic cleft of RPA70N binds multiple checkpoint proteins, including RAD9, to regulate ATR signaling.* Mol Cell Biol, 2008. **28**(24): p. 7345-53.

108. Weisshart, K., P. Taneja, and E. Fanning, *The replication protein A binding site in simian virus 40 (SV40) T antigen and its role in the initial steps of SV40 DNA replication.* J Virol, 1998. **72**(12): p. 9771-81.

109. Bansbach, C.E., et al., *The annealing helicase SMARCAL1 maintains genome integrity at stalled replication forks.* Genes Dev, 2009. **23**(20): p. 2405-14.

110. Collins, K.L., et al., *The role of the 70 kDa subunit of human DNA polymerase alpha in DNA replication.* Embo J, 1993. **12**(12): p. 4555-66.

111. Dornreiter, I., W.C. Copeland, and T.S. Wang, *Initiation of simian virus 40 DNA replication requires the interaction of a specific domain of human DNA polymerase alpha with large T antigen.* Mol Cell Biol, 1993. **13**(2): p. 809-20.

112. Weisshart, K., et al., *Protein-protein interactions of the primase subunits p58 and p48 with simian virus 40 T antigen are required for efficient primer synthesis in a cell-free system.* J Biol Chem, 2000. **275**(23): p. 17328-37.

113. Dornreiter, I., et al., *Interaction of DNA polymerase alpha-primase with cellular replication protein A and SV40 T antigen.* Embo J, 1992. **11**(2): p. 769-76.

114. Nasheuer, H.P., et al., *Purification and functional characterization of bovine RP-A in an in vitro SV40 DNA replication system.* Chromosoma, 1992. **102**(1 Suppl): p. S52-9.

115. Braun, K.A., et al., *Role of protein-protein interactions in the function of replication protein A (RPA): RPA modulates the activity of DNA polymerase alpha by multiple mechanisms.* Biochemistry, 1997. **36**(28): p. 8443-54.

116. Corn, J.E. and J.M. Berger, *Regulation of bacterial priming and daughter strand synthesis through helicase-primase interactions.* Nucleic Acids Res, 2006. **34**(15): p. 4082-8.

117. Huang, S.G., et al., *Stoichiometry and mechanism of assembly of SV40 T antigen complexes with the viral origin of DNA replication and DNA polymerase alpha-primase.* Biochemistry, 1998. **37**(44): p. 15345-52.

118. Dornreiter, I., et al., *SV40 T antigen binds directly to the large subunit of purified DNA polymerase alpha.* Embo J, 1990. **9**(10): p. 3329-36.

119. Langston, L.D., C. Indiani, and M. O'Donnell, *Whither the replisome: emerging*

perspectives on the dynamic nature of the DNA replication machinery. Cell Cycle, 2009. **8**(17): p. 2686-91.

120. Copeland, W.C. and T.S. Wang, *Enzymatic characterization of the individual mammalian primase subunits reveals a biphasic mechanism for initiation of DNA replication.* J Biol Chem, 1993. **268**(35): p. 26179-89.

121. Kuchta, R.D. and G. Stengel, *Mechanism and evolution of DNA primases.* Biochim Biophys Acta, 2010. **1804**(5): p. 1180-9.

122. Aravind, L. and E.V. Koonin, *Phosphoesterase domains associated with DNA polymerases of diverse origins.* Nucleic Acids Res, 1998. **26**(16): p. 3746-52.

123. Makiniemi, M., et al., *A novel family of DNA-polymerase-associated B subunits.* Trends Biochem Sci, 1999. **24**(1): p. 14-6.

124. Desdouets, C., et al., *Evidence for a Cdc6p-independent mitotic resetting event involving DNA polymerase alpha.* Embo J, 1998. **17**(14): p. 4139-46.

125. Matsumoto, T., T. Eki, and J. Hurwitz, *Studies on the initiation and elongation reactions in the simian virus 40 DNA replication system.* Proc Natl Acad Sci U S A, 1990. **87**(24): p. 9712-6.

126. Tsurimoto, T., T. Melendy, and B. Stillman, *Sequential initiation of lagging and leading strand synthesis by two different polymerase complexes at the SV40 DNA replication origin.* Nature, 1990. **346**(6284): p. 534-9.

127. Gai, D., et al., *Insights into the oligomeric states, conformational changes, and helicase activities of SV40 large tumor antigen.* J Biol Chem, 2004. **279**(37): p. 38952-9.

128. Cavanagh, J., Fairbrother, W. J., Palmer, A.G., and Skelton, N.J., *Protein NMR Spectroscopy: Principles and Practice*. 1996, San Diego: Academic Press. 533-553.

129. Cornilescu, G., F. Delaglio, and A. Bax, *Protein backbone angle restraints from searching a database for chemical shift and sequence homology.* J Biomol NMR, 1999. **13**(3): p. 289-302.

130. Guntert, P., *Automated NMR structure calculation with CYANA.* Methods Mol Biol, 2004. **278**: p. 353-78.

131. Case, D.A., *AMBER*, S.F. University of California, Editor. 2006.

132. Nuutinen, T., et al., *The solution structure of the amino-terminal domain of human DNA polymerase epsilon subunit B is homologous to C-domains of AAA+ proteins.* Nucleic Acids Res, 2008. **36**(15): p. 5102-10.

133. Collins, K.L. and T.J. Kelly, *Effects of T antigen and replication protein A on the initiation of DNA synthesis by DNA polymerase alpha-primase.* Mol Cell Biol, 1991. **11**(4): p. 2108-15.

134. Melendy, T. and B. Stillman, *An interaction between replication protein A and SV40 T antigen appears essential for primosome assembly during SV40 DNA replication.* J Biol Chem, 1993. **268**(5): p. 3389-95.

135. Matsuo, H., et al., *Identification by NMR Spectroscopy of Residues at Contact Surfaces in Large, Slowly Exchanging Macromolecular Complexes.* Journal of the American Chemical Society, 1999. **121**(42): p. 9903-9904.

136. Shereda, R.D., et al., *SSB as an organizer/mobilizer of genome maintenance complexes.* Crit Rev Biochem Mol Biol, 2008. **43**(5): p. 289-318.

137. Duderstadt, K.E. and J.M. Berger, *AAA+ ATPases in the initiation of DNA replication.* Crit Rev Biochem Mol Biol, 2008. **43**(3): p. 163-87.

138. Makowska-Grzyska, M. and J.M. Kaguni, *Primase directs the release of DnaC from DnaB.* Mol Cell, 2010. **37**(1): p. 90-101.

139. Moldovan, G.L., B. Pfander, and S. Jentsch, *PCNA, the maestro of the replication fork.* Cell, 2007. **129**(4): p. 665-79.

140. Murakami, Y. and J. Hurwitz, *DNA polymerase alpha stimulates the ATP-dependent binding of simian virus tumor T antigen to the SV40 origin of replication.* J Biol Chem, 1993. **268**(15): p. 11018-27.

141. Manosas, M., et al., *Coupling DNA unwinding activity with primer synthesis in the bacteriophage T4 primosome.* Nat Chem Biol, 2009. **5**(12): p. 904-12.

142. Pandey, M., et al., *Coordinating DNA replication by means of priming loop and differential synthesis rate.* Nature, 2009. **462**(7275): p. 940-3.

143. Moyer, S.E., P.W. Lewis, and M.R. Botchan, *Isolation of the Cdc45/Mcm2-7/GINS (CMG) complex, a candidate for the eukaryotic DNA replication fork helicase.* Proc Natl Acad Sci U S A, 2006. **103**(27): p. 10236-41.

144. Gambus, A., et al., *GINS maintains association of Cdc45 with MCM in replisome progression complexes at eukaryotic DNA replication forks.* Nat Cell Biol, 2006. **8**(4): p. 358-66.

145. Aparicio, T., et al., *The human GINS complex associates with Cdc45 and MCM and is essential for DNA replication.* Nucleic Acids Res, 2009. **37**(7): p. 2087-95.

146. Evrin, C., et al., *A double-hexameric MCM2-7 complex is loaded onto origin DNA during licensing of eukaryotic DNA replication.* Proc Natl Acad Sci U S A, 2009. **106**(48): p. 20240-5.

147. Remus, D., et al., *Concerted loading of Mcm2-7 double hexamers around DNA during DNA replication origin licensing.* Cell, 2009. **139**(4): p. 719-30.

148. Moarefi, I.F., et al., *Mutation of the cyclin-dependent kinase phosphorylation site in simian virus 40 (SV40) large T antigen specifically blocks SV40 origin DNA unwinding.* J Virol, 1993. **67**(8): p. 4992-5002.

149. Miles, J. and T. Formosa, *Evidence that POB1, a Saccharomyces cerevisiae protein that binds to DNA polymerase alpha, acts in DNA metabolism in vivo.* Mol Cell Biol, 1992. **12**(12): p. 5724-35.

150. Kouprina, N., et al., *CTF4 (CHL15) mutants exhibit defective DNA metabolism in the yeast Saccharomyces cerevisiae.* Mol Cell Biol, 1992. **12**(12): p. 5736-47.

151. Williams, D.R. and J.R. McIntosh, *Mcl1p is a polymerase alpha replication accessory*

factor important for S-phase DNA damage survival. Eukaryot Cell, 2005. **4**(1): p. 166-77.

152. Zhu, W., et al., *Mcm10 and And-1/CTF4 recruit DNA polymerase alpha to chromatin for initiation of DNA replication.* Genes Dev, 2007. **21**(18): p. 2288-99.

153. Gambus, A., et al., *A key role for Ctf4 in coupling the MCM2-7 helicase to DNA polymerase alpha within the eukaryotic replisome.* Embo J, 2009. **28**(19): p. 2992-3004.

154. Im, J.S., et al., *Assembly of the Cdc45-Mcm2-7-GINS complex in human cells requires the Ctf4/And-1, RecQL4, and Mcm10 proteins.* Proc Natl Acad Sci U S A, 2009. **106**(37): p. 15628-32.

155. Tsutsui, Y., et al., *Genetic and physical interactions between Schizosaccharomyces pombe Mcl1 and Rad2, Dna2 and DNA polymerase alpha: evidence for a multifunctional role of Mcl1 in DNA replication and repair.* Curr Genet, 2005. **48**(1): p. 34-43.

156. Tanaka, H., et al., *Ctf4 coordinates the progression of helicase and DNA polymerase alpha.* Genes Cells, 2009. **14**(7): p. 807-20.

157. Tanaka, H., et al., *Replisome progression complex links DNA replication to sister chromatid cohesion in Xenopus egg extracts.* Genes Cells, 2009. **14**(8): p. 949-63.

158. Moser, B.A., et al., *Differential arrival of leading and lagging strand DNA polymerases at fission yeast telomeres.* Embo J, 2009. **28**(7): p. 810-20.

159. MacDougall, C.A., et al., *The structural determinants of checkpoint activation.* Genes Dev, 2007. **21**(8): p. 898-903.

160. Marians, K.J., *Understanding how the replisome works.* Nat Struct Mol Biol, 2008. **15**(2): p. 125-7.

161. Ilves, I., et al., *Activation of the MCM2-7 helicase by association with Cdc45 and GINS proteins.* Mol Cell, 2010. **37**(2): p. 247-58.

162. Tanaka, T. and K. Nasmyth, *Association of RPA with chromosomal replication origins*

requires an Mcm protein, and is regulated by Rad53, and cyclin- and Dbf4-dependent kinases. Embo J, 1998. **17**(17): p. 5182-91.

163. Walter, J. and J. Newport, *Initiation of eukaryotic DNA replication: origin unwinding and sequential chromatin association of Cdc45, RPA, and DNA polymerase alpha.* Mol Cell, 2000. **5**(4): p. 617-27.

164. Smelkova, N.V. and J.A. Borowiec, *Dimerization of simian virus 40 T-antigen hexamers activates T-antigen DNA helicase activity.* J Virol, 1997. **71**(11): p. 8766-73.

165. Huang, H., et al., *Structure of a DNA polymerase alpha-primase domain that docks on the SV40 helicase and activates the viral primosome.* J Biol Chem, 2010. **285**(22): p. 17112-22.

166. Henricksen, L.A., C.B. Umbricht, and M.S. Wold, *Recombinant replication protein A: expression, complex formation, and functional characterization.* J Biol Chem, 1994. **269**(15): p. 11121-32.

167. Gurney, E.G., S. Tamowski, and W. Deppert, *Antigenic binding sites of monoclonal antibodies specific for simian virus 40 large T antigen.* J Virol, 1986. **57**(3): p. 1168-72.

168. Spence, S.L. and J.M. Pipas, *SV40 large T antigen functions at two distinct steps in virion assembly.* Virology, 1994. **204**(1): p. 200-9.

169. Lilyestrom, W., et al., *Crystal structure of SV40 large T-antigen bound to p53: interplay between a viral oncoprotein and a cellular tumor suppressor.* Genes Dev, 2006. **20**(17): p. 2373-82.

170. Ahuja, D., et al., *A structure-guided mutational analysis of simian virus 40 large T antigen: identification of surface residues required for viral replication and transformation.* J Virol, 2009. **83**(17): p. 8781-8.

171. Murakami, Y., et al., *Species-specific in vitro synthesis of DNA containing the polyoma virus origin of replication.* Proc Natl Acad Sci U S A, 1986. **83**(17): p. 6347-51.

172. Schneider, C., et al., *Species-specific functional interactions of DNA polymerase*

alpha-primase with simian virus 40 (SV40) T antigen require SV40 origin DNA. Mol Cell Biol, 1994. **14**(5): p. 3176-85.

173. Simmons, D.T., *Adv virus Res*. 2000. 75-134.

174. Park, P., et al., *The cellular DNA polymerase alpha-primase is required for papillomavirus DNA replication and associates with the viral E1 helicase.* Proc Natl Acad Sci U S A, 1994. **91**(18): p. 8700-4.

175. Masterson, P.J., et al., *A C-terminal helicase domain of the human papillomavirus E1 protein binds E2 and the DNA polymerase alpha-primase p68 subunit.* J Virol, 1998. **72**(9): p. 7407-19.

176. Conger, K.L., et al., *Human papillomavirus DNA replication. Interactions between the viral E1 protein and two subunits of human dna polymerase alpha/primase.* J Biol Chem, 1999. **274**(5): p. 2696-705.

177. Zavitz, K.H. and K.J. Marians, *ATPase-deficient mutants of the Escherichia coli DNA replication protein PriA are capable of catalyzing the assembly of active primosomes.* J Biol Chem, 1992. **267**(10): p. 6933-40.

178. Gabbai, C.B. and K.J. Marians, *Recruitment to stalled replication forks of the PriA DNA helicase and replisome-loading activities is essential for survival.* DNA Repair (Amst), 2010. **9**(3): p. 202-9.

179. Bailey, S., W.K. Eliason, and T.A. Steitz, *Structure of hexameric DnaB helicase and its complex with a domain of DnaG primase.* Science, 2007. **318**(5849): p. 459-63.

180. Wang, G., et al., *The structure of a DnaB-family replicative helicase and its interactions with primase.* Nat Struct Mol Biol, 2008. **15**(1): p. 94-100.

181. Thomsen, N.D. and J.M. Berger, *Running in reverse: the structural basis for translocation polarity in hexameric helicases.* Cell, 2009. **139**(3): p. 523-34.

182. Pyle, A.M., *How to drive your helicase in a straight line.* Cell, 2009. **139**(3): p. 458-9.

183. McGeoch, A.T., et al., *Organization of the archaeal MCM complex on DNA and implications for the helicase mechanism.* Nat Struct Mol Biol, 2005. **12**(9): p. 756-62.

184. Braithwaite, A.W., et al., *Mouse p53 inhibits SV40 origin-dependent DNA replication.* Nature, 1987. **329**(6138): p. 458-60.

185. Gannon, J.V. and D.P. Lane, *p53 and DNA polymerase alpha compete for binding to SV40 T antigen.* Nature, 1987. **329**(6138): p. 456-8.

186. Lee, J.B., et al., *DNA primase acts as a molecular brake in DNA replication.* Nature, 2006. **439**(7076): p. 621-4.

187. Tanner, N.A., et al., *Single-molecule studies of fork dynamics in Escherichia coli DNA replication.* Nat Struct Mol Biol, 2008. **15**(2): p. 170-6.

188. Hamdan, S.M., et al., *Dynamics of DNA replication loops reveal temporal control of lagging-strand synthesis.* Nature, 2009. **457**(7227): p. 336-9.

189. Ott, R.D., Y. Wang, and E. Fanning, *Mutational analysis of simian virus 40 T-antigen primosome activities in viral DNA replication.* J Virol, 2002. **76**(10): p. 5121-30.

190. Bell, S.P. and A. Dutta, *DNA replication in eukaryotic cells.* Annu Rev Biochem, 2002. **71**: p. 333-74.

191. Zegerman, P. and J.F. Diffley, *Phosphorylation of Sld2 and Sld3 by cyclin-dependent kinases promotes DNA replication in budding yeast.* Nature, 2007. **445**(7125): p. 281-5.

192. Tanaka, S., et al., *CDK-dependent phosphorylation of Sld2 and Sld3 initiates DNA replication in budding yeast.* Nature, 2007. **445**(7125): p. 328-32.

193. Wohlschlegel, J.A., et al., *Xenopus Mcm10 binds to origins of DNA replication after Mcm2-7 and stimulates origin binding of Cdc45.* Mol Cell, 2002. **9**(2): p. 233-40.

194. Xu, X., et al., *MCM10 mediates RECQ4 association with MCM2-7 helicase complex during DNA replication.* Embo J, 2009. **28**(19): p. 3005-14.

195. Ricke, R.M. and A.K. Bielinsky, *A conserved Hsp10-like domain in Mcm10 is required to stabilize the catalytic subunit of DNA polymerase-alpha in budding yeast.* J Biol Chem, 2006. **281**(27): p. 18414-25.

196. Chattopadhyay, S. and A.K. Bielinsky, *Human Mcm10 regulates the catalytic subunit of DNA polymerase-alpha and prevents DNA damage during replication.* Mol Biol Cell, 2007. **18**(10): p. 4085-95.

197. Robertson, P.D., et al., *Domain architecture and biochemical characterization of vertebrate Mcm10.* J Biol Chem, 2008. **283**(6): p. 3338-48.

198. Ricke, R.M. and A.K. Bielinsky, *Mcm10 regulates the stability and chromatin association of DNA polymerase-alpha.* Mol Cell, 2004. **16**(2): p. 173-85.

199. De Falco, M., et al., *The human GINS complex binds to and specifically stimulates human DNA polymerase alpha-primase.* EMBO Rep, 2007. **8**(1): p. 99-103.

200. Kukimoto, I., H. Igaki, and T. Kanda, *Human CDC45 protein binds to minichromosome maintenance 7 protein and the p70 subunit of DNA polymerase alpha.* Eur J Biochem, 1999. **265**(3): p. 936-43.

201. Pacek, M., et al., *Localization of MCM2-7, Cdc45, and GINS to the site of DNA unwinding during eukaryotic DNA replication.* Mol Cell, 2006. **21**(4): p. 581-7.

202. Lou, H., et al., *Mrc1 and DNA polymerase epsilon function together in linking DNA replication and the S phase checkpoint.* Mol Cell, 2008. **32**(1): p. 106-17.

203. Lee, C., et al., *Alternative mechanisms for coordinating polymerase alpha and MCM helicase.* Mol Cell Biol, 2009. **30**(2): p. 423-35.

204. Taneja, P., et al., *A dominant-negative mutant of human DNA helicase B blocks the onset of chromosomal DNA replication.* J Biol Chem, 2002. **277**(43): p. 40853-61.

205. Bird, L.E., et al., *Mapping protein-protein interactions within a stable complex of DNA primase and DnaB helicase from Bacillus stearothermophilus.* Biochemistry, 2000. **39**(1): p. 171-82.

206. Lu, Y.B., et al., *Direct physical interaction between DnaG primase and DnaB helicase of Escherichia coli is necessary for optimal synthesis of primer RNA.* Proc Natl Acad Sci U S A, 1996. **93**(23): p. 12902-7.

207. Bhattacharyya, S. and M.A. Griep, *DnaB helicase affects the initiation specificity of Escherichia coli primase on single-stranded DNA templates.* Biochemistry, 2000. **39**(4): p. 745-52.

208. Johnson, S.K., S. Bhattacharyya, and M.A. Griep, *DnaB helicase stimulates primer synthesis activity on short oligonucleotide templates.* Biochemistry, 2000. **39**(4): p. 736-44.

209. Dunn, J.J. and F.W. Studier, *Complete nucleotide sequence of bacteriophage T7 DNA and the locations of T7 genetic elements.* J Mol Biol, 1983. **166**(4): p. 477-535.

210. Lee, S.J. and C.C. Richardson, *Interaction of adjacent primase domains within the hexameric gene 4 helicase-primase of bacteriophage T7.* Proc Natl Acad Sci U S A, 2002. **99**(20): p. 12703-8.

211. Toth, E.A., et al., *The crystal structure of the bifunctional primase-helicase of bacteriophage T7.* Mol Cell, 2003. **12**(5): p. 1113-23.

212. Lao-Sirieix, S.H., et al., *Structure of the heterodimeric core primase.* Nat Struct Mol Biol, 2005. **12**(12): p. 1137-44.

213. Warren, E.M., et al., *Physical interactions between Mcm10, DNA, and DNA polymerase alpha.* J Biol Chem, 2009. **284**(36): p. 24662-72.

214. Robertson, P.D., et al., *Solution NMR structure of the C-terminal DNA binding domain of Mcm10 reveals a conserved MCM motif.* J Biol Chem, 2010. **285**(30): p. 22942-9.